A popular antidepressant drug and its metabolite induce toxicity *via* beta-amyloid and a serotonin transporter-dependent mechanism

A Thesis Submitted to the

College of Graduate and Postdoctoral Studies

In Partial Fulfillment of the Requirements

For the degree of Master of Science

In the Department of Psychiatry

University of Saskatchewan

Saskatoon

By:

Kaeli Jean Knudsen

PERMISSION TO USE:

In presenting this thesis/dissertation in partial fulfillment of the requirements for a graduate degree from the University of Saskatchewan, I agree that the Libraries of this University may make it freely available for inspection. I further agree that permission for copying of this thesis/dissertation in any manner, in whole or in part, for scholarly purposes may be granted by the professor or professors who supervised my thesis/dissertation work or, in their absence, by the Head of the Department or the Dean of the College in which my thesis work was done. It is understood that any copying or publication or use of this thesis/dissertation or parts thereof for financial gain shall not be allowed without my written permission. It is also understood that due recognition shall be given to me and to the University of Saskatchewan in any scholarly use which may be made of any material in my thesis/dissertation.

DISCLAIMER:

Reference in this thesis/dissertation to any specific commercial products, process, or service by trade name, trademark, manufacturer, or otherwise, does not constitute or imply its endorsement, recommendation, or favoring by the University of Saskatchewan. The views and opinions of the author expressed herein do not state or reflect those of the University of Saskatchewan, and shall not be used for advertising or product endorsement purposes.

Requests for permission to copy or to make other uses of materials in this thesis/dissertation in whole or part should be addressed to:

Head of the department of Psychiatry
College of Medicine
107 Wiggins Avenue
University of Saskatchewan
Saskatoon, Saskatchewan, S7N 5E5, Canada

OR

Dean
College of Graduate and Postdoctoral Studies
University of Saskatchewan
116 Thorvaldson Building, 110 Science Place
Saskatoon, Saskatchewan, S7N 5C9, Canada

Abstract

Depression increases the risk of Alzheimer disease (AD); however, some of this risk might be associated with the type of antidepressant drug used to treat the depression. Indeed, a significant risk has been associated with selective serotonin reuptake inhibitors (SSRIs). SSRIs increase synaptic serotonin levels by inhibiting the serotonin transporter (SERT). It has been reported that SERT can transport molecules other than serotonin. One such molecule is the 14 kDa protein α-synuclein (a protein which accumulates in the Parkinson disease brain). Therefore, it is possible that the AD-related, 4 kDa beta-amyloid (Aβ), may also be transported by SERT, and the inhibition of SERT by SSRIs could inadvertently result in the intracellular accumulation of Aβ and, ultimately, cell death and plaque formation (a hallmark of AD pathology).

Caenorhabditis elegans (*C. elegans*) and mammalian cell culture were used to study the effects of selected SSRIs, i.e. Fluoxetine and its major metabolite, nor-Fluoxetine, on the accumulation of Aβ. The expression of $A\beta_{1-42}$ in our transgenic *C. elegans* strain is under the control of the muscle promoter and is therefore specific to the muscle. Any accumulation causes a loss of motility/paralysis phenotype. Both Fluoxetine and nor-Fluoxetine exacerbated paralysis in *C. elegans* expressing $A\beta_{1-42}$. To confirm a role for the worm analogue of SERT, MOD-5, in this effect, a worm was generated that carried the $A\beta_{1-42}$ peptide on a truncated MOD-5 background. Paralysis was also exacerbated in this cross-bred worm strain (*versus* the parental strain that just expressed the $A\beta_{1-42}$ peptide), even in the absence of SSRI treatment. The degree of paralysis in a worm that carried the $A\beta_{1-42}$ peptide on a TPH-1 (tryptophan hydroxylase) null background (thus, inhibiting the synthesis of serotonin) was similar to that in the parental strain that just expressed the $A\beta_{1-42}$ peptide. Thus, any paralysis in this worm model was not dependent on any change in in serotonin availability. The experiments based on mammalian cell cultures, although showing promise, were not as conclusive and need further optimization.

Given the increased practice of prescribing SSRIs for off-label purposes, a significant number of individuals could be unknowingly put at risk for AD through a mechanism based on inhibition of SERT-mediated transport and intracellular accumulation of Aβ peptides. These observations will hopefully lead to a change in prescription practices.

Acknowledgments

I would like to thank my research supervisors, Dr. Carlos Carvalho and Dr. Darrell Mousseau. To Dr. Carvalho for initially giving me a chance to gain research experience in the summer after the second year of my undergraduate degree and allowing me to continue with further research under his supervision and to Dr. Mousseau for allowing me the opportunity to expand my skill set (without forcing me to work with mice). I am also appreciative to both of my supervisors for their endless support, whether it was motivationally, instructionally, intellectually, or financially. I would also like to thank my other Advisory Committee member, Dr. Jennifer Chlan for her added guidance on this project. A "thank you" is also owed to the other members of the Carvalho and Mousseau laboratories, both past and present, for their help and expertise over the years. I would like to acknowledge the funding that made this research possible. Dr. Mousseau is the Saskatchewan Research Chair in *Alzheimer disease and related dementia* funded jointly by the Alzheimer Society of Saskatchewan and the Saskatchewan Health Research Foundation; Dr. Carvalho is funded by an NSERC-Discovery grant and by the Canadian Foundation for Innovation (CFI); and I was awarded the College of Medicine CoMGRAD Graduate Student Scholarship. Finally, I want to thank my parents for all of their support during my university education, but especially throughout this Master's degree. They both provided constant encouragement and endured many conversations where they acted as my sounding board when working through experimental and analytical problems.

Table of Contents

List of Tables

List of Figures

List of Abbreviations

50p	50% of the worms are paralyzed
5-HIAA	5-hydroxyindoleacetic acid
5-HIAL	Serotonin aldehyde
5-HT	5-hydoxytryptamine/Serotonin
5-HTT	Serotonin transporter
Aβ	Beta-amyloid
AD	Alzheimer disease
AICD	Amyloid precursor protein intracellular C-terminal domain, roughly 50 amino acids in length
Ala	Alanine
ALDH	Aldehyde dehydrogenase
ApoE	Apolipoprotein E
APP	Amyloid precursor protein
APS	Ammonium persulfate
BACE	β-secretase
BMI	Body mass index
BSA	Bovine serum albumin
C. elegans	*Caenorhabditis elegans*
CSF	Cerebrospinal fluid
C83	α-C-terminal fragment of APP, 83 amino acids in length
C99	β-C-terminal fragment of APP, 99 amino acids in length
dH_2O	Distilled water
DMEM	Dulbecco modified eagle medium
DMEM/F12	Dulbecco modified eagle medium and nutrient mixture F-12
DNA	Deoxyribonucleic acid
DOC	Deoxycholate

ECL	Enhanced luminol-based chemiluminescent
E. coli	*Escherichia coli*
FBS	Fetal bovine serum
G. biloba	*Ginkgo biloba*
HEK	Human embryonic kidney
HEPES	4-(2-hydroxyethyl)-1-piperazineethanesulfonic acid
HNTG	HEPES – NaCl - Triton X-100 – Glycerol
Ile	Isoleucine
Ind	Indiana
IP	Immunoprecipitation
kDa	KiloDalton
LB	Lysogeny broth
MAO	Monoamine oxidase
MAO-A/MAO-B	Monoamine oxidase-A/Monoamine oxidase-B
MAOI	Monoamine oxidase inhibitor
NFT	Neurofibrillary tau tangles
NGM	Nematode growth media
Opti-MEM	Opti-modified eagle medium
OP_{50}	Uracil auxotroph *E. coli* strain used as food for *C. elegans* culturing
PAGE	Polyacrylamide gel electrophoresis
PBS	Phosphate-buffered saline
PET	Positron emission tomography
p3	Produced by cleavage of APP with α-secretase and γ-secretase; 24-26 amino acids in length
RIPA	Radioimmunoprecipitation assay
RT	Room temperature
sAPPα	Soluble APP fragment
SERT	Serotonin transporter (synonymous with 5-HTT)

SDS	Sodium dodecyl sulfate
SNRI	Serotonin-noradrenaline reuptake inhibitor
SORL	Sortilin-related receptor
SSRI	Selective Serotonin Reuptake Inhibitor
Swe	Swedish
T2D	Type-2 diabetes
TBI	Traumatic brain injury
TBS	Tris-buffered saline
TBST	Tris-buffered saline containing Tween-20
TCA	Tricyclic antidepressant
TeCA	Tetracyclic antidepressant
TEMED	Tetramethylethylenediamine
WBS	Worm bleaching solution
WB	Western blot
WT	Wild-type

1 Introduction

1.1 Alzheimer disease

Alzheimer disease (AD) is a neurodegenerative disorder that is responsible for almost 70% of dementia cases[1]. AD primarily affects thought, language, and memory; however, as this disease progresses, some motor dysfunction can also occur. Typical cognitive symptoms are mild forgetfulness that can grow to be more severe over time; confusion with names and simple math problems; forgetting everyday tasks; difficulties speaking and understanding speech; problems with reading and writing; behavioural changes; and anxious, aggressive, or aimless behaviour[2]. The impairment seen in people with AD is the result of synaptic damage, degeneration of axons, and atrophy within many regions of the brain including the hippocampus, entorhinal cortex, ventricles, amygdala, putamen, caudate, thalamus, and much of the cortex[3].

Although the indicators for diagnosing AD post-mortem are distinct, this is the only time that a definite diagnosis can be determined. However, in recent years, new technologies and research have allowed for other markers, such as cerebrospinal fluid (CSF) levels of the cytoskeletal protein tau and the hydrophobic, 4 kDa peptide beta-amyloid (Aβ), used to detect AD and its development[4]. Many genes are thought to be implicated, but very few have been confirmed to have a direct influence on the development of this disorder. An allele of apolipoprotein E (*ApoE ε4*)[5–7], mutations within presenilin 1 and 2 (*PSEN-1 and PSEN-2*), and the amyloid precursor protein (*APP*)[8,9] can influence the risk for, and development of, AD by regulating the generation and/or clearance of the Aβ-like peptides. When dysfunctional, Aβ is prevented from being cleared from the brain (*i.e.* APOE ε4) or converted into hydrophobic variants (*i.e.* APP, PSEN1, PSEN2), all of which aid in the formation of plaques[1]. In addition to these four genes, the sortilin-related receptor (*SORL1*) also influences the risk for AD as it is involved in trafficking APP intracellularly[10]. The five genes discussed are summarized in Table 1. Outside of these, any other genes studied have not produced reliable results or shown a consistent relationship with the development of AD[10].

Table 1.1: Summary of genes associated with AD.

Gene	Protein	Animal System	Impact on Aβ
ApoE ε4[5,6]	Apolipoprotein E ε4	Human[5]	ApoE normally binds Aβ; however, the APOE ε4 variant does not, resulting in less clearance of Aβ from the brain and accumulation of plaques[5]
PSEN-1[11]	Presenilin-1	Human and *C. elegans*[11]	PS-1 is the catalytic core of γ-secretase[12], an enzyme required for cleavage of APP. Mutations in PSEN-1 cause an increased production of longer Aβ variants[13].
PSEN-2[14,15]	Presenilin-2	Human[14]	PS-2 is another component of the enzyme used to cleave APP. Mutations in this gene have been found to be associated with an increase in Aβ[16].
APP[8]	Amyloid precursor protein	Human[8]	Mutations in this gene alter processing, causing an increase in Aβ[17].
SORL1[18]	Sortilin-related receptor1	Human[19]	This protein is involved in the sorting of APP and determines whether APP is directed through a recycling pathway or a breakdown pathway, producing Aβ[19].

Brain tissues from AD patients present two molecular hallmarks, neurofibrillary tangles (NFTs) and amyloid plaques, that appear to contribute to the disease symptoms[2]. NFTs are composed of 10 nm diameter fibrils and consist primarily of Tau protein, a microtubule-associated protein that is misfolded when hyperphosphorylated[20]. The NFTs have a helical shape when fibrils pair up[21]. Neuronal degeneration caused by NFTs typically begins in the medial temporal lobe in the allocortex and continues to the multimodal association area, proceeding through six stages described as Braak stages[22]. The transentorhinal region has NFT accumulation in Stage I, followed by an affected entorhinal cortex proper and CA1 of the hippocampus in Stage II. By Stage III these filaments are found in the limbic structures, which progress into the amygdala, thalamus, and claustrum in the subsequent stage. In Stage V, NFTs are present in multimodal regions, and by Stage VI, the primary sensory, motor, and visual areas have NFT accumulation[22].

Amyloid plaques are also very common within the brains of people with AD, but it has been shown that people can still develop dementia without having significant amyloid deposition[23], while there is strong evidence of significant amyloid plaque in certain cognitively intact elderly individuals[24]. Therefore, the role of the 'plaque' remains contentious; however, soluble Aβ peptides are known to exert toxic effects on cells[25]. APP can be metabolized via two distinct pathways. One pathway produces Aβ peptides through cleavage by β-secretase and γ-secretase[26] and the other is produced by α-secretase and γ-secretase. α-Secretase cleaves at a site within the Aβ peptide sequence and impedes the generation of the intact peptide, thus supporting a neuroprotective, anti-AD role for this enzyme. The specific physiological roles of the full APP peptide are not well known[27]; however, it has been reported that APP is involved in embryogenesis[28], neurite outgrowth[29], neuronal migration[30], and regulating neural progenitor cell proliferation in adult brains[31], with the conclusion that the physiological role of APP within the brain is one of neuroprotection[27]. Along with post-translational modifications, processing of APP can therefore lead to different Aβ isoforms and APP metabolites.

The dominant isoform of amyloid within plaques is $A\beta_{1\text{-}42}$. Total Aβ content does not increase in AD, but instead alterations in β-secretase activity will favor the generation of $A\beta_{1\text{-}42}$[32]. This is a very hydrophobic peptide with a higher rate of fibrillization due to two additional residues, both hydrophobic, on the C-terminus (*i.e.* Ile and Ala), resulting in a much greater likelihood of its aggregation[26] intracellularly after being produced by the secretory pathway within the endoplasmic reticulum[33]. As mentioned above, there are many variants of amyloid that are

found within the brain due to the different pathways involved in APP cleavage. These other isoforms are also present within the plaques or, if they are soluble, can remain diffuse. Both soluble and insoluble Aβ may contribute to the total amyloid burden within the brain, but there are contradictory data about the actual physiological role of Aβ[34,35]. However, a loss of synaptic plasticity is highly associated with $A\beta_{1-42}$ deposition within the cells compared to Aβ being released extracellularly[25]. Aβ accumulation within brain regions is more variable than the progression of tau tangles with the multimodal association area often showing the highest level of aggregation. After the associate cortex, the entorhinal cortex, hippocampus, basal ganglia, brainstem nuclei, and cerebellum are affected by the accumulation of Aβ, but to a lesser extent[34], in addition to the primary sensory, visual, and motor areas[35]. Braak and Braak described the progression of Aβ accumulation by separating the advancement into three stages[22]. The first, Stage A, begins with accumulation within the basal area of the frontal, temporal, and occipital lobes. The accumulation progresses into the multimodal association regions and hippocampus in Stage B. Finally, Stage C is characterized by plaques in all areas of the primary cortex. During this final stage, plaques can be present within the cerebellum, striatum, hypothalamus, subthalamic nucleus, thalamus, and red nucleus, as well[22].

Typically, once the patient is given a clinical diagnosis of AD, their NFT and Aβ aggregation has reached Braak Stages V/VI and Stage C of NFTs and Aβ, respectively[22]. As NFTs and Aβ accumulate within different areas of the brain, their presence, especially that of NFT, is associated with degeneration of those specific regions. The progression of the accumulation of toxic proteins is responsible for the cognitive symptoms displayed by individuals with AD. As the disease progresses, any areas affected by degeneration enlarges; the functions and behaviours controlled by these brain regions are also affected, producing neurological symptoms. Early neurofibrillary degeneration results in isolation of the medial temporal lobe from the subcortical nuclei and multimodal association area, causing the characteristic symptom of AD (*i.e.* short-term memory) by reducing the stimuli received from these regions[36]. Further cognitive decline occurs as accumulation moves into the cortical areas. This degeneration includes damage to the prefrontal cortex resulting in high-order executive dysfunction; apraxia caused by degeneration of the parietal cortex, visuospatial navigation and visuoperceptive mistakes due to deficits within the occipitoparietal cortex, and deterioration of the anterior temporal cortex causing semantic memory loss, finally resulting in severe dementia[22,36]. NFTs are also positively correlated with the presence

of microgliosis and astrocytosis, both of which are signs of substantial neuronal loss, and increased atrophy[3,37].

The distribution and extent of the plaque and tangle aggregation are also informative, in addition to obvious atrophy, in determining the pathology of AD at autopsy; however, there have been advances in diagnostic tools allowing for more accurate AD diagnosis earlier in the disease process[38]. Cerebrospinal fluid (CSF), which circulates throughout the brain and helps to remove 'waste', can be an effective reflection of pathological changes in the brain. Testing CSF for some indication as to the risk for AD developing later in life centers on levels of Aβ, total tau, and hyperphosphorylated tau[38]. However, little differences are seen between mild cognitive impairment and the onset of AD[4], thus CSF levels of these proteins are not yet reliable markers for assessing the early stages of disease progression. In addition, amyloid levels can be viewed using positron emission tomography (PET) imaging, but this method also has its limitations[39]. In individuals with mild to moderate dementia, 10-35% of the cases present with negative scans when using PET to look for amyloid deposition[23]. Although these biomarkers do allow for a more confident diagnosis when combined with clinical measures, especially in the early stages[40], the results above suggest that the diagnostic tests prior to autopsy are not completely accurate in their determination of AD and that reliable pathology markers have still not been found.

There is also research that suggests that AD may be transmissible[41,42], as with other prion diseases. The prion paradigm describes a commonality between a number of neurodegenerative disorders where aggregation of a toxic protein is found[43]. Some evidence has shown that inoculation of a non-primate brain with AD brain homogenates can result in the formation of Aβ plaques[42]; therefore, Aβ may be the prion-like peptide resulting in the neurodegeneration seen within AD. Prion diseases are associated with neuronal loss, astrocytosis, and the accumulation of misfolded prion protein[44,45], all of which are very similar to pathologies consistent with AD. If Aβ is able to be transmitted throughout the brain furthering deterioration, this would have an impact on how we should be pharmacologically treating AD.

Although a specific 'cause' that might explain what triggers an AD-like pathology is not presently known, there are several factors associated with the development of AD. Lifestyle, physical, and psychological aspects all appear to play a role in how vulnerable a person is to this neurodegenerative disorder. Diet plays a large role in most physical health concerns and treatments, and as such it is not surprising that a balanced diet consisting of unprocessed, whole

foods helps to reduce the risk of AD[10,46,47]. As well, consistent physical activity appears to reduce the risk of AD for many reasons. Physical activity can increase glucose utilization, oxygen extraction, cerebral blood flow, and capillary density; all of which have been shown to promote better cognition and decrease amyloid plaque formation in rodents[48]. Both increased blood flow and capillary density would promote clearance of the amyloid peptide and preclude the formation of plaques; thus, physical activity appears to indirectly play a role. Cognitive activities are also associated with reduced risk for AD in both younger and older groups of people[10,49]. In contrast, some pre-existing disorders and diseases may increase an individual's vulnerability to AD[49]. Cerebrovascular disease including hemorrhagic infarcts, ischemic cortical infarcts, and vasculopathies can lead to direct damage of brain regions important in memory function and may increase accumulation of Aβ[10]. Type-2 diabetes (T2D) also doubles the risk of AD[50,51], likely due to both cerebrovascular and non-cerebrovascular mechanisms involved with T2D[52]. As well, traumatic brain injury (TBI) increased a person's risk for AD when compared to individuals with no history of TBI[53]. Metabolic syndrome has also been shown to have a positive association with cognitive dysfunction[54]. Consistent with metabolic syndrome, high body mass index (BMI) and obesity are also thought to make an individual more vulnerable to AD[49]. The psychological side of health can also influence the development of AD; individuals facing consistent stress were found to have an increased risk[49].

In addition to the structural and metabolic changes observed in AD, various mood disorders, such as anxiety[55–57] and depression[58–60] have been associated with an increased risk of developing AD. A change in mood implies changes in monoaminergic neurotransmitters systems, for example the serotonin system[61]. Thus, changes in serotonin (5-HT) and its contribution in mood disorders[62] suggests that alterations in this monoamine system could be a risk for developing AD. This reduction in serotonin is the result of lesions in the brainstem nuclei that synthesize this monoamine and can also be seen in early stages of AD[63,64].

Depression was found to increase a person's risk for AD, with each subsequent depressive episode being associated with an increase in risk[49,65]. Although all the factors described show an association with the development for AD, a limitation that must be considered is that this relationship may be only correlational without any actual cause. As well, many of the risk factors are related to one another, and have a greater chance of being present together. Whether they have an additive effect, need to be present together for the risk to be increased, or mask the effect of

another inconspicuous agent is still not clear, but a reduction in serotonin levels have been consistently associated with AD[63,64].

1.2 Depression

Of the AD risk factors described above, one of the most common is depression. In Canada, one fourth of residents will suffer from a form of depression severe enough to require treatment within their lifetime[66]. Depression is more prevalent in women and this trend is consistent from younger teens through to older adults[67,68]. Although everyone experiences some depressive symptoms at different points throughout their lives, in those that suffer from clinical depression the mood disorder intrudes upon the individual's life. These people may experience constant sadness, anxiety, or an absence of feelings; changes in their regular sleep pattern resulting in too much or too little sleep; change in appetite, causing an associated weight change; loss of interest in their usual activities; irritability and restlessness; treatment resistant physical symptoms, such as digestive issues or chronic pain; difficulties concentrating, recalling memories, or making decisions; fatigue; feelings of worthlessness, hopelessness, or guilt; and suicidal thoughts[69]. In addition to these, males may experience "depressive equivalents" in place of emotional symptoms[68]. Men are more likely to show more irritability, anger, emotional numbness, and self-distraction through workaholism, substance use, womanizing, and gambling[68]. Most of these symptoms are not identified as symptoms *per se* in the Diagnostic and Statistical Manual of Mental Disorders[70]; however, many of these behaviours can be ways to distract from depressive thoughts. Although depression is thought to occur more in women[67], this may simply be due to how depression is defined for both sexes.

As there are different types of depression, the causes of this mood disorder differ. For example, evidence has shown that clinical depression can be the result of a combination of environmental factors[71], including stress, loss of family/friends, humiliation, failure, experiencing abuse, conflict, illness, financial crisis, and the physiological responses to these personal experiences. Experiences affect people differently, leading to the idea that there may also be genetic influences to depression[72]; possibly having the largest impact in a person's vulnerability to depression.

In addition, there are biochemical and anatomical differences in the brains of individuals with depression compared to mentally healthy controls. Differences in production and synaptic

availability of the monoamines dopamine, norepinephrine, and serotonin are likely the primary cause of depressive symptoms[73]. This notion was supported when compounds that increase availability of monoamines, by preventing their enzymatic breakdown, were shown to also reduce symptoms of depression[73] and as such, the regions that synthesize these neurotransmitters, including the ventral tegmental area, locus coeruleus, and the raphe nuclei, have been targets of studies on depression[73]. Structural imaging has also shown that clinical depression is associated with enlarged lateral ventricles, reduced grey and white matter within the prefrontal cortex[74], and decreased volumes of the amygdala[75] and hippocampus[76].

1.3 Antidepressant drugs

A combination of psychotherapy and pharmacotherapy is the usual treatment of depression and allows both the dysfunctional biochemical pathways and the depressive thoughts they produce to be treated. In Canada from 2007 to 2011, 4.2% of men aged 25-44 and 8.2% aged 45-64 were prescribed at least one antidepressant drug. In both age groups, 9.3%, and 17.2%, of women were prescribed an antidepressant drug[77]. These numbers also include prescriptions for an antidepressant drug as an off-label treatment, *e.g.* for indications such as chronic pain or sleep disorders, and obviously does not consider individuals who were treated for depression using non-pharmacological interventions (*e.g.* cognitive behavioural therapy). As changes in monoamine availability is likely the cause of depressive symptoms[73], mechanisms for monoaminergic regulation are the targets for pharmacological therapy. A summary of commonly prescribed classes of antidepressant drugs can be seen in Table 2.

Table 1.2: Classes of antidepressant drugs and their putative modes of action.

Antidepressant Drugs	Mode of Action
Monoamine oxidase inhibitors	Block monoamine oxidases from breaking down monoamines within neurons, glial cells, and in the synapse[78].
Tricyclic antidepressants	Associate with serotonin and noradrenaline uptake transporters, blocking transport of transmitters[79].
Selective serotonin reuptake inhibitors	Prevent the uptake of serotonin by selectively inhibiting the serotonin transporter[80].
Serotonin noradrenaline reuptake inhibitors	Inhibit the uptake of serotonin and noradrenaline, increasing their availability in the synapse[81].

1.3.1 A brief history of the development of antidepressant drugs

Pharmaceuticals have been used as treatment for depression since compounds were found to have antidepressant properties in the 1950s. The first observation of antidepressant effects was after treatment with isonicotinylhydrazine, later called Isoniazid, which was being used to treat tuberculosis[82]. Iproniazid was then synthetically produced based on the structure of Isoniazid and found to have higher antitubercular properties in humans[83]. In addition to being a tuberculosis treatment, it was observed that Iproniazid caused heightened energy and improved mood in tuberculosis patients[84]. It began to be prescribed as an antidepressant drug and was found to cause an improved mood, increased interest and tolerance of social situations, and a healthy weight gain[85]. These compounds were found to alter levels of neurotransmitters, including serotonin, by inhibiting the enzyme responsible for serotonin degradation, i.e. monoamine oxidase (MAO). As such, they were named MAO inhibitors (MAOIs), and were the first category of pharmaceuticals used to treat depression[86].

As with most medications, there were many side effects associated with their use[87–89], thus further research was done. Chlorpromazine, a compound originally synthesized in 1883 for the textile industry, was found to have antidepressant properties when tested on patients with psychotic symptoms[90]. The structure-activity relation studies of Chlorpromazine led to the development of the first tricyclic antidepressant (TCA) drug. Imipramine, was the original serotonin uptake inhibitor, which led to the increased availability of serotonin within the synapse and was available as an antidepressive treatment by the 1960s[91].Yet, TCA drugs, because they also targeted histaminergic and cholinergic systems, also had unwanted side effects such as dizziness, lethargy, and some cognitive changes.

This led to the development of more selective reuptake inhibitors. A category of antidepressant drugs that was developed shortly after the MAOIs and TCAs were the tetracyclic antidepressant drugs; however, this class has not remained a popular option for treatment.

The first class of antidepressant drugs designed to target a specific transporter were the selective serotonin reuptake inhibitors (SSRIs)[92]. The first of the SSRIs developed was Fluoxetine; it increased serotonin availability by inhibiting its uptake from the synapse back into the presynaptic neuron[80]. Fluoxetine was shown to successfully reduce depressive symptoms following its introduction in the early 1980s. However, Fluoxetine treatment had a delay in response time and roughly 30% of patients were unresponsive to the treatment[93].

As it had been hypothesized that both serotonin and noradrenaline have roles in depression[81], another category of compounds was produced that would enhance the availability of both monoamines within the brain. This class of antidepressant drugs is known as the serotonin-noradrenaline reuptake inhibitors (SNRIs) and they can bind to both serotonin and noradrenaline reuptake transporters[94].

1.3.2 Categories of antidepressant drugs

1.3.2.1 Monoamine oxidase inhibitors

The first antidepressant drugs discovered were the MAOIs[86], specifically with the use of Iproniazid. As the name of this category of antidepressant drugs suggests, these drugs prevent the monoamine oxidase (MAO) enzyme from breaking down monoamines in neurons, glial cells, and within the synapse. The MAOs degrade excess neurotransmitters from these areas and allow for regulation of appropriate levels of neurotransmitter availability around neurons. For example, serotonin is broken down to serotonin aldehyde (5-HIAL), then is converted to 5-hydroxyindoleacetic acid (5-HIAA) by aldehyde dehydrogenase (ALDH)[95]. This increase in synaptic concentration of neurotransmitters potentiate neurotransmitter binding to the respective receptors[78]. There are two forms of this enzyme: MAO-A and MAO-B. The isoenzymes can metabolize many compounds, but both have higher affinities for certain monoamines. MAO-A metabolizes serotonin, adrenaline, and noradrenaline, but has higher affinity for serotonin and noradrenaline; while MAO-B is able to break down dopamine, benzylamine, and β-phenylethylamine[96], with a preference for the latter two[97]. As well as breaking down different monoamines, the two isoenzymes are found in different neurons. MAO-A is found in catecholaminergic neurons[98] and is more abundant in the locus coeruleus, an area of the brain with the greatest number of noradrenergic neuronal cell bodies[99]. In contrast, MAO-B is found in serotonergic neurons, histaminergic neurons, and in glial cells[98], therefore, its greatest abundance is in the raphe nuclei, which is where all of the brain's serotonin cell bodies are found[99]. As stated, these enzymes control monoamines in and around the neurons. If any of these neurotransmitters are produced in concentrations that are too high to be regulated locally (through breakdown by intracellular MAOs after being transported back into the neuron) and are allowed to diffuse into an adjacent synapse, then extracellular MAOs will degrade any of the diffused neurotransmitter excess so that they cannot impede proper signalling or act as false neurotransmitters at these

adjacent sites[100]. In addition to neurons, MAOs are also expressed in many peripheral tissues where these isozymes typically are present in the same tissues and organs[101].

The original MAOIs were successful at reducing depressive symptoms, however they did have some unwanted side effects, which arose due to the irreversible inhibition of both MAO-A and MAO-B[102]. Inhibiting both isoenzymes prevents the breakdown of many monoamines, allowing their availability to increase. Tyramine is one such monoamine that accumulates upon MAO inhibition and can represent a problem in individuals with a diet that includes food and beverages that are high in tyramine by ingesting foods and beverages including soft cheeses, fermented sausages, yogurt, wine, and beer containing yeast[103]. Toxic levels of unprocessed tyramine can displace other monoamines with similar structure (including dopamine, adrenaline, and noradrenaline) from vesicles, and bind to their respective receptors in their place. This displacement can lead to vasoconstriction, causing a rise in blood pressure and heart rate[103]. Other side effects that have been observed due to tyramine accumulation are jaundice, nephrotoxicity, and fatal hepatic cell damage[87–89].

As it was known that MAO-A was the isoform associated with the antidepressant effect, when MAOIs were developed, they were targeted to bind to the A isoenzyme selectively, but reversibly[104]. The recovery from MAOIs that irreversibly bind both MAO-A and MAO-B is dependent on the time it takes neurons to synthesize new MAOs to metabolize the neurotransmitters. MAOIs can be eliminated faster than the body can synthesize new MAOs, thus these antidepressant drugs are not efficient[103]. However, MAOIs that can reversibly inhibit MAO-A have a shorter reaction time also allowing for a quicker recovery rate since the drug can dissociate from the enzyme. As dissociation occurs, more of the MAOI can be metabolized and eliminated[103], allowing the newer generation of MAOIs to have fewer negative side effects compared to the first generation. As the newer MAOIs allow MAO-B to metabolize tyramine[104], the potential for a hypertensive response is also reduced[103]. Although there are some extra precautions that need to be taken when using MAOIs to treat depression, they can still be very successful at combating depressive symptoms.

1.3.2.2 Tricyclic antidepressant (TCA) drugs

The TCA Imipramine was observed to have antidepressant effects around the same time as Iproniazid, giving more support to the theory that increasing the availability of monoamines is a

way to treat depression[81,105]. TCAs accomplish this by binding to serotonin and noradrenaline uptake transporters[79], and preventing the uptake of these monoamines into the presynaptic terminal where they might be degraded by MAO. However, TCAs are not very selective as they can also bind to serotonin receptors[106], muscarinic cholinoceptors[107], histamine receptors[108], and α-adrenoceptors[109]. The promiscuity of these compounds is likely what causes the range of side-effects seen in patients prescribed TCAs. As stated above, the side effects of these compounds include dizziness, vomiting, weight change, indigestion, fatigue, constipation, headaches, and decreased sex drive[110].

1.3.2.3 Selective serotonin reuptake inhibitors (SSRIs)

As serotonin was known to have a role in depression[81], new antidepressant drugs were developed to specifically target and inhibit serotonin reuptake transporters. The first SSRI designed was Fluoxetine[80], which continues to be widely prescribed to treat depression and more recently for many other off-label disorders and symptoms. The treatment was successful in many patients and was associated with very few complications; however, the rate of treatment resistance was not reduced with the introduction of SSRIs[111] indicating that there were still unexplained differences between individuals (or the type of depression that they suffered from)[112,113].

1.3.2.4 Serotonin-noradrenaline reuptake inhibitors (SNRIs)

Availability of both serotonin and noradrenaline were reported to be simultaneously reduced in depression. Since some patients were not responsive to SSRIs, new compounds were developed to increase the availability of both monoamines[81]. To accomplish this, SNRIs were designed to bind to both serotonin and noradrenaline reuptake transporters. The initial compounds in this drug category had variable affinities for these targets[114–116]. In addition, these compounds are not as selective as SSRIs and depending on the actual SNRI, they are able to bind secondary receptors[114–116]. The lack of selectivity accounts for the range in tolerability in depressive patients[117,118].

All antidepressant drugs described above have been shown to alleviate the symptoms of depression, although there is no one compound, or class of compound, that has been found to have a 100% success rate at improving depressive symptoms in all patients (*i.e.* regardless of type of depression). As well, when remission does occur, it is typically after weeks of treatment and does

not occur with the first treatment tried. Trial-and-error is often used to determine which medication is best tolerated in the individual. While treating the depressive symptoms present, some side effects still accompany pharmacotherapy such as nausea, constipation, headaches, fatigue, weight changes, or a reduced sex drive[110,119].

1.3.3 Serotonin Transporter (SERT)

SERT is the target for antidepressant uptake inhibitors, such as TCAs, SNRIs, and SSRIs; the latter of which has the greatest selectivity and specificity for this transporter. Evidence suggests that there are distinct binding sites on the transporter for TCAs and for SSRIs, as the uptake inhibitors do not produce consistent effects within patients[120,121]. Although the compounds can act quickly and inhibit serotonin uptake, the antidepressant effects only occur after more than a week of treatment[122]. The delay suggests that the antidepressive actions are the result of long-term adaptive changes, including down-regulation or desensitization of receptors, caused by the increased availability of serotonin[122].

As with other related neurotransmitter transporters, SERT has a 12-transmembrane domain structure[123]. This transporter is bidirectional, but typically transports one Na^+ and one Cl^- with every serotonin molecule from the extracellular space into the pre-synaptic neuron, with the removal of one K^+ ion into the synaptic cleft[122,124]. SERT terminates serotonin neurotransmission by removing the monoamine from the synaptic cleft back into the presynaptic cell[125] to be either metabolized by MAO and forming 5-HIAA or packaged into new secretory vesicles by the vesicular monoamine transporter[126]. The region of the brain with the greatest abundance of serotonergic neurons is the raphé nucleus (localized within the brainstem)[126], thus this transporter is more prominent in these neurons.

There are some studies showing that sex does not have an effect on the efficacy of antidepressant drugs[127–129], however, many studies have shown that females show greater improvement in mood when treating their depression with an SSRI[130–133] and treatment in males is more successful with TCAs[131,134–136]. The sex difference in efficacy suggests that either SERT is not structurally the same when comparing females and males or that the transporters are the same but are not modulated by other proteins the same way between the sexes. This is further supported by the theory that there are two binding sites on the uptake transporter. Their affinity

may be different between the two sexes, allowing TCAs to be more successful in males and SSRIs to produce better effects in females.

1.3.4 The effects of metabolism

Many of the antidepressant (uptake inhibitor) drugs have active metabolites, so it is important to consider how the liver might contribute to the profile of any antidepressant drug. Although all tissues have some metabolic capabilities, the liver is the main organ involved in metabolic processes[137]. Within the liver, cytochrome P450 enzymes are a superfamily of hemethiolate enzymes that mainly metabolize xenobiotic compounds, including clinically used drugs[138,139]. Of the many polymorphic P450 enzymes, six are involved in the metabolism of most clinically relevant antidepressant drugs: CYP2D6, CYP3A4, CYP2C9, CYP2CI9, CYP1A2, and CYP2E1[137].

There are many factors that influence the rate a compound is metabolized and, therefore, affecting the pharmacokinetics of the drug. Aside from the range of genetic polymorphisms of digestive enzymes, age and sex are two important factors that can affect a person's metabolism[140–142]. This is especially important for prodrugs, which require transformation to their active metabolites for activity, and for compounds that have toxic metabolites[143].

1.3.4.1 Metabolism and age

The increase in life expectancy, reflected in lower mortality rates, is resulting in an aging population[144]. An older population brings with it many physiological changes and deterioration[145], most of which negatively affect metabolism. Of these, alterations in liver function exert a great influence on the "aging" physiology and this affects how drugs are metabolized and cleared from the body[141]. With age comes a decrease in organ volume that can range from 20-40%[146] and reduced blood flow, slowing the delivery of the compound to the organ and its metabolism by 40-60%[141]. Clearance of drugs is more dependent upon the latter; if the drugs cannot be transferred efficiently to be metabolized (*e.g.* in the case of Fluoxetine, it is absorbed from the gastrointestinal tract and is delivered to the liver to be metabolized[137]), that will greatly influence their pharmacokinetics (*i.e.* how drugs are distributed throughout the body) as well as the types of compounds produced and their relative availability. For example, nor-Fluoxetine, the major demethylated metabolite of Fluoxetine, has a much longer half-life (*e.g.* seven to fifteen days) in

comparison to Fluoxetine (*e.g.* one to three days)[147], and both are found to have similar mechanisms of actions and affinities for SERT. Since metabolism slows with age, this breakdown would be relatively slower in older individuals, who will display lower levels of nor-Fluoxetine. Interestingly, treating older patients with Fluoxetine may be safer because of the slower breakdown of the drug,[148] allowing for less nor-Fluoxetine to be produced.

1.3.4.2 Metabolism and sex

The differences in anatomy and tissue composition between the sexes result in differences in the ability to metabolize compounds. Sex differences in liver metabolism, hormone levels, body weight, volume of plasma, plasma protein levels, gastric emptying, gastric acid secretion, enzyme activity, and body fat are known to affect the pharmacokinetics of a drug[142]. Antidepressant drugs are lipophilic in nature and, as such, have an affinity for adipose tissue; women tend to have a greater percentage of body fat and adipose tissue, which could explain the greater distribution of antidepressant drugs found within a female body[149]. Specifically, Fluoxetine is highly lipophilic and, has a longer half-life than most other SSRIs. In addition, the half-life of nor-Fluoxetine is much longer, and brain levels of this compound have been found to be 2-fold elevated over Fluoxetine at steady state[150]. Women also metabolize Fluoxetine to nor-Fluoxetine faster than men[151], and the metabolite remains longer in females[152], possibly due to slower gastric clearance and acid secretion from changes in estrogen[153].

Inconsistencies in metabolism studies could be due to methodological differences used. These include the demographic studied, class of antidepressant drug used, variation in the treatment regimen, statistical analysis, and age of female patients[142]. The varied estrogen levels throughout the onset and duration of menopause could have great effects on the efficacy of a drug and its metabolism. As stated above, estrogen levels have been found to influence gastric motility[142]. If the participants in the studies were not at the same stage of their menstrual cycle with similar sex hormone levels, differences in metabolism could be present. This may be another factor that needs to be considered, otherwise comparisons between the individuals in the study may be inaccurate.

1.4 Project Goal

This project aims to determine the effect of SSRIs on the intracellular accumulation of Aβ in a cell and whole organism models.

1.4.1 *Caenorhabditis elegans* as a model of AD

The nematode, *C. elegans*, has a short lifespan of around 25 days, which provides an excellent model for aging and neurodegeneration studies. Its rapid turnover from embryo to reproductive mature adult is a benefit for genetic manipulation and high sample sizes in a short period of time. In addition, synchronized generations can be easily obtained through a bleaching process of multigenerational populations that kills larvae and adults leaving only the embryos (protected by their egg shells)[154]. Since *C. elegans* have only a small number of neurons compared to a human brain, the muscle cells provide an effective predictive *in vivo* model to test the effects of antidepressant drugs on the accumulation of Aβ and investigate the genetic machinery modulating its effects in an intact organism. This nematode has been extensively used as an entry model system in aging studies because it offers a faster and suitable platform to screen for the genetic and cell biology underpinnings of aging cells.

C. elegans does express an ortholog of APP, APL-1 (amyloid precursor-like-1); however, APL-1 does not have β-secretase (BACE) sites[155] and because of this, APL cannot be cleaved to an Aβ variant. As well, this species does not express a BACE ortholog[155]. This is beneficial for surrogate AD studies because transgenic worms have been constructed to express human sequences producing Aβ peptide variants[155,156], enabling the study of any effects of the protein with fewer interfering endogenous factors. The worm strains utilized in this project express one of two Aβ peptide variants, $A\beta_{1\text{-}42}$ or $A\beta_{3\text{-}42}$, and are controlled by a muscle promoter. As the transgene expression is restricted to muscle cells, this results in a progressive paralysis phenotype to be analyzed. The degree of paralysis can be used to screen for effects of drugs or mutations on Aβ accumulation.

1.4.2 Cell culture as a model of AD

As with *C. elegans*, cell cultures are advantageous model systems for studying the molecular hallmarks of AD. Cell culture allows the systemic and behavioural effects observed in live worms to be translated to a mammalian system and studied in relevant cell types at the

molecular level. Although the worms are suitable to study neurodegenerative disorders, the transgenic strains used in this study were produced to over-express Aβ in their muscle cells, which makes it difficult to extrapolate to the neuronal context. Conversely, cell culture can directly model these processes in neuronal-like cells, which are more comparable to the accumulation seen in the human brain. As well, this model can be used to quantitatively study the role of SSRIs in the dynamic changes of Aβ localization, intracellularly or, if exported, in the media.

There are AD mouse models available that can be used to study the effects in a mammalian organism closer in evolutionary divergence to humans; however, *C. elegans* and cell culture together provide models that are more easily manipulated and provide a more direct method to test the hypotheses. *C. elegans* allow for functional assays to study the effects of SSRIs on Aβ-mediated toxicity and mammalian cell culture can be used to display whether Aβ can be exported. As this study focuses on the accumulation of Aβ as a contributing factor to the development of AD, the use of a mouse model would have produced more challenges to overcome. Firstly, mouse models can take from 2 to 15 months to age enough for plaque deposition and from 3 to 17 months for cognitive deficits to occur[157], and the timeline varies between the mouse lines. Because of the additional time required, the sample size would suffer. Secondly, a mouse is much more complex than a nematode; although there are models of both mice and *C. elegans* that lack the serotonin transporter, in a mouse there would be more additional effects to consider. For example, mice that are homozygous for the null mutation of SERT produce increased anxiety-like behaviours[158], which could interfere in behavioural assays to test for depressive symptoms when mimicking the pharmacological inhibition of SERT. As stated, worms have many conserved pathways that can be studied and a less complex nervous system, allowing for fewer possible interfering targets.

1.4.3 Project Rationale

An association exists between depression and AD, with those suffering from depression early in life having an increased risk for AD later in life[159]. In addition, both depression and AD are associated with a decrease in serotonin and noradrenaline. In AD this reduction of monoamine transmitters is the result of brainstem lesions, which are present early in disease progression; in patients with comorbid depression and AD, this damage is exacerbated[63,64]. However, a study by Kessing and colleagues (2009), suggests that any risk of AD associated with a diagnosis of depression may be exacerbated by the type of treatment used for depression rather than depression

itself[120]. It was found that individuals with depression who developed dementia were twice as likely to have been treated with an SSRI compared to individuals who did not develop AD[120]. SNRIs displayed a lesser risk of 1.5x; and TCAs showed no effect or reduced the risk of AD[120,160]. All the people studied had been diagnosed with clinical depression, therefore depression itself must not be the factor amplifying their risk for AD, as not all showed the same risk for AD. Aside from these findings, the literature discussing a potential association between Aβ accumulation and SERT is minimal.

The use of antidepressant drugs to combat depression and off-label purposes is very common[77], and with the continued use of these medications, chronic side effects will begin to be observed. The acute effects of compounds can be evident after the initial treatments, but long-term effects are not known until the drug has been in use for many years. As our knowledge about antidepressant drugs grows, changes may be required in prescribing compounds for treating depression. Some studies have produced data suggesting that chronic use of antidepressant drugs is associated with dementia, with people suffering from dementia being twice as likely to have taken antidepressant drugs compared to individuals that did not have dementia[161]. As well, the earlier depression occurs in an individual, the probability for antidepressant drug use and possible polypharmacy will increase. Of the people who experience one depressive episode, 50% will suffer a second event, and 80% of those individuals will have at least one more[70]. Chronic depression can result in chronic antidepressive treatment, which will just have compounding effects and further risk for polypharmacy.

SERT is thought to only be involved with the transport of serotonin, however, it has been shown that α-synuclein, which typically is associated with Parkinson's disease and the dopamine transporter[162], was able to bind to SERT,[163] suggesting that there may also be a link to Parkinson's disease. α-Synuclein was found to directly bind to SERT and cause negative modulation of the transporter by competing with serotonin[163]. An argument could be made that as serotonin is derived from tryptophan, its size would be comparable to an amino acid, but, since Aβ peptides range from 40-42 amino acids in length, the possibility that Aβ could be cleared through SERT or associate with this transporter is unlikely. However, the theory of the association between SERT and Aβ cannot be eliminated based on the size of this peptide given that α-synuclein can interact and modulate SERT[163], and is a much larger peptide consisting of 140 amino acids[164]. If proteins involved with the pathology of AD, such as Aβ, can be removed from the cell through this

transporter, treatment with a compound that blocks the transporter would also prevent the removal of this toxic protein. Thus, treatment with SSRIs would prevent Aβ transport, aiding in intracellular accumulation of Aβ and facilitating the formation of amyloid plaques, displayed in Figure 1. The progression of experiments performed in this study are discussed in Figure 2.

1.4.4 Research Hypothesis

SSRI treatments, particularly Fluoxetine and nor-Fluoxetine, may contribute to AD by enhancing the accumulation of intracellular Aβ peptides through inhibition of SERT.

1.4.5 Project objectives

The specific objectives studied are:

1) To determine if Fluoxetine and nor-Fluoxetine treatments lead to an intracellular accumulation of Aβ in a *C. elegans* transgenic model.
2) To determine if Fluoxetine and nor-Fluoxetine prevent Aβ removal via SERT in mammalian cell cultures.

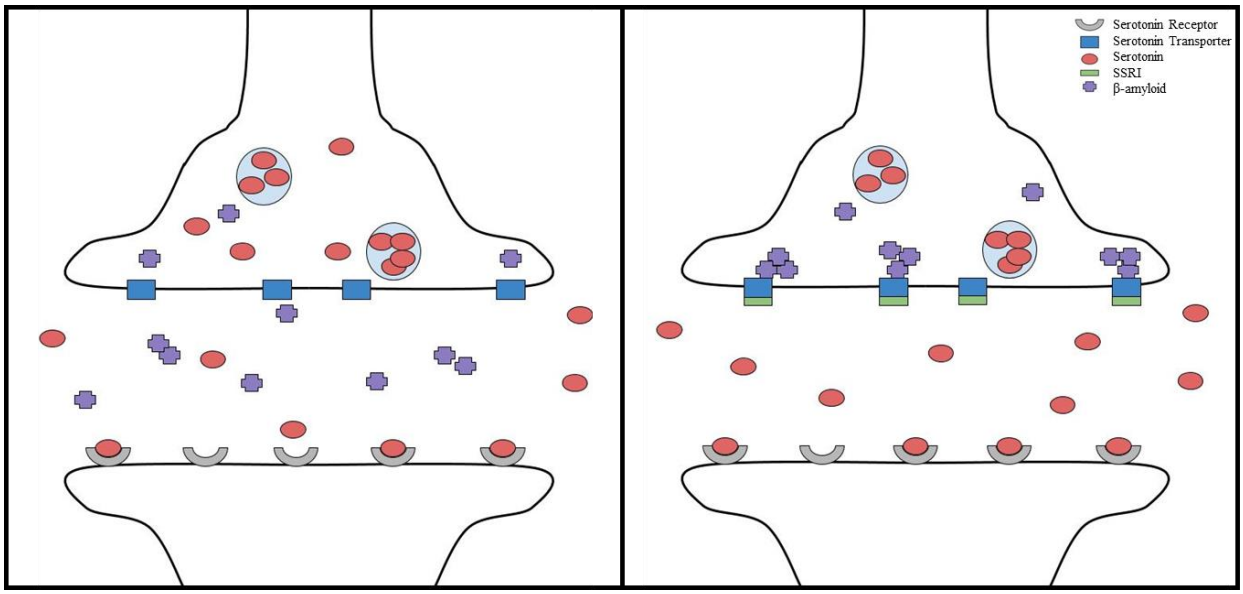

Figure 1.1: The proposed effect of SSRIs on Aβ deposition in neurons.

The role of SSRIs is to bind and inhibit SERT from being able to transport serotonin into the presynaptic neuron, increasing the availability of this monoamine within the synapse. It is theorized that SERT does not select only for serotonin and that Aβ is moved out of the neuron through these transporters, seen in the left panel. The right panel depicts inhibition of Aβ movement and the resulting accumulation of the toxic peptide within the presynaptic neuron, near the membrane of the cell.

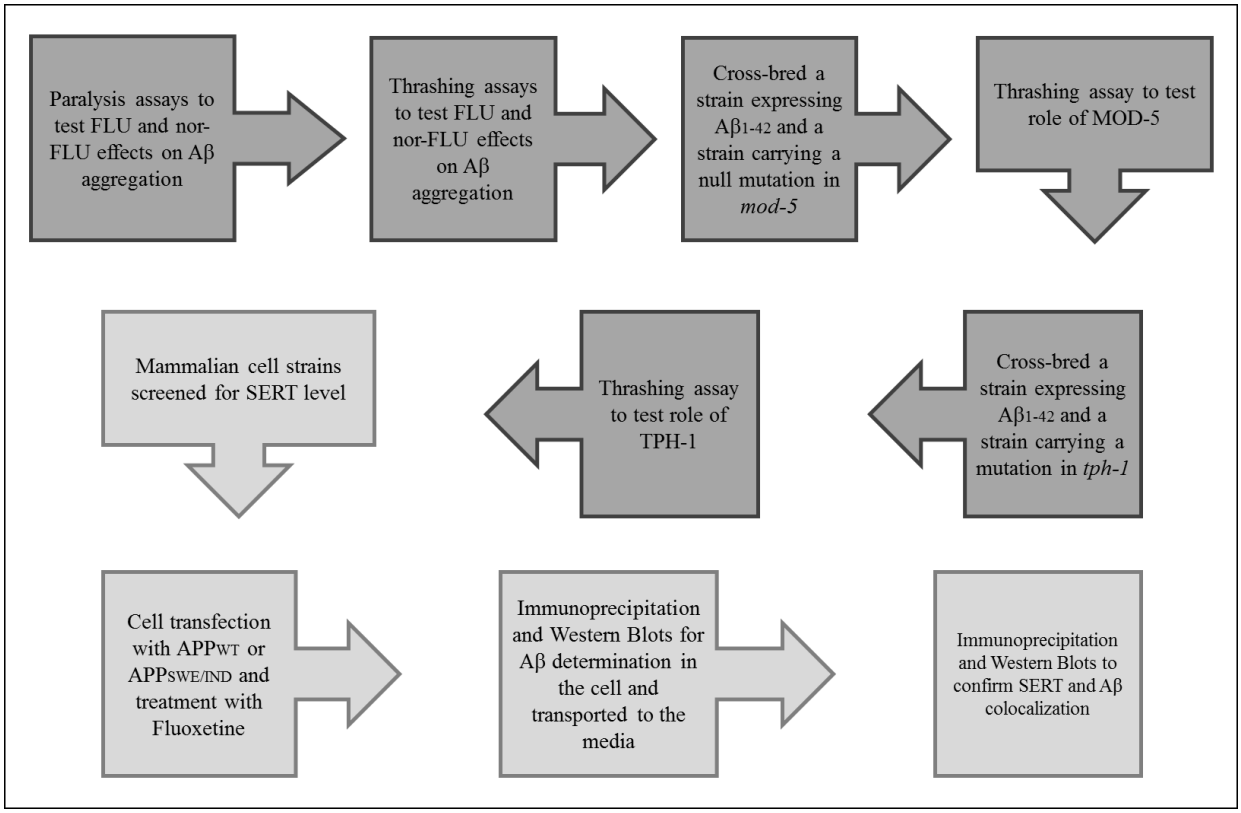

Figure 1.2: Experiment flowchart.

The first model used was *C. elegans* (depicted in dark gray), to show the effects of Fluoxetine or nor-Fluoxetine treatment on the accumulation of Aβ by studying the paralysis phenotype produced. To optimize the strategy utilized, first a paralysis assay was employed to determine if there was a difference in paralysis rate with Fluoxetine or nor-Fluoxetine treatment. However, this assay only allows qualitative data to be collected, so a thrashing assay was used to quantify paralysis by analysing thrashing behaviour. To ensure that the worm analogue of SERT, MOD-5, interacts with SSRIs, a strain that expresses $A\beta_{1\text{-}42}$ was crossed in a *mod-5* mutant. This new strain was used to molecularly mimic the pharmacological inhibition of the serotonin transporters with a thrashing assay. As SSRIs alter serotonin availability, a strain that expresses $A\beta_{1\text{-}42}$ was cross-bred to also have a *tph-1* (tryptophan hydroxylase) mutant background. This mutation prevents serotonin from being produced by lacking tryptophan hydroxylase. A thrashing assay was used to determine if altering the levels of serotonin changes thrashing behaviour. The second model, seen in light gray, is mammalian cell culture, used to test the location of AB with Fluoxetine treatment. The cells were transfected with one of two types of human APP. Immunoprecipitation and Western blotting were then used to determine whether the AB could be found in the media, or if its transportation was prevented with treatment with Fluoxetine. As well, immunoprecipitation and Western blots were used to look for any interaction between Aβ variants and SERT.

2 Materials and Methods

2.1 Materials

2.1.1 *C. elegans* Strains

Table 2.1: *C. elegans* strains utilized throughout this study.

Strain	Genotype	Source	Reference	Purpose
CL2122	*dvIs15* [(pPD30.38) *unc-54*(vector) + (pCL26) *mtl-2*::GFP]	Chris Link; University of Colorado	Fay et al., 1998[165]	Control strain for paralysis and thrashing assays
Cl2120	*dvIs14* [(pCL12) *unc-54*::A-beta-1-42 + (pCL26) *mtl-2*::GFP]	Chris Link; University of Colorado	Fay et al., 1998[165]	To study the effects of SSRIs on $A\beta_{3-42}$
GMC101	*dvIs100* [*unc-54p*::A-beta-1-42::*unc-54* 3'-UTR + mtl-2p::GFP]	Gawain McColl; The Florey Institute of Neuroscience	McColl et al., 2012[155]	To study the effects of SSRIs on $A\beta_{1-42}$
CB61	*dpy-5(e61)* I	Sydney Brenner; Medical Research Council Laboratory of Molecular Biology	Brenner S, 1974[166]	Used in crossing schemes
MT9772	*mod-5(n3314)* I	H. Robert Horvitz; MIT	Ranganathan et al., 2001[167]	To test whether SSRIs act on the worm analogue of SERT
CB128	*dpy-10(e128)* II	Sydney Brenner; Medical Research Council Laboratory of Molecular Biology	Brenner S, 1974[166]	Used in crossing schemes
MT15434	*tph-1(mg280)* II	H. Robert Horvitz; MIT	Sze et al., 2000[168]	To test whether serotonin has a role in the reduced thrashing phenotype

Table 2.2: *C. elegans* genes

Gene	Protein/Role
Mod-5	Serotonin transporter
Tph-1	Tryptophan hydroxylase
Dpy-5	Group I procollagen; when mutated produces a dumpy (smaller and wider than WT worms) phenotype
Dpy-10	Cuticle collagen protein; when mutated produces a dumpy (smaller and wider than WT worms) phenotype
DvIs100	Transgene consisting of a UNC-54 muscle promoter vector, $A\beta_{1-42}$, and a green fluorescent protein marker
DvIs14	Transgene consisting of a UNC-54 muscle promoter vector, $A\beta_{1-42}$ which gets cleaved to $A\beta_{3-42}$, and a green fluorescent protein marker
DvIs15	Transgene consisting of a UNC-54 muscle promoter vector and a green fluorescent protein marker

2.1.2 Cell Lines

Table 2.3: Cell lines used throughout this study.

Cell Line	Organism	Tissue	Morphology	Reference
HEK293	Human	Embryonic kidney	Neuronal-like	ATCC: CRL-3249
HT22	Mouse	Hippocampus	Neuronal	Maher and Davis, 1996
SH-SY5Y	Human	Neuroblastoma	Epithelial	ATCC: CRL-2266
N2a	Mouse	Neuroblastoma	Neuronal	ATCC: CCL-131

2.1.2.1 Cell pellets for initial SERT screen

Before determining which cell line would be used to test the effects of Fluoxetine and nor-Fluoxetine, a variety of human and mouse cell lines were screened for levels of SERT.

2.1.3 Plasmids

Three plasmids carrying different alleles of APP were used to transfect cells: pcDNA3.1 (Invitrogen) empty vector, pcDNA3.1/APP_{WT}, and pcDNA3.1/$APP_{Swe/Ind}$. APP_{WT} is the common form found within humans, while $APP_{Swe/Ind}$ is an allele that carries two mutations within APP (a two amino acid substitution and a point mutation, respectively) that results in a greater production of Aβ. The plasmids containing the APP inserts were cloned using *Hind-III* at the 5' end and *Xba-I* at the 3' end to contain APP_{WT} or $APP_{Swe/Ind}$.

2.1.4 Equipment and Reagents

Table 2.4: Reagents

Reagent	Manufacturer	Catalogue Number	Lot Number
Tris Base	Fisher Scientific	BP154-1	164826
Glycine	Fisher Scientific	BP381-1	166210
SDS	J.T. Baker	L050-07	E07619
Methanol	Fisher Scientific	AU52-4	171488
Sodium Chloride	Fisher Scientific	S271-3	167532
Glycerol	Anachemia	AC-4674	770328R
β-mercaptoethanol	Sigma	M-3148	102K0025
Bromo-Blue	Sigma	B-5525	4143657
Sulfuric Acid	Fisherbrand	UN1830	114275
Bistris	Sigma	1B9754	SLBH8220V
Bicine	Sigma	B8660	SLBR5204V
Triton X-100	Sigma	9002-93-1	
30% Acrylamide/Bis	Bio-Rad	161-0158	
40% Acrylamide/Bis	Bio-Rad	161-0144	
Urea	Sigma	U5378-1KG	SLBH3423V
Isopropanol	Fisher Scientific	A416-4	143620
DMEM (1X)	Gibco	11885-084	1848586
DPBS (1X)	Gibco	14190-144	1806048
DMEM/F12	Gibco	11330-032	1869010
Opti-MEM+GlutaMAX	Gibco	51985-034	1868987
Recovery Cell Culture Freezing Medium	Gibco	12684-010	18855679
Fetal Bovine Serum	Gibco	12483-020	
Trypsin/EDTA	Gibco	R-001-100	
Bovine Serum Albumin	Sigma	A3912-100G	SLBL5766V
Total Protein Kit, Micro Lowry, Peterson's Modification	Sigma-Aldrich	TP0300-1KT	020M6096
Qiagen HiSpeed® Plasmid Maxi Kit	Qiagen	12663	157037836
PageRuler Prestained Protein Ladder	Thermo Scientific	26616	00568726
Specter Low Range Ladder	Thermo Scientific	26628	00551160
C-TERM antibody	Sigma	A8717	43M4B16
6E10	Bio Legend	803002	B226151
4G8	Bio Legend	800702	B198888
ST45A5	Santa Cruz		L1316
22C11	EMD Millipore	MAB348	2793862
Anti-mouse 800	LI-COR	925-32210	C70712-11

Protein A Sepharose Beads	GE Healthcare	17-5280-02	10229487
Protein G Sepharose Beads	GE Healthcare	17-0618-05	10232495
Goat-anti-mouse IgG	Bio-Rad	170-6516	
TEMED	Bio-Rad	1610-0801	
Lipofectamine	Invitrogen	11668-019	
SERT	Biorbyt	Orb13226	
Sodium Chloride	BioShop	SOD001.205	6E43489
Peptone	BioShop	PEP403.500	6D43152
Agar Powder	Anachemia	02116-380	16E106578
Calcium Chloride	BioShop	CCL555.500	2A23595
Magnesium Sulfate	BioShop	MAG513.500	1L22952
Ethyl Alcohol 95%	Commercial Alcohols	P016EA95	24061
Cholesterol	Alfa Aesar	A11470	I14W043
Potassium Phosphate Monobasic	BioShop	PPM302.1	6D43352
Potassium Hydroxide	BioShop	PHY202.1	1C20501
Sodium Phosphate Dibasic	Sigma-Aldrich	57907-500	086H0066
Glycerol	Fisher BioReagents	BP229.1	168402
Javex	[Commercial Product]		
Bio-Tryptone	BioShop	TRP402.500	6D43153
Yeast Extract	BioShop	YEX401.500	1L22941

Table 2.5: Equipment

Equipment	**Manufacturer**	**Model**
Fume hood	H.H. Hawkins LTD	115/230
Stirrer and Hot Plate	Corning	PC-351
Power Pac	Bio-Rad	Power Pac 300
Water Bath	Fisher Scientific	2340
Centrifuge (15ml tubes)	International Equipment Co.	
Bio-Safety Cabinet	Microzone Corporation	Bio Klone 2
Cell Culture Incubator	Thermo Scientific	HERACell VIOS 160i
Microcentrifuge	Bio-Rad	S586354
Heat Block	Fisher Scientific	Isotemp 2001
Scale	Mettler Toledo	M51045
Rocker	VWR	Standard Analog Rocker
-80°C Freezer	Thermo Scientific	Forma 88000 Series
Spectrophotometer	Molecular Devices	Spectra Max M5
LI-COR	Mandel	Odyssey
Nanodrop	Thermo Scientific	NANODROP 2000c
Vortex	Scientific Industries	Vortex Genie 1
Impulse Sealer	Uline	KF-300H
Incubator	Fischer Scientific	Isotemp
Shaking Incubator	Thermo Scientific	MaxQ 4000
Media Dispenser	Wheaton	Unispense
Microscope	Nikon	Nikon SMZ 745
Light Transformer	Nikon	Transformer XN
Fluorescence Microscope	Nikon	Nikon H550L
Transformer	Lumen Dynamics	X-CITE Series 120
Pipet-Aid	Drummond	

2.2 Methods

2.2.1 *C. elegans* maintenance and crossing strategies

2.2.1.1 Maintenance

All *C. elegans* strains were maintained on 60mm plates with normal growth medium (NGM) at 16°C in a Fisher Scientific Isotemp® incubator and fed the OP_{50} strain of *E. coli*. The coding sequence to express $A\beta_{1-42}$ or $A\beta_{3-42}$ follows the *unc-54* muscle enhancer and includes a green fluorescent marker (the complete transgenes are *dvIs100* or *dvIs14*, respectively). Strains were maintained at 16ºC prior to the paralysis and thrashing assays. Protein accumulation increases considerably at higher temperatures (25°C) and worms display a progressive paralysis phenotype[155,156]. To ensure synchronous populations, plates were kept at the same temperatures and experiments with different strains/treatments were performed in parallel on the same days.

2.2.1.2 Breeding

To test whether Fluoxetine and nor-Fluoxetine effects on thrashing behaviour depended on proper transport and serotonin synthesis, strains expressing muscle $A\beta_{1-42}$ (*dvIs100*) in *mod-5* (serotonin tranporter) and *tph-1*-depleted (tryptophan hydroxylase) backgrounds, respectively, were constructed.

2.2.1.2.1 Generating males

Males were isolated from the progeny of heat shocked young adult hermaphrodites that were incubated at 30ºC for 4 hours[169]. Heat shock at this temperature increases frequency of X chromosome non-disjunction during meiosis without compromising fertility. Monosomic X0 worms in *C. elegans* develop as normal males. Rare males (X0) that resulted from non-disjunction events in XX oocytes were isolated from the progeny of heat shocked worms and subsequently mated with virgin hermaphrodites. Upon mating, a 1:1 XX/X0 (hermaphrodite/male) progeny ratio can be generated and 50% male populations maintained.

2.2.1.2.2 Generating *mod-5;dvIs100* worms

To ensure that the SSRIs being tested were indeed acting on the serotonin transporter, the effects of genetically inhibiting its function in the worm was tested. The hypothesis was that any genetic inhibition of SERT function would mimic the pharmacological inhibition seen with

Fluoxetine and nor-Fluoxetine. The steps to achieve this cross are displayed and discussed in Figures 3 and 4. An intermediate strain was required in the production of *mod-5;dvIs100* and the steps in the cross strategy are displayed in Figures 3 and 4.

Although *dvIs100* males (GMC101; $A\beta_{1-42}$ transgene) could be crossed with *mod-5* hermaphrodites (MT9772) to produce *mod-5;dvIs100* worms, it would be difficult to identify *mod-5* animals from siblings heterozygous for *mod-5*, as *mod-5/+* worms are overtly WT and only display abnormal behaviour in response to exogenous serotonin. To evade the need for molecular screening for the *mod-5*(n3314) mutations or, alternatively, individually testing progeny for serotonin hypersensitive phenotypes, the cross strategy took advantage of a phenotypic marker allele, *dpy-5*(e61) linked to the *mod-5* locus on chromosome I. Dumpy worms are viable, though significantly smaller than the WT which allows for identification of *dpy-5* homozygotes on plates with non-dumpy worms. The first part of this strategy required the introduction of the Aβ-containing transgene (*dvIs100*) into the *dpy-5* background (Figure 3) while in the subsequent steps, the *dpy-5 mod-5* + chromosome was selected out of the self-fertilized progeny of *dpy-5 mod-5 +/dpy-5 + mod-5* hermaphrodites, therefore eliminating any other unrecombined genotype with the exception of *dpy-5+ mod-5* homozygotes, as shown in Figure 4.

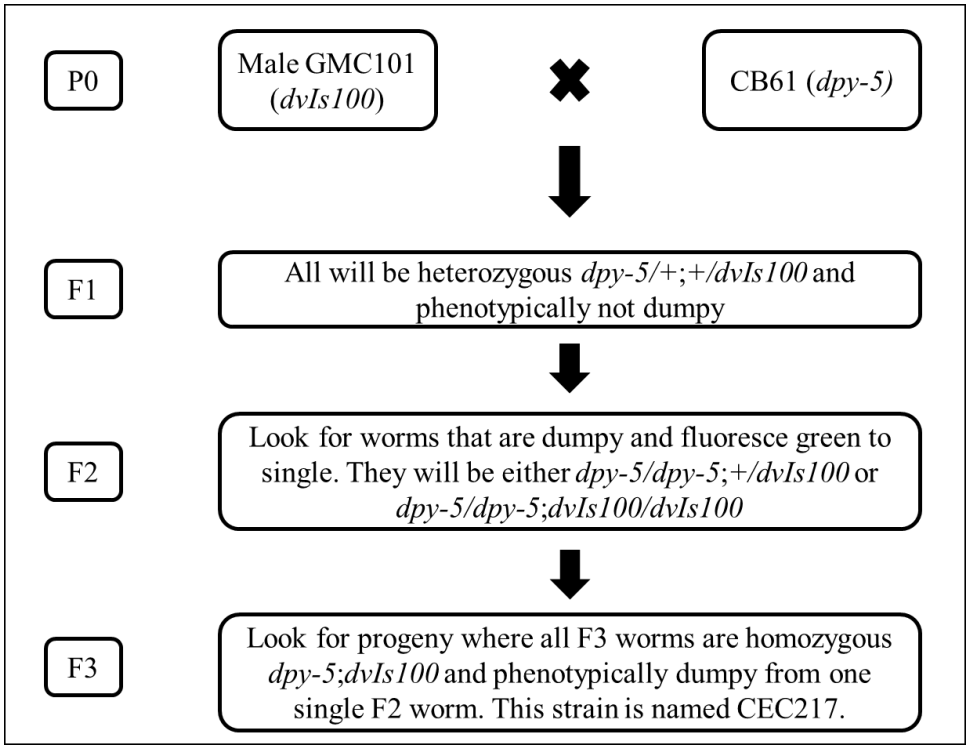

Figure 2.1: Cross scheme for generating *dpy-5;dvIs100* worms.

Although the GMC101 and MT9772 strains could be crossed to produce a *mod-5;dvIs100* mutant worm, it would be difficult to determine which worms produced were homozygous for the *mod-5* mutation, which were heterozygous, and which were the product of no cross occurring. To avoid this eventuality, an additional step was required so that there would be a phenotype to select against and allow for selection of the *mod-5* mutation. Male GMC101 worms and hermaphroditic CB61 worms were allowed to mate on two mating plates to breed overnight. (Mating plates are regular NGM plates with a small drop of OP_{50} in the center so that the worms stay in the same area, increasing the frequency of meetings.) The next day, the CB61 worms were picked onto individual seeded NGM plates (called singling) to isolate their progeny form the other progeny of the other "mothers". Once the eggs were laid, the "mother" was removed so that only F1 progeny was on the plates. If the cross has occurred, the F1 generation will all be *dpy-5+/+dvIs100* and appear non-dumpy, with possibly faint green fluorescence along the body muscle due to the GFP marker gene within *dvIs100.* F1 worms are then singled, then the F2 generation was scored for worms that showed a dumpy phenotype and had green fluorescence along their body muscle to single. These worms were either homozygous for both *dpy-5* and *dvIs100,* or homozygous for *dpy-5* and heterozygous for *dvIs100*. To ensure the worms are homozygous for both genes, the F3 generation was scored for progeny that all show a dumpy phenotype and fluoresce green. These worms were *dpy-5;dvIs100* and the strain named CEC216.

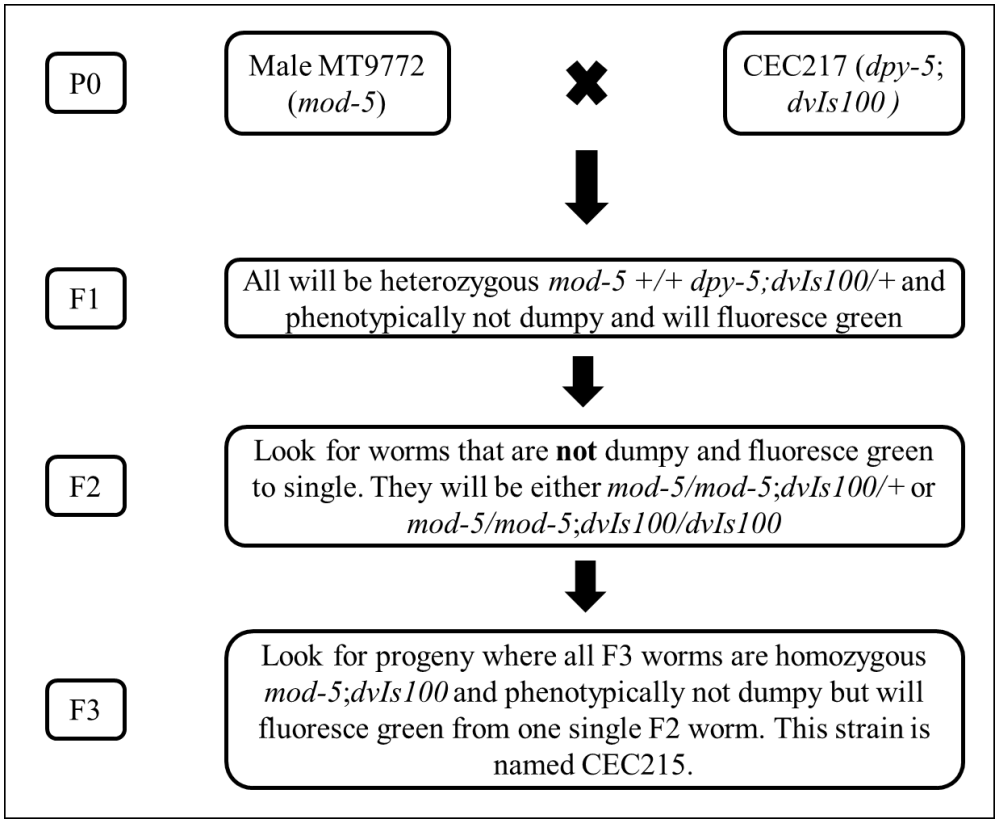

Figure 2.2: Cross scheme for generating *mod-5;dvIs100* worms.

To complete the second portion of the cross to have worms that produce $A\beta_{1-42}$ that also lack the serotonin transporter, MT9772 males and hermaphroditic CEC216 worms were crossed overnight. The next day, CEC216 worms were singled onto seeded NGM plates, and once they had laid their eggs, the "mother" was removed. If the cross occurred, all worms are *mod-5 +/+ dpy-5;dvIs100/ +*. Within the F2 generation, worms that show a non-dumpy phenotype and have green fluorescence along their body muscle were to singled. Since both dpy-5 and mod-5 are on chromosome I[166,167], if the dumpy phenotype is not seen, this signifies that the worm is homozygous for the *mod-5* mutation. The final step of this cross was to scan plates of F3 progeny for the non-dumpy and green phenotype in all the worms from the same F2 parent, showing that the F2 worm and its offspring are *mod-5;dvIs100.* This strain was named CEC215.

2.2.1.2.3 Generating *tph-1;dvIs100*

To ensure that the reduced thrashing phenotype observed in untreated $A\beta_{1-42}$ expressing worms (GMC101 – *see* results) was not the result of altered serotonin levels, worms deficient in serotonin synthesis, because of a mutation in tryptophan hydroxylase (TPH-1), were generated. Because serotonin itself has been directly implicated in normal *C. elegans* locomotion behaviour, this genotype served as a negative control to ensure that reduced locomotion in GMC101 worms was not an intrinsic product of $A\beta_{1-42}$ influencing serotonin levels, but instead the consequence of progressive $A\beta_{1-42}$ peptide accumulation in muscle cells. An intermediate dumpy marker strain (*dpy-10*), linked to *tph-1* on chromosome II was used in a two-step strategy to produce *tph-1;dvIs100.* The crossing scheme is indicated in Figures 5 and 6.

2.2.2 Synchronization

Worm cuticles are permeable to NaOH such that larvae and adult worms die if exposed to it. In contrast, egg shells provide an impenetrable barrier that protect embryos from caustic environments. By treating a mixed population on a plate with a bleaching solution and recovering viable eggs, a new developmentally synchronized population of hatching larvae representing a 12-hour window of time (the time required to undergo embryogenesis) can be reconstituted. The protocol is shown below.

a. Wash the worms and eggs off with Worm Bleaching Solution (WBS) and transfer into 1.5 mL Eppendorf tubes; this is the first step of the preparation for the paralysis assay or thrashing assay and as such is referred to as Day 1.
b. Centrifuge at 10000 rpm for 2 minutes, then remove the supernatant.
c. Resuspend the pelleted worms and eggs with 1000 µL M9 Buffer.
d. Centrifuge the samples again at 10000 rpm for 2 minutes and repeat steps c and d two more times so that the eggs are rinsed three times.
e. Resuspend the pellet in 500 µL of fresh M9 Buffer and pipette onto NGM plates without OP_{50}.
f. The following day wash the hatched L1 worms off the plate with 1.0 mL of M9 Buffer, centrifuge at 5000 rpm for 2 minutes, remove most of the supernatant, and plate the worms onto a seeded NGM plate.

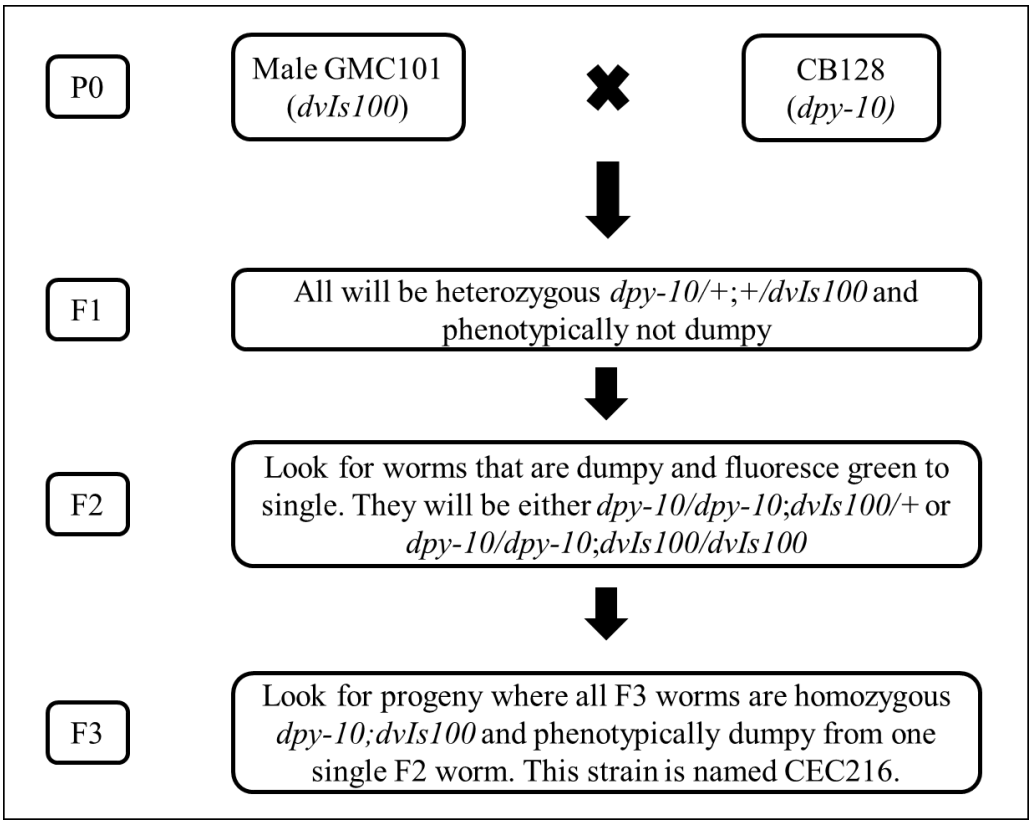

Figure 2.3: Cross scheme for generating *dpy-10;dvIs100* worms.

To determine whether serotonin played a role in the thrashing behaviour, worms that encode the sequence for $A\beta_{1-42}$ and lack tryptophan hydroxylase activity were produced. Male GMC101 worms were crossed with hermaphroditic CB128 worms overnight on mating plates. The CB128 worms were then singled and removed once the eggs were laid. Within the F1 generation, if the cross occurred, all worms should be *dpy-10 +/+ dvIs100,* and appear non-dumpy, with possibly faint green fluorescence along the body muscle, if any. F1 worms were singled and left to self-fertilize; from the F2 generation, worms showing the dumpy phenotype and green fluorescence along their body muscle were singled to score the F3 generation. Plates with all worms expressing the dumpy phenotype and green fluorescence were homozygous *dpy-10;dvIs100.* This strain was named CEC217.

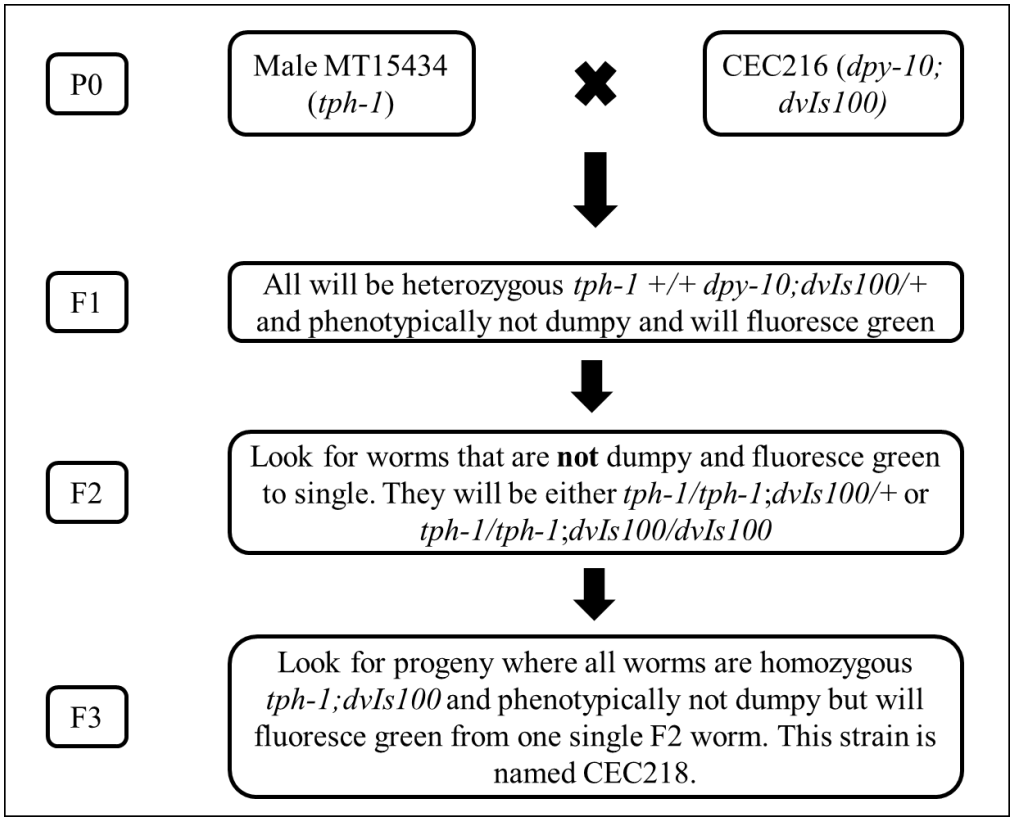

Figure 2.4: Cross scheme for generating *tph-1;dvIs100* worms.

To complete the second portion of the cross, male MT15434 worms hermaphroditic CEC217 worms were crossed overnight. The CEC217 worms were singled, left to lay eggs, then removed so only the F1 generation would remain. If the cross occurred, all worms should be heterozygous for *tph-1+/+ dpy-10;dvIs100/ +*, appearing non-dumpy and possibly with faint green fluorescence along the body muscle. These worms were singled and left to self-fertilize, then the F2 generation was scored for worms that showed a non-dumpy phenotype and had green fluorescence along their body muscle to single. Since both dpy-10 and tph-1 are on chromosome II[166], if we do not see the dumpy phenotype, we can assume that the worm is homozygous for the *tph-1* mutation. The final step of this cross was to scan plates of F3 progeny for the non-dumpy and green phenotype in all the worms from the same F2 parent, showing that the F2 worm and its offspring were homozygous *tph-1;dvIs100.* This strain was named CEC218.

2.2.3 Heat-killed Bacteria

Live bacteria, used as food for *C. elegans* cultures can metabolize Fluoxetine[170]. To control for the potential interference of bacteria-derived SSRI metabolites contributing to Aβ accumulation in worm tissues, heat-killed *E. coli* were used. The bacteria were killed using the following steps:

a. Inoculate lysogeny broth (LB) with bacteria and incubated at 37ºC overnight.
b. Centrifuge the LB and bacteria mixture in an Eppendorf Centrifuge 5804 at 4 500 rpm for 10 minutes in 50 mL Falcon tubes until all the *E. coli* has formed a pellet at the bottom of the tubes.
c. Remove the supernatant
d. Resuspend the pelleted bacteria in 5 mL of fresh LB.
e. Pipette 1 mL of this solution into 1.5 mL Eppendorf tubes and place into a VWR Analog Heatblock at 70ºC for 30 minutes.
f. Collect the heat-killed *E. coli* in a 15 mL Falcon tube until required to seed the treatment plates. This protocol is based on the description by Ren and colleagues[170].

To ensure that the heated *E. coli* had been killed, three 15 mL Falcon tubes with 3 mL of LB were tested. One was not inoculated and used as a negative control to ensure that the LB itself had not been contaminated; one tube was inoculated with the *E. coli* before it was heated to be used as a positive control; and the last was inoculated with the heated bacteria. All are incubated at 37ºC overnight to test for growth.

2.2.4 Paralysis assays

As a simple visual readout to indirectly test the potential effect of SSRIs on the accumulation of Aβ in live *C. elegans*, populations of worms expressing *dvIs100* (GMC101) with different drug treatments were analysed in different time-points for changes in the previously described Aβ-dependent, paralysis curve. In the context of GMC101, paralysis, defined as the absence of detectable core movement on a solid medium, is an induced phenotype resulting from the ectopic accumulation of a human peptide in muscle cells of these worms. The deposition of Aβ peptides in these cells is thought to lead to progressive paralysis and, ultimately, paralysis of the whole organism. Previously, other laboratories had characterized the rate of paralysis in GMC101 animals as a function of time as an experimental platform to screen for conserved genes

that influence Aβ toxicity[171,172]. Though not directly informative on neuronal Aβ toxicity, this assay was therefore a natural experimental entry point to functionally probe whether SSRI treatment could disturb the normal progression of Aβ accumulation significantly enough to influence a whole organism level response (movement).

The following steps describe the assay:

a. On day one, inoculate a flask with sterile LB media with OP_{50} and place it in a Thermo Scientific MaxQ 4000 shaker incubator overnight at 37ºC at 165 rpm; the drug will be administered by mixing it with the OP_{50}. Synchronize the strains using the protocol above and prepare 35 mm NGM plates to use for the treatments later.
b. On day two, once the eggs have hatched, move L1 worms by washing with 1000 µL M9 buffer onto NGM plates seeded with OP_{50}. As well, seed the 35 mm plates with 100 µL of OP_{50} or the OP_{50} + drug mixture composed of 1 µM or 10 µM Fluoxetine or nor-Fluoxetine diluted in dH_2O. Once seeded, leave the plates on the bench (at 20ºC) until the bacterial and drug lawn has dried, then move them into a 4ºC fridge to prevent desiccation.
c. On day four the worms have reached the L4 stage. Pick 15 worms with a platinum wire onto each of the treatment plates. Twelve hours after the worms are picked onto the plates is the first time-point to score for paralysis.
d. Score the worms at 18, 20, 22, 24, 26, 28, 30, 32, 34, 36, and 42-hour time-points.

Paralysis was assigned to animals that showed loss of movement in the central body region (region from head to tail) that prevented further foraging behaviour. Some remaining head and tail side-to-side swaying may still be displayed even in fully immobile GMC101 animals, as the paralysis only occurs throughout the body muscle cells. These worms were scored as paralyzed for the purpose of this analysis[171]. To exclude dead animals from being scored as paralyzed, immobile worms were gently prodded with a platinum wire to check for the normal head backing response to touch stimuli. Only the worms that did show a retractile response were scored as paralyzed, while those that did not respond were discarded.

2.2.5 Thrashing assays

Because of the variability in measuring movement against a solid, high friction surface where varying levels of movement impairments are hard to distinguish, this paralysis assay is

prone to experimental biases, tends to overestimate or underestimate paralysis depending on the level of functional compromise, and is therefore best used as a qualitative indicator of a phenotypic trend. An alternative assay that measures number of thrashes over time on liquid can be used as a quantitative way to address minor movement impediments before full paralysis ensues. The assay is based on a worm being placed in a drop of M9 Buffer and the number of complete side-to-side lateral swimming movements in a specified amount of time recorded. Because the number of thrashes corresponds to muscle vigor, values can be assigned and compared against a standard genetic background (WT, etc.) or treatment. To prevent external factors, such as age, from influencing the analysis, thrashing behaviour was quantified in the same timeline and with the same drug regimes used for the paralysis assays (see above). One thrash was assigned to a single lateral bend of the body as the head and tail point towards the same side. Measurements were taken on day 5, either at hour 18 or 24, and one on day 6, at hour 42 or 36, respectively. Individually, 5 worms were picked off each treatment plate in 5 µL of M9 Buffer on a glass slide and given 20 seconds to acclimatize to the new media. Thrashing was manually counted for the following 30 seconds using a Nikon SMZ 745 microscope.

2.2.6 Maintaining cell lines

2.2.6.1 HEK293, N2a, and HT22

These cells were grown in DMEM + 10% FBS in a Thermo Scientific HERACell VIOS 160i incubator at 5% CO_2 and 37ºC.

2.2.6.2 SH-SY5Y

These cells were grown in DMEM/F12 + 10% FBS in a Thermo Scientific HERACell VIOS 160i incubator at 5% CO_2 and 37ºC.

2.2.7 Transfecting cells

Cells were overexpressed with APP to study the effects of SSRIs on the accumulation of Aβ. Cell transfections were performed using the following protocol:

a. Split the cells so that by the day that they are harvested, they are at 90% confluency, requiring the transfection to be set up at 50-70% confluency, depending on the rate of growth of the cells.

b. Make a master-mix for each experiment to minimize any differences between plates, with enough for one extra plate included for any pipetting error. For each plate, include 900 µL OPTI-MEM reduced serum media and 9 µg of either pcDNA3.1 vector, pcDNA3.1/$APP_{WT,}$ or pcDNA3.1/$APP_{Swe/Ind}$ per plate to make up the two Solution As. The plasmids were amplified using the Qiagen HiSpeed® Plasmid Maxi Kit.
c. Solution B consists of 900 µL OPTI-MEM reduced serum media and 27 µL Lipofectamine Reagent per plate.
d. Add Solution A and the appropriate amount of Solution B together and gently mix and allow them to incubate for 15 minutes.
e. While incubating, aspirate off the media on the plates and rinse with 7.5 mL warm serum-free media, then also aspirate this off.
f. After the incubation period has elapsed, 7.2 mL serum-free media per plate is added to each combined Solution A and B then gently mixed.
g. Pipette 9.0 mL of the Solution A, Solution B, and serum-free mixture gently onto each plate of cells, according to the treatment they are to receive.
h. Return the cells to the Thermo Scientific HERACell VIOS 160i incubator for 6 hours.
i. After the 6 hours, supplement the media with 9.0 mL DMEM + 20% FBS and add in 18 µL of Fluoxetine for a 10 µM treatment or 45 µL for a 25 µM treatment. Nothing extra is added for the 0 µM treatment, aside from the supplemental media.
j. After 24 hours, remove the plates from the incubator and place them on ice to stop any additional metabolism.
k. Collect the media in a 15 mL Falcon tube and centrifuge it to collect any cells that are not adhered to the plate. Remove the supernatant to a 50 mL Falcon tube to freeze the media in until ready to IP.
l. Gently rinse cells with 6mL of cold 1x PBS, then aspirate the 1x PBS off.
m. Pipette 3 mL TE to plates to detach cells. Allow them to sit for a few minutes.
n. Use a P1000 micropipette to wash the cells off the plate with the TE and add it to the cells in the 15 mL tube.
o. Rinse the rest of the cells off with 6 mL of cold DMEM + 10% FBS and add it to the 15 mL tube with cells, then centrifuge for two minutes to pellet cells.

p. Discard the supernatant.
q. Resuspend the cells with 500 µL of cold 1x PBS and move the cell solution into a 1.5 mL microcentrifuge tube.
r. Rinse the 15 mL tube with an additional 500 µL of cold 1x PBS to retrieve any cells left and add it to the same microcentrifuge tube
s. Pellet the cells by centrifugation with 5 000 rcf for 2 minutes, then discard the supernatant. Store the cell pellet in a freezer until time to lyse.

2.2.8 Cell lysis

The cells were harvest from 15 cm diameter cell culture plates, described above and pelleted by centrifugation. The pellets were stored at -20°C until needed. During the cell lysis steps, cell pellet was kept on ice. The following steps were used to lyse the pellets:

a. Make a 1x RIPA/1x PIC Buffer from frozen stock supplies of 10x RIPA and 100x PIC and dilute with millipore water.
b. Resuspend the cell pellet in 600 µL of 1x RIPA/1x PIC Buffer and incubate on ice for 30 minutes.
c. Centrifuge the samples at 12 000 rcf for 10 minutes at 4ºC.
d. Transfer the supernatant to a new tube. This is the soluble fraction that will be used throughout future tests. The remaining pellet comprises the insoluble fraction and is frozen for later uses.

2.2.9 Sequential immunoprecipitation (IP) of the soluble fraction

As APP is able to be cleaved into a multitude of different variants, a sequential IP was used to help isolate some of the larger populations of amyloid peptides after protein determination was completed using the Total Protein Kit, Micro Lowry, Peterson's Modification. All IPs were set up in triplicate, with two sets containing 300 µg, one to use to test for Aβ using a urea gel and one to test for any interactions between SERT and Aβ using a 10% SDS-PAGE gel. The lysis protocol used allows proteins to remain in their typical conformation, also maintaining the integrity of interactions between proteins. Because of this, an antibody can be used to pull out Aβ then probing for SERT to detect any interactions. The third replica was set up with 100 µg of protein to look for

the levels of sAPPα using a 10% SDS-PAGE gel. The first step of the sequential IP uses a C-Term antibody to pull out full length APP, C99, C83, and AICD fragments. The following step uses 6E10, which binds amino acids 1-17, and pulls out Aβ and sAPPα.

The following steps were used to begin the C-Term IP:

a. Add the volume of the soluble fraction necessary for 300 µg or 100 µg to 1x RIPA/1x PIC Buffer for a final volume of 400 µL.
b. For the samples with 300 µg, add 4.5 µL of the C-Term antibody diluted 1 in 4 in 5% BSA in 1x RIPA/1x PIC Buffer and 60 µL of 50% slurry of Protein A sepharose beads. To the samples with 100 µg of protein, add 1.5 µL of the C-Term antibody diluted 1 in 4 in 5% BSA in 1x RIPA/1x PIC Buffer and 20 µL of 50% slurry of Protein A sepharose beads.
c. Vortex and leave to rotate overnight at 4ºC.
d. The following day centrifuge the samples at 5 000 rcf for 2 minutes at 4ºC.
e. Transfer the supernatant into a new microcentrifuge tube for the 6E10 IP and store in the 4ºC fridge until it is set up.
f. Wash the beads with 500 µL of HNTG buffer, vortex, and centrifuge at 5 000 rcf for 2 minutes.
g. Discard the supernatant and repeat step f twice, so that three washes have been completed
h. For the final wash removal, use a 30-gauge needle to remove the remainder of the HNTG buffer off the beads
i. Add 20 µL of 2x Laemmli buffer to the beads and vortex. Freeze the samples until they are run on gels.

The 6E10 IP follows a very similar procedure as used for the C-Term IP. The supernatant from the 300 µg C-Term IP had 4.5 µL of 6E10 antibody and 60 µL of 50% slurry of Protein G sepharose beads added. The supernatant from the 100 µg IPs receive 1.5 µL 6E10 antibody and 20 µL 50% slurry of Protein G sepharose beads. Vortex the samples and leave them to rotate overnight at 4ºC. The wash steps are the same as described above for the C-Term IP.

2.2.10 Immunoprecipitation from media

To measure the levels of Aβ in the media, a 6E10 IP was performed using the following steps:

a. Add 9.0 µL 6E10 antibody and 60 µL of 50% slurry of Protein G sepharose beads to the media.
b. Vortex the tubes and put the samples on a rotator overnight at 4ºC.
c. The following day centrifuge the samples at 5 000 rcf for 5 minutes, then transfer the supernatant to a new tube to save.
d. Use 500 µL of HNTG buffer to resuspend the beads and transfer them to a microcentrifuge tube.
e. Use an additional 500 µL of HNTG buffer to rinse the tube and add it to the same microcentrifuge tube and vortex.
f. Centrifuge the samples at 5 000 rcf for 2 minutes then remove the supernatant.
g. Repeat the washes with 1.0 mL two more times for a total of three washes.
h. Use a 30-gauge needle to remove the remaining buffer from the beads.
i. Add 20 µL of 2x LB to the samples and vortex. Freeze the samples until they are run later.

2.2.11 Western Blotting

2.2.11.1 Antibodies

Full length APP was detected in cell lysate using a mouse anti-APP antibody, 22C11. This antibody binds to the N-terminus spanning amino acid residues 66 to 81 and can detect three forms of APP; immature at 110 kDa, sAPPα at 120 kDa, and the mature form at 130 kDa[173]. The immature APP species is N-glycosylated while the mature species of APP is N- and O-glycosylated and has a sulfated tyrosyl residue, causing its molecular weight to be higher.

The soluble N-terminal fragment of APP, i.e. sAPPα, was identified using the 22C11 antibody. First cell lysates were immunodepleted with an antibody that binds to the C-terminus of APP. This removes full length APP and the C-terminal C99, C83, and AICD fragments by binding to amino acid residues 66-81. As sAPPα lacks the C-terminus epitope, this peptide remains in the supernatant.

As Aβ peptides also lack the C-terminus epitope, they also remain in the supernatant and can be immunoprecipitated using the mouse monoclonal 6E10 anti-Aβ antibody. 6E10 binds to the N-terminal spanning amino acid residues 1 to 17.

SERT levels were detected in resolved cell lysates with a rabbit polyclonal anti-SERT antibody. SERT from Biorbyt binds to amino acid residues 411-490 of the human transporter.

The secondary used to detect all the mouse primary antibodies was anti-mouse in the 800 infrared dye channel to be visualized with LICOR. The antibody is used at a dilution of 1:20 000.

The secondary used to detect rabbit antibodies was anti-rabbit in the 800 infrared dye channel, visualized using LI-COR. This antibody was used at a dilution of 1:20 000.

2.2.11.2 Urea/SDS-PAGE Protocol

Urea/SDS-PAGE gels are composed of three separate layers: the comb gel, stacking gel, and the resolving gel. Table 1 in Appendix A displays the constituents that the gels are composed of. The protocol to make and run these gels is as follows:

a. Dissolve the urea in separation buffer and 40% acrylamide overnight in a 10 mL flask on a stir plate at RT.
b. The following day add 10% SDS and gently mix.
c. Add 10% APS, made fresh on the day the gel is cast, and TEMED in sequence with mixing in between.
d. Pour 3900 µL of the resolving gel for each plate with 1.0 mm spacers, then pipette a thin layer of H_2O saturated butanol on top to remove bubbles and make the top of the gel level.
e. Once solidified, rinse off the butanol with dH_2O and allow it to dry before the next layer is poured.
f. Combine all components of the stacking gel and mix, then add the 10% APS and TEMED, with mixing between. Immediately pour 900 µL of the stacking gel above the resolving gel along with a layer of butanol.
g. After the stacking gel has solidified, rinse the butanol off with dH_2O.
h. Combine the components for the comb gel, adding 10% APS and TEMED last with mixing between, and pour to the top of the plates and place the comb quickly after.
i. Once completely solidified, rinse the plates with dH_2O and gently remove the comb.

j. Set the unit up with the plates cast that day. Add 1X Cathodic Buffer (0.2 M Bicine + 0.1 M NaOH + 0.25% SDS as final concentrations made from 32.6 g Bicine + 4 g NaOH + 2.5 g SDS in 1000 mL ddH_2O) to the inner chamber and 1x Anodic buffer (2.0 M Tris + 0.5 M H_2SO_4 as final concentrations made from 242 g Tris + 27.8 mL H_2SO_4 in 1000 mL ddH_2O) to the outer chamber.
k. Load the appropriate volume of sample and Specter Low Range ladder, run the gels at 15 mA per plate for roughly three hours.
l. Once the gels have finished running, transfer in Transfer Buffer at 65 mA for two hours.
m. Briefly move the membranes to dH_2O, then boil in a petri dish with 100 mL of 1x PBS for 3 minutes.
n. After boiling, block the membranes with 5% milk in 1x TBS for 1 hour.
o. Wash the membranes three times for roughly 10 minutes each in 1x TBST to remove excess blocking solution.
p. Probe the membranes in the primary antibody overnight at 4ºC on a rocker.
q. The following day wash the membranes three times for roughly 10 minutes each in 1x TBST.
r. Probe the membranes in the appropriate secondary antibody at RT for 1 hour on a rocker.
s. Wash the membranes three times for roughly 10 minutes each in 1x TBST then visualize using LI-COR.

The samples, roughly 25 µL, were resolved alongside 5 µL of Specter Low Range Ladder. The type of gel and concentration of primary used to probe are described in the corresponding figure legend to the experiment run.

When visualizing with LI-COR, the settings used are an intensity of 10.0, quality of low, and resolution of 84nm using the 800 channel.

To save membranes for a later use, they are bagged in 1x TBS and stored at 4ºC.

2.2.11.3 SDS-PAGE

Western blots are composed of two layers: the stacking gel and the resolving gel. The components of the gels are displayed in Table 2 of Appendix A. The protocol to make and run these gels is as follows:

a. Combine the components of the resolving gel and gently mix.
b. Add 10% APS, made fresh on the day the gel is cast, and TEMED in sequence with mixing in between.
c. Pour 4300 µL of the resolving gel for each plate with 1.0 mm spacers, then pipette a thin layer of H_2O saturated butanol on top to remove bubbles and make the top of the gel level.
d. Once solidified, rinse off the butanol with dH_2O and allow it to dry before the next layer is poured.
e. Combine all components of the stacking gel and mix, then add the 10% APS and TEMED, with mixing between. Immediately pour the stacking gel to the top of the plates and place the comb quickly after.
f. Set the unit up with the solidified plates cast that day. Add 1X Running Buffer (25mM Tris HCl + 192 mM Glycine + 0.1% SDS as final concentrations made from 30.3 g Tris Base + 144.0 g Glycine + 10 g SDS to a total volume of 1.0 L in dH_2O, then diluted 1 in 10 with dH_2O) to the inner and outer chambers.
g. Load the appropriate volume of sample and PageRuler Prestained Protein ladder, run the gels at 50 V for 30 minutes then at 180 V for roughly another hour for completion.
h. Once the gels have finished running, transfer in Transfer Buffer (25 mM Tris HCl + 192 mM Glycerol + 3.75% SDS + 20% MeOH as final concentrations made from 12 g Tris Base + 57.6 g Glycine + 150 mg SDS + 800 mL Methanol diluted to a volume of 4 L with dH_2O) at 230mA for 90 minutes.
i. Block the membranes with 5% milk in 1x TBS for 1 hour.
j. Wash the membranes three times for roughly 10 minutes each in 1x TBST to remove excess blocking solution.
k. Probe the membranes in the primary antibody overnight at 4ºC on a rocker.

l. The following day wash the membranes three times for roughly 10 minutes each in 1x TBST.
m. Probe the membranes in the appropriate secondary antibody at RT for 1 hour on a rocker.
n. Wash the membranes three times for roughly 10 minutes each in 1x TBST then visualize using LI-COR.

The samples, roughly 25 µL, were resolved alongside 5 µL of PageRuler Prestained Protein Ladder. The type of gel and concentration of primary used to probe are described in the corresponding figure legend to the experiment run.

As with the urea/SDS-PAGE gels, the regular WBs were also visualized with LI-COR, at an intensity of 10.0, quality of low, and resolution of 84nm using the 800 channel.

To save membranes for a later use, they are bagged in 1x TBS and stored at 4ºC.

2.2.12 Statistical analyses using SPSS software

2.2.12.1 Kaplan-Meier Test

As the data points from the paralysis assays can be statistically analyzed similarly to survival curves, the Kaplan Meier test was used to determine whether the type of drug treatment altered the rate of paralysis associated with Aβ accumulation in control animals (CL2122), $A\beta_{3-42}$-producing worms (CL2120), and $A\beta_{1-42}$-producing worms (GMC101). If a difference was seen between the vehicle, 1µM and 10µM, additional Kaplan-Meier tests were used to compare two treatments at a time using a corrected α of 0.0167.

2.2.12.2 Kruskal Wallis and Mann Whitney U Tests

The data collected from the thrashing assays was not normally distributed (forming a bell-shaped, symmetrical curve around the mean), thus a Kruskal Wallis and subsequent Mann Whitney U post-hoc tests were used to determine whether each treatment (vehicle, 1µM Fluoxetine or nor-Fluoxetine, or 10 µM Fluoxetine or nor-Fluoxetine) had different effects on the thrashing behaviour of *C. elegans*. Mann Whitney U tests were utilized to analyze the groups pairwise using a corrected value of $\alpha = 0.0125$ as each set of data was compared four times.

3 Results

3.1 Fluoxetine does not influence Aβ-associated paralysis in *C. elegans*.

The effects of the SSRI, Fluoxetine, on modulating Aβ accumulation was initially investigated using a paralysis paradigm. Increasing Aβ production in muscle cells of transgenic *C. elegans* (CL2120 and GMC101) results in a progressive paralysis phenotype[155,165]. Measurement of the percentage of paralyzed animals as a function of time can therefore be a useful, albeit indirect, assessment of Aβ accumulation. When plotted on a curve, these rates provide a dynamic picture of Aβ toxicity. If Fluoxetine can alter the rate of Aβ production or accumulation in these worms, it follows that paralysis rates will likely reflect this effect. For instance, a precipitated spike in paralysis as indicated by reaching 50% of paralyzed (50p) worms at an earlier time-point than that observed for untreated controls would suggest that Fluoxetine potentiates Aβ accumulation. Conversely, a delay in reaching 50p on a paralysis curve would be consistent with a protective role for this drug.

Using this experimental approach, worms treated with either a vehicle or one of two concentrations of Fluoxetine were scored for complete paralysis, *i.e.* when no central body movement is detectable. In these assays, GMC101 ($A\beta_{1-42}$) and CL2120 ($A\beta_{3-42}$) populations displayed a profile of increasing paralysis overtime that agrees with previous reports[155] (Figure 7). As indicated in the paralysis curves in Figure 7A and 7C and demonstrated by calculating the relevant *P* values in Table 1 in Appendix B, Fluoxetine treatment did not significantly skew the paralysis response of worms expressing Aβ peptides in muscle tissue.

A factor potentially interfering with these results relates to the metabolism of Fluoxetine to nor-Fluoxetine by live *E. coli*. The direct role of nor-Fluoxetine in the context of the paralysis assay must therefore be separately addressed (*see* Section 3.2, below) as it possibly contributes (acts in synergy with Fluoxetine) or masks (competes for binding with Fluoxetine) Aβ accumulation in these backgrounds. Nor-Fluoxetine is also the major Fluoxetine metabolite in humans, suggesting that bacterially-processed Fluoxetine could be altering the molar ratio of these SSRIs compounds on plates and potentially altering the behavioural responses observed in these assays[174]. To avoid this potential confound, Fluoxetine was added to bacterial lawns made of dead *E. coli*. In these plates, bacterial contribution to nor-Fluoxetine concentrations at the expense of Fluoxetine inputs should not be a factor.

Interestingly, when comparing the motility responses of worms exposed to Fluoxetine on live *versus* dead *E. coli* lawns, noticeable differences in the rate of paralysis could be observed (Figure 7). When the drug was delivered on live *E. coli* food the 50p time-point was reached at 32 hours in vehicle-treated $A\beta_{3-42}$-producing animals (CL2120) as compared to 34 hours in Fluoxetine treated CL2120 worms, where the vehicle treated worms continue to worsen until the final time-point of 42 hours while the Fluoxetine treated plateaued (Figure 7A; $P = 0.241$), indicating a potential protective effect of Fluoxetine on Aβ accumulation. However, the same treatments when repeated on a heat-killed bacteria substrate, resulted in a premature paralysis of Fluoxetine-treated CL2120 worms when compared to control (Figure 7C; $P = 0.355$) suggesting that the delay in paralysis establishment of the genetically identical worms growing on live, metabolizing bacteria plates may be accounted by a reduced Fluoxetine intake, higher nor-Fluoxetine concentrations, the presence of another Fluoxetine metabolite or several of these factors in combination. It is important to note that as the data were not statistically different no conclusion can be made.

With respect to the $A\beta_{1-42}$-producing worms (GMC101), and consistent with previous reports[155] implicating more robust accumulation of $A\beta_{1-42}$ in AD, paralysis rates were generally higher in early time-points as compared to CL2120 worms (comparing Figure 7A to 7B and 7C to 7D). However, the perceived effect of bacteria substrates insofar as modulating paralysis rates observed for CL2120 worms was not reproducible in GMC101 animals; whether Fluoxetine was delivered in live or dead bacteria did not seem to alter the overall paralysis response as compared to untreated $A\beta_{1-42}$ expressing worms (comparing Figure 7B and 7D). These results could represent intrinsic differences between the Aβ peptides, though the lack of statistical significance between these datasets more likely reflect sample specific variations. In addition, a concentration-dependent effect could not be found between the 1 µM and 10 µM Fluoxetine treatments (Table 1 of Appendix B).

3.2 Nor-Fluoxetine does not influence Aβ-associated paralysis in *C. elegans*.

Nor-Fluoxetine, a by-product of Fluoxetine metabolism, has a much longer half-life than its parent compound[147]. As nor-Fluoxetine has a slower turnover rate in the body, it could have clinically relevant roles in explaining outlasting or delayed effect of SSRI treatment, particularly with respect to Aβ toxicity in patients with a chronic, lifelong use of SSRIs. To dissect the consequence of nor-Fluoxetine exposure to Aβ accumulation in *C. elegans*, the paralysis assay

protocol performed for Fluoxetine (*see* Section 3.1) were repeated using pure nor-Fluoxetine added to plates with live and dead bacteria (Figure 8).

Despite the lack of solid evidence in support of a significant effect of Fluoxetine and nor-Fluoxetine in paralysis rates, some interesting observations suggest that these two drugs may have an additive effect. Treating GMC101 worms with different concentrations of Fluoxetine yielded similar 50p time-points, occurring at around 32-34 hours (Figure 7). When GMC101 worms growing in live *E. coli* were treated with nor-Fluoxetine these populations reached 50p 2 to 4 hours later at 36 hours, pointing to differences in the response to these related SSRIs. Interestingly, in GMC101 populations exposed to 10 µM nor-Fluoxetine on dead bacterial lawns where no source of Fluoxetine existed, 50p was reached much sooner at 32 hours than in the treatment with 1 µM Fluoxetine (50p = 42 hours) and no treatment control (50p = 42 hours) (Figure 8D). This treatment thus supports a dose-dependent role of nor-Fluoxetine in driving progressively more accumulation in $A\beta_{1\text{-}42}$ expressing worms when compared to Fluoxetine. In this interpretation, providing pure nor-Fluoxetine to worms from the start of the treatment bypasses the slower processing of Fluoxetine metabolism (by bacteria and/or worms) and nor-Fluoxetine accumulation (in worms) presumably speeding up the process of Aβ accumulation in muscle. Though an interesting possibility, these conclusions are currently not statistically supported ($P = 0.135$). Further work to reproduce these results is necessary.

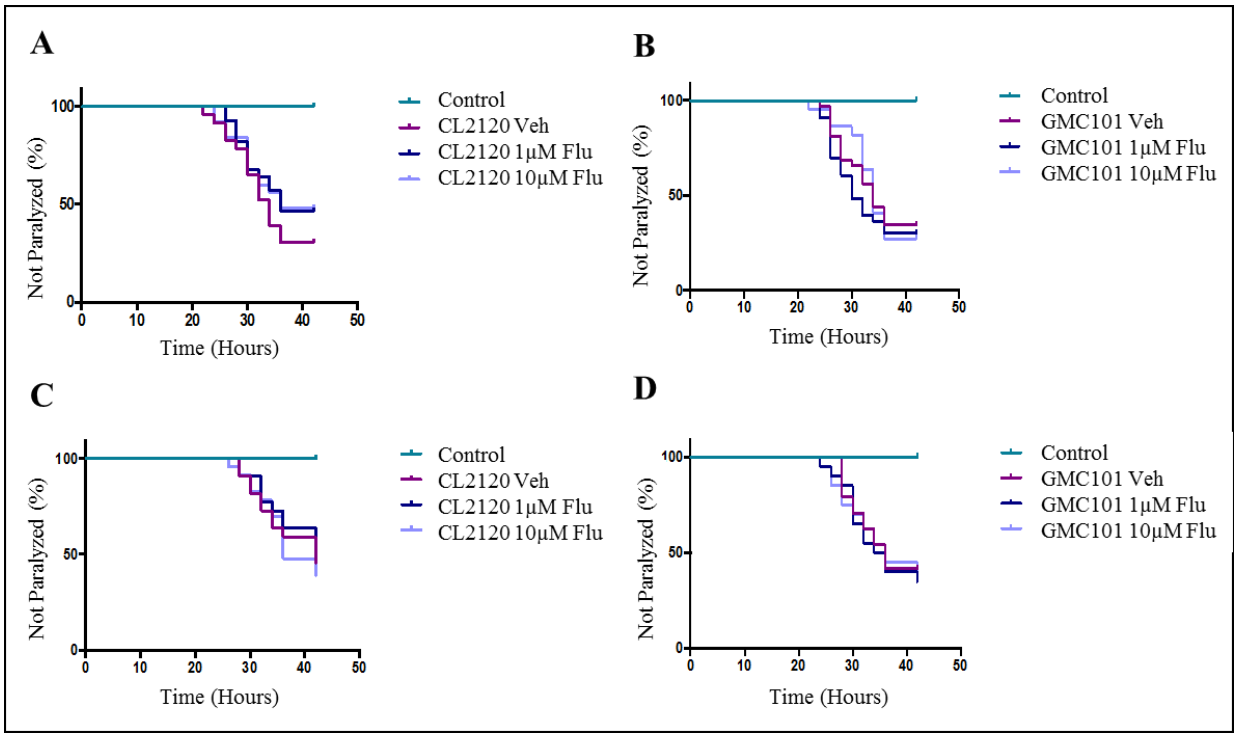

Figure 3.1: Fluoxetine does not influence Aβ-associated paralysis in $A\beta_{3-42}$ (CL2120) and $A\beta_{1-42}$ (GMC101) worms.

The control strain used for the paralysis assays is CL2122, which does not express and accumulate any form of Aβ. (A) CL2120 worms treated with live *E. coli* and Fluoxetine. (B) GMC101 worms treated with live *E. coli* and Fluoxetine. (C) CL2120 worms treated with dead *E. coli* and Fluoxetine. (D) GMC101 worms treated with dead *E. coli* and nor-Fluoxetine. All four panels show a range of paralysis trends, none of which were found to be significantly different from the vehicle treatment or the control strain.

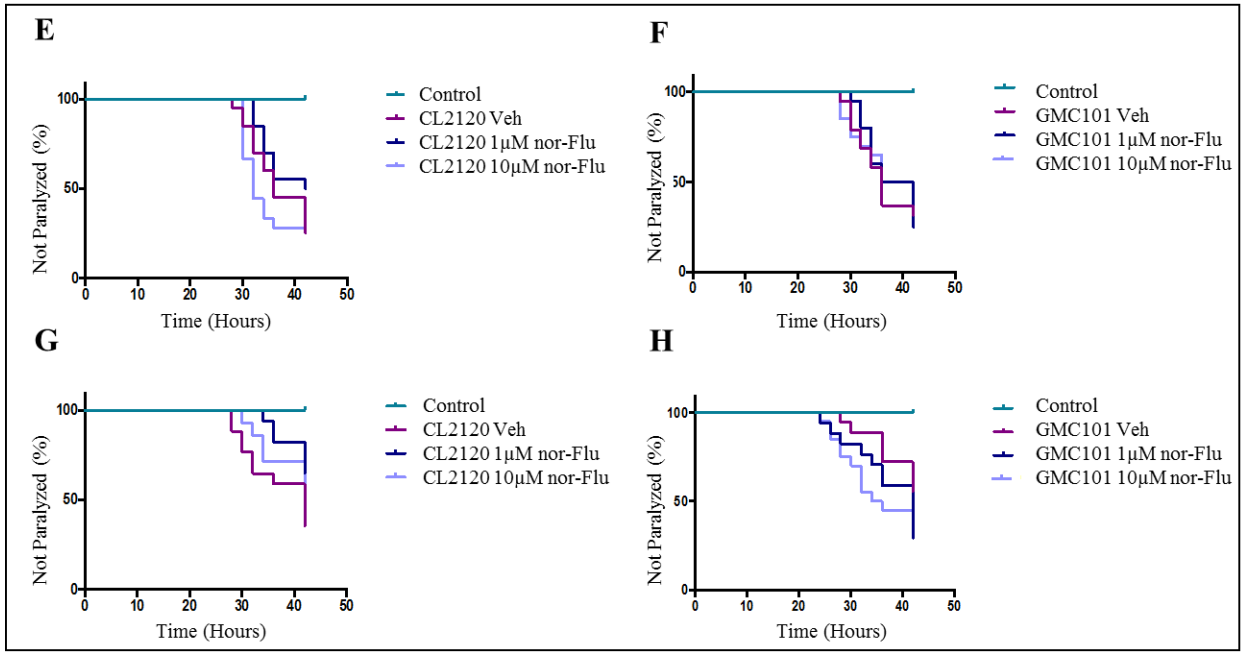

Figure 3.2: Nor-Fluoxetine does not influence Aβ-associated paralysis in $A\beta_{3\text{-}42}$ (CL2120) and $A\beta_{1\text{-}42}$ (GMC101) worms.

The control strain used for the paralysis assays is CL2122, which does not express and accumulate any form of Aβ. Panel (E) displays CL2120 worms treated with live *E. coli* and nor-Fluoxetine. (F) GMC101 worms treated with live *E. coli* and nor-Fluoxetine. (G) CL2120 worms treated with dead *E. coli* and nor-Fluoxetine. (H) GMC101 worms treated with dead *E. coli* and nor-Fluoxetine. All paralysis assays did not show any statistically significant difference between the two nor-Fluoxetine treatments and the vehicle treatment or with the control strain.

3.3 Thrashing behaviour is a better indicator of Aβ-induced paralysis in *C. elegans*.

Although the conclusion from the paralysis assays presented in Sections 3.1 and 3.2 did not support a role for Fluoxetine and nor-Fluoxetine in enhancing the Aβ-dependent paralysis phenotype in *C. elegans*, technical drawbacks of the assay have to be considered. The all-or-nothing assessment for paralyzed *versus* non-paralyzed phenotypic outcomes as proxy for muscle function does not capture slighter, more gradual loss of movement that likely occurs as the cell's capacity to process newly synthesized Aβ peptide is overcome. In this restricted scenario, the potential physiologically significant effects of SSRIs in *C. elegans* motility would not be accounted for if the time of paralytic onset was not ultimately affected. Likewise, because paralysis may not necessarily imply an endpoint in muscle function but simply a compounded effect beyond a threshold in which the remaining muscle activity is unable to propel movement, the assay equally ignores further muscle deterioration that could occur after the onset of paralysis. This assay is therefore blind to the continuum of possible physiological opportunities for Aβ regulation before and after the onset of complete paralysis and biased towards underestimating movement deterioration before paralysis while discarding the effects on left-over muscle activity after worms became immobile on the solid media. It is possible that SSRI-mediated modulation of Aβ accumulation does occur and is physiologically relevant but cannot be captured by the paralysis assay as it has been applied here. This can also be said about the thrashing assay, however, since quantifying thrashing is more sensitive to smaller differences in paralysis rate to be detected in the liquid media, and not just scored as paralyzed or not, it does offer a better alternative experiment to use.

To overcome the limitations of the paralysis assay and introduce a better quantitative assessment of the state of muscular function in Aβ expressing worms, thrashing assays were used. This assay consists of placing worms in liquid and scoring the frequency of lateral swimming. Reduced thrashing correlates with natural tissue deterioration in aging animals and has been extensively used as an index to evaluate the effects of new mutations and drugs on muscle and neuronal function[175]. Because these movements occur in a low resistant media, milder compromises in muscle function can be detected and quantified. In addition, worms perceived as paralyzed on agar plates can display residual movement observed as reduced thrashing rates in liquid, allowing for further characterization. Thus, thrashing quantification could, in principle,

resolve the issues of under- and overestimations of the consequences of Aβ accumulation in the paralysis assay used above.

As proof of concept to the suitability of using the thrashing assay for measuring Aβ-induced paralysis, the range of thrashing rates for Aβ expressing worms (CL2120 and GMC101) treated with vehicle alone were initially determined (Figure 9 and 10). As reported previously, and in contrast to the results from the paralysis assay, $A\beta_{3\text{-}42}$ worms do not show the same Aβ toxicity as seen with $A\beta_{1\text{-}42}$ peptides (observed as a reduction in thrashing throughout the time-points tested) when compared with transgenic control worms that do not produce Aβ peptides (CL2122; Figure 7), consistent with the lower Aβ accumulate potential expected in these worms[155]. The difference seen within this strain between the two assays could be from the subjectivity of the paralysis assay or due to overestimation of paralysis caused by the added resistance of the solid media that the worms were scored on. In this context, and assuming SSRIs do influence thrashing behaviour through the regulation of Aβ accumulation, no significant effect on thrashing would be anticipated in treatments with Fluoxetine or nor-Fluoxetine. Indeed, culturing CL2120 in dead bacteria substrates containing these drugs does not significantly alter the range of thrashing rates (Figure 9; $0.141 \leq P \leq 0.638$, Tables 3 and 6 in Appendix B). In contrast, $A\beta_{1\text{-}42}$ worms have been shown to accumulate Aβ and paralyze as a result[155]. Consistent with these results, GMC101 worms ($A\beta_{1\text{-}42}$) displayed a dramatic reduction in thrashing rates as compared to control animals (CL2122) in all time-points (Figure 10). Importantly, the compromise in muscle function, evidenced by reduced thrashing in $A\beta_{1\text{-}42}$ worms, is progressively and significantly worsened in later time-points (comparing vehicle treated GMC101 datasets in Figure 10A and 10D; $P < 0.001$) demonstrating a dose-dependent effect of Aβ in the reduction of thrashing behaviour. Together, the results with vehicle treated CL2120 (Figure 9) and GMC101 (Figure 10) worms reveal in more detail the dynamics of paralysis derived from Aβ production and accumulation in muscle cells and validates the use of this experimental approach to re-test a role of SSRIs in these processes.

3.4 Fluoxetine and nor-Fluoxetine exacerbate the reduction in thrashing in $A\beta_{1\text{-}42}$-expressing worms.

To investigate whether SSRIs could disturb the normal kinetics of paralysis observed in $A\beta_{1\text{-}42}$ worms, Fluoxetine and nor-Fluoxetine were added to dead bacteria and fed to GMC101 worms. The thrashing behaviour of these worms was recorded at different time-points of adult life,

all chosen before complete paralysis transpires (reported previously to occur by 48 hours after being shifted to 25°C[155]) and compared to the response of control animals that did not express any Aβ peptide (CL2122). As observed in Figure 10, treatment with SSRIs leads to a substantial shortening of the time in which clear effects on movements can be detected in GMC101 worms, with animals showing a detectable reduction in thrashing behaviour already at 18 hours (Figure 10A), at a time when no overt paralysis was observed in the paralysis assay (*see* Figure 7D). This finding supports the limitations of the paralysis assay insofar as assessing pre-paralysis compromise in thrashing of Aβ expressing worms, as suggested above. While treatment with Fluoxetine and nor-Fluoxetine resulted in a significant reduction in thrashing rates relative to control worms in all time-points tested, for the most part and with the exception of the 18 hour time-point (Figure 10A, Tables 4 and 7 in Appendix B), these effects were not dose-dependent (Figure 10B, 10C, and 10D). One possible explanation for these results considers that the only two doses tested (1 µM and 10 µM) may not cover the necessary range to induce detectable variation given the limited resolution of the paralysis assay. A final assessment of whether increasing Fluoxetine concentrations can impact protein aggregate loads in these cells should be performed by testing $A\beta_{1-42}$-expressing worm lysates using Western Blots (WBs). These animals have been collected, but not processed at this time. Finally, comparisons between Fluoxetine and nor-Fluoxetine-induced reduction in thrashing failed to reveal any significant differences. It appears that both compounds have a similar bioactive role in limiting movement presumably because of increased Aβ accumulation or oligomerization in muscle cells. Considering the shared chemical properties of these compounds, it is likely that both act on the same target to regulate Aβ expression, accumulation, or processing. Under the hypothesis of this thesis, this mechanism could involve co-opting the serotonin transport system (*see* below). However, it is also possible that these SSRIs act synergistically in different pathways. Controlled assays providing different molar ratios of Fluoxetine/nor-Fluoxetine to Aβ-expressing worms in thrashing assays would be important to dissect possible functional interaction of these drugs, an important and clinically relevant aspect of this analysis considering the co-existence of these molecules in patient's brains.

Overall, the results presented in this section support a role of SSRIs as potentiators of Aβ-mediated toxicity in a transgenic model organism and point to important limitations of using the paralysis assay on solid surfaces for quantitative measurements of Aβ-driven paralysis. In line with

these findings, thrashing counts on animals grown on heat-killed *E. coli* were used henceforth to investigate the downstream effectors of SSRIs in worms.

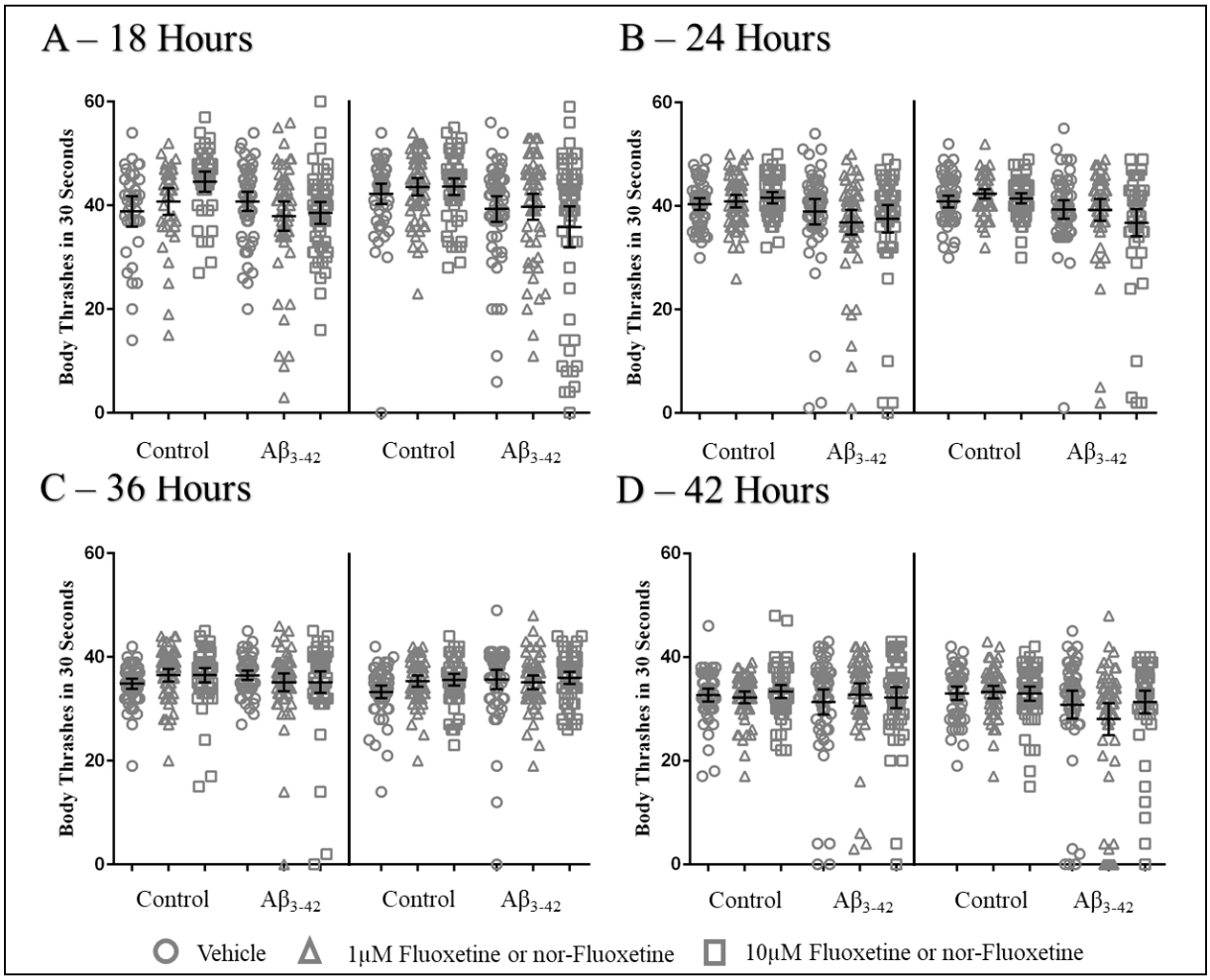

Figure 3.3: Fluoxetine or nor-Fluoxetine do not influence thrashing in Aβ3-42-expressing worms.

The data on the left side of the graphs represent worms treated with Fluoxetine and that on the right side were treated with nor-Fluoxetine and the error bars represent the 95% confidence interval. The "Control" data is collected for worms that do not produce Aβ (CL2122). Each strain and treatment combination represent the thrashing of ≤ 60 worms. Panel (A) represents the thrashing data collected after 18 hours of treatment, (B) is the data after 24 hours of treatment, (C) shows the data after 36 hours of treatment, and (D) is the thrashing data after 42 hours of treatment. At all time-points, Fluoxetine and nor-Fluoxetine treatment did not cause a significant difference in thrashing compared to the vehicle treatment in CL2120 ($A\beta_{3-42}$) worms. The vehicle used in the thrashing assays was dead *E. coli*.

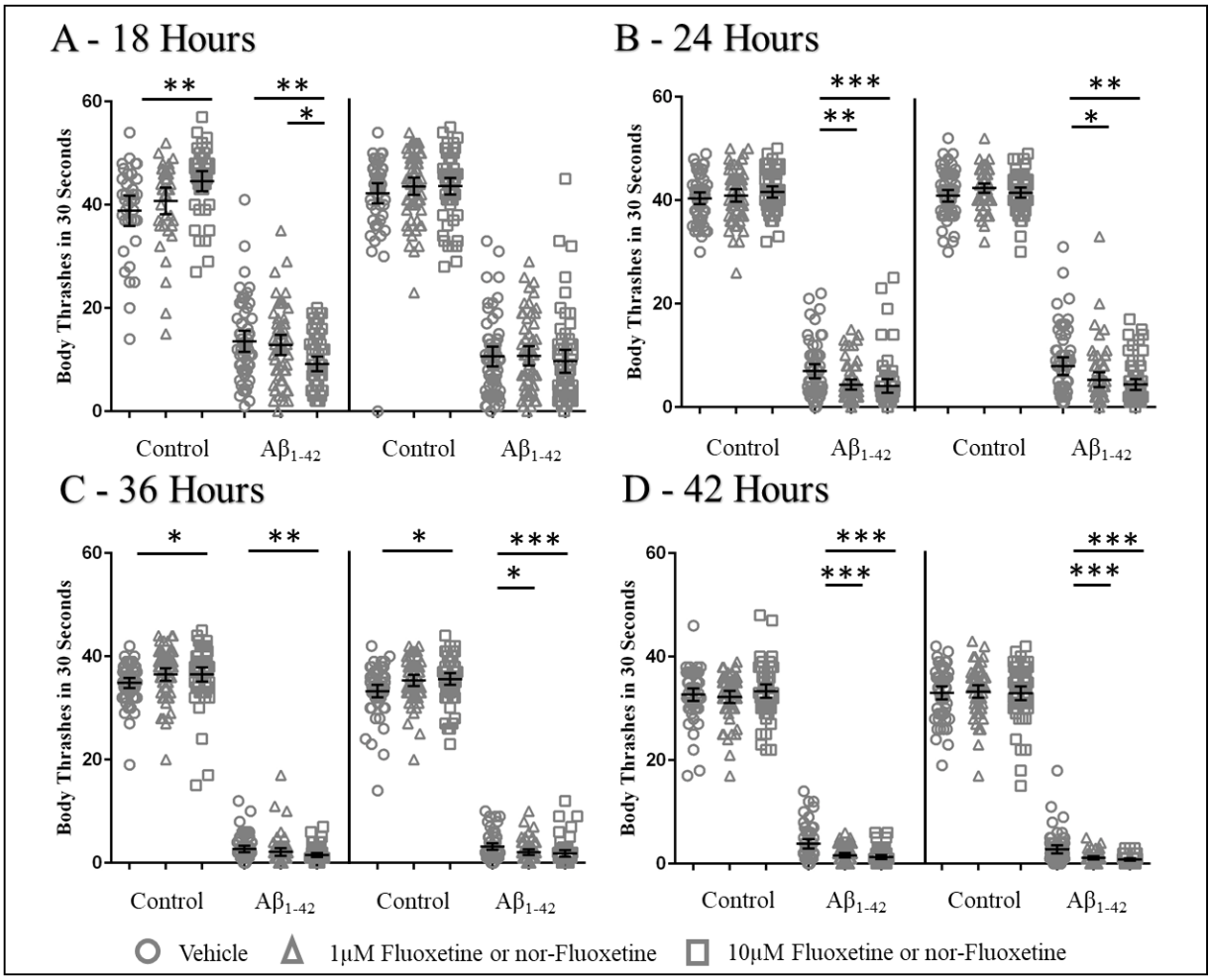

Figure 3.4: Fluoxetine and nor-Fluoxetine exacerbate the reduction in thrashing in Aβ$_{1-42}$-expressing worms.

The data presented on the left side of the graphs are worms treated with Fluoxetine and the right side are those treated with nor-Fluoxetine and the error bars represent the 95% confidence interval. The data presented in Figure 9 are from worms treated and tested at the same time as the data displayed in this figure, with the "Control" (CL2122) data being from the same worms. Each strain and treatment combination represent the thrashing of ≤ 60 worms. Panel (A) represents the thrashing data collected after 18 hours of treatment, (B) is the data after 24 hours of treatment, (C) shows the data after 36 hours of treatment, and (D) is the thrashing data after 42 hours of treatment. The vehicle used in the thrashing assays was dead *E. coli*. After 24, 36, and 42 hours, a statistically significant difference is seen between the GMC101 (Aβ$_{1-42}$) worms treated with the vehicle and 10μM of Fluoxetine or nor-Fluoxetine. At the same time-points as above there is also a difference between the vehicle and 1μM of Fluoxetine and nor-Fluoxetine, except at 36 hours. However, there are also no differences found between the 1μM and 10μM treatments after 18 hours. One asterisk denotes $0.0167 > P > 0.001$, two asterisks represent $P = 0.001$, and three asterisks show a significance level of $P < 0.001$.

3.5 SERT/MOD-5 is required for Fluoxetine/nor-Fluoxetine-dependent exacerbation of thrashing reduction in Aβ expressing worms.

SSRIs promote serotonergic signalling by inhibiting postsynaptic serotonin uptake from synaptic clefts/neuromuscular junctions through binding to SERT, the ionotropic serotonin transporter on the membrane of neurons. Moreover, hypersensitivity to exogenous serotonin can lead to paralysis in worms through regulation of acetylcholine release in synapses. Deregulation of endogenous serotonin transport induced by SSRI treatment alone, however, cannot explain the reduced thrashing behaviour observed in GMC101 worms, since this effect required Aβ expression (*see* the unaffected thrashing behaviour of CL2122 worms treated with SSRIs in Figure 9 and 10). Alternatively, SERT has been proposed to bind and export other substrates, particularly α-synuclein[163], supporting a role of this transporter on diminishing the load of neurotoxic peptides. In this scenario, impairment of SERT-mediated transport using SSRIs may hinder the cell's ability to remove Aβ peptides resulting in the formation of Aβ accumulates and, in the worm model, exacerbating the reduction in thrashing behaviour.

Using clinically relevant drugs to treat the worms not only allows for translational relevance of these data, but, because of known pharmacology of these drugs, we can assume that they are acting on the worm analogue of SERT, MOD-5. However, there is always the possibility that these drugs, or any other drug, is eliciting an effect that is "off-target", *i.e.* not acting through its expected target and mechanism. To test the possibility that SERT/MOD-5 mediates the sensitivity to Fluoxetine and nor-Fluoxetine in the context of muscle function in GMC101 worms, animals expressing $A\beta_{1-42}$ (*dvIs100*) in a null *mod-5* background (*n3314*) were generated. MOD-5, the *C. elegans* SERT homolog, is expressed in motor neurons and is required for synaptic inhibition at neuromuscular junctions[176]. Importantly, MOD-5 has also been demonstrated to be a target of Fluoxetine in worms[167]. Thus MOD-5 appears to be present in the right place and have chemical affinity for SSRI ligands, both of which are requirements if this transporter is indeed behind the enhanced thrashing reduction observed in GMC101 worms. This theory is supported by evidence from Kullyev and colleagues where they showed that serotonin could not be detected in neurons with serotonin transporters in worms treated with Fluoxetine[177]. If Fluoxetine and nor-Fluoxetine act by antagonizing MOD-5-dependent Aβ export in these cells, genetic depletion of *mod-5* should replicate the phenotypes triggered by the pharmacological inhibition of this transporter using SSRIs, as characterized above for GMC101 worms. Indeed, in the absence of

SSRI treatment, depleting *mod-5* in $A\beta_{1-42}$ (CEC215) using a null mutation (*n3314*) resulted in statistically significant reduction in thrashing behaviour compared to GMC101 animals at all four time-points tested ($P < 0.001$, Table 8 of Appendix B), suggesting that lack of MOD-5 activity is sufficient for the exacerbated reduction in thrashing observed upon SSRI treatment (Figure 11). As confirmed throughout these assays, the reduction in thrashing requires the *dvIs100* ($A\beta_{1-42}$) transgene expressing in muscle, such that *mod-5* mutants alone are expectedly wildtype insofar as thrashing behaviour (Figure 11). Transporter as well as ligand are thus necessary to yield the paralysis phenotype. Presumably, binding of Fluoxetine and/or nor-Fluoxetine to MOD-5 in $A\beta_{1-42}$ (GMC101) worms to saturation levels could inactivate the transporter, leading to a comparable MOD-5 depleted phenotype that is achieved in an actual *mod-5* mutant. It follows that the reduction in thrashing behaviour observed in untreated *mod-5*;$A\beta_{1-42}$ (CEC215) worms (Figure 11) should not only be significantly more robust than in $A\beta_{1-42}$ (GMC101) animals but also similar to the rates observed in $A\beta_{1-42}$ worms treated with Fluoxetine and/or nor-Fluoxetine (Figures 9 and 10). When directly compared, CEC215 worms do not show a statistically significant difference in thrashing behaviour ($P \geq 0.092$), supporting the above hypothesis.

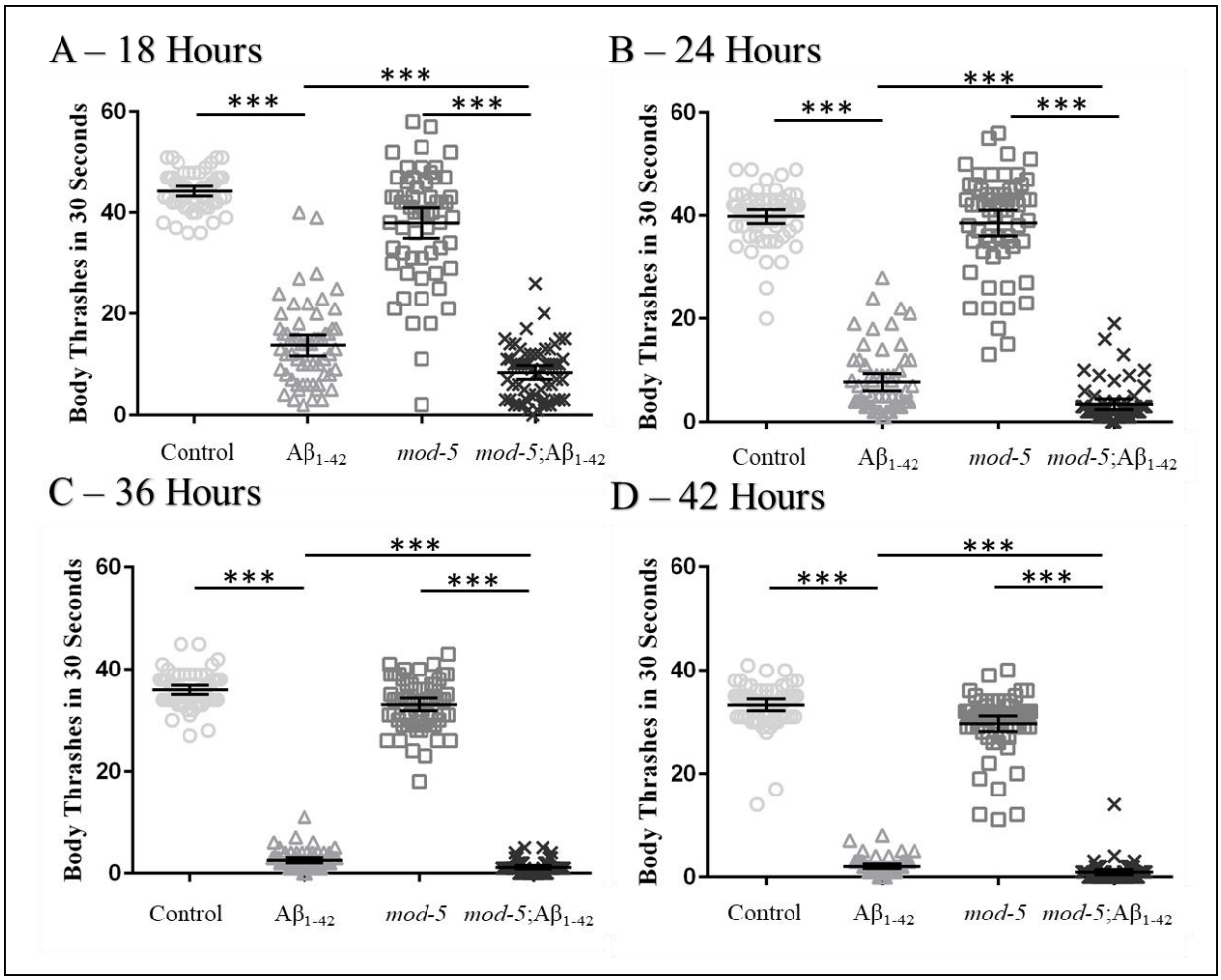

Figure 3.5: A non-functional MOD-5 exacerbates the reduction in thrashing in Aβ3-42-expressing worms.

Sixty worms of each strain were scored at each time-point in a thrashing assay to study the role of the serotonin transporter in the paralysis phenotype. The "Control" data is collected for worms that do not produce Aβ (CL2122). Panel (A) represents the thrashing data collected after 18 hours of treatment, (B) is the data after 24 hours of treatment, (C) shows the data after 36 hours of treatment, and (D) is the thrashing data after 42 hours of treatment. Three asterisks show a significance level of $P < 0.001$.

3.6 Serotonin is dispensable for MOD-5/SSRI-mediated regulation of Aβ-induced paralysis.

SSRIs were developed to increase the availability of serotonin, but there is always the possibility that a phenotype seen could be serotonin-independent and, indeed, serotonin-independent functions of SSRIs have been reported in worms. For instance, while serotonin is required for SSRI-induced hyperenhanced slowing response, *mod-5* mutants exposed to high concentrations (2.9 mM) of Fluoxetine display contraction of nose muscles followed by paralysis, suggesting that these compounds have alternative targets aside from the canonical serotonin transporter[167]. Conceivably, serotonin displacement to the cleft in *mod-5*;Aβ_{1-42} mutants could in itself impact intracellular Aβ loads indirectly. If serotonin is at all involved in Aβ toxicity observed in Aβ_{1-42} worms, for instance, the reduced thrashing phenotype in these animals should be suppressed or heightened by genetically eliminating serotonin signalling in the neuromuscular junction. This hypothesis was tested by producing a *tph-1*;Aβ_{1-42} (CEC218) that is impaired in serotonin production, but has normal MOD-5 mediated transport. As indicated in Figure 12, *tph-1(mg280)* mutants showed a range of thrashing responses significantly different than the control CL2122 worms that do not express Aβ peptides at all time-points except 18 hours ($P \leq 0.006$, Table 9 in Appendix B). Although this contradicts a previous report that swimming behaviour is not affected by impairment in serotonin production (*tph-1*) or transport (*mod-5*)[178], when looking at the distribution of the data points the difference observed appears to be between the range of the two data sets, with worms showing both more and less thrashing behaviour than the controls, and the 95% confidence intervals overlap each other at all time-points except at 42 hours (Figure 12; $P < 0.001$). When *tph-1* is introduced in Aβ_{1-42} expressing worms, however, a pattern of thrashing rates consistent with that observed for Aβ_{1-42} (GMC101) worms is present in all four time-points tested (Figure 12; $0.021 \leq P \leq 0.594$, Table 9 in Appendix B). These results suggest that the absence of endogenous serotonin delivered to the neuromuscular junction by motor neurons does not disrupt the kinetics of Aβ accumulation in muscle cells and supports the conclusion that serotonin-independent roles of MOD-5, presumably exacerbated by SSRI treatment, mediate Aβ toxicity in this model.

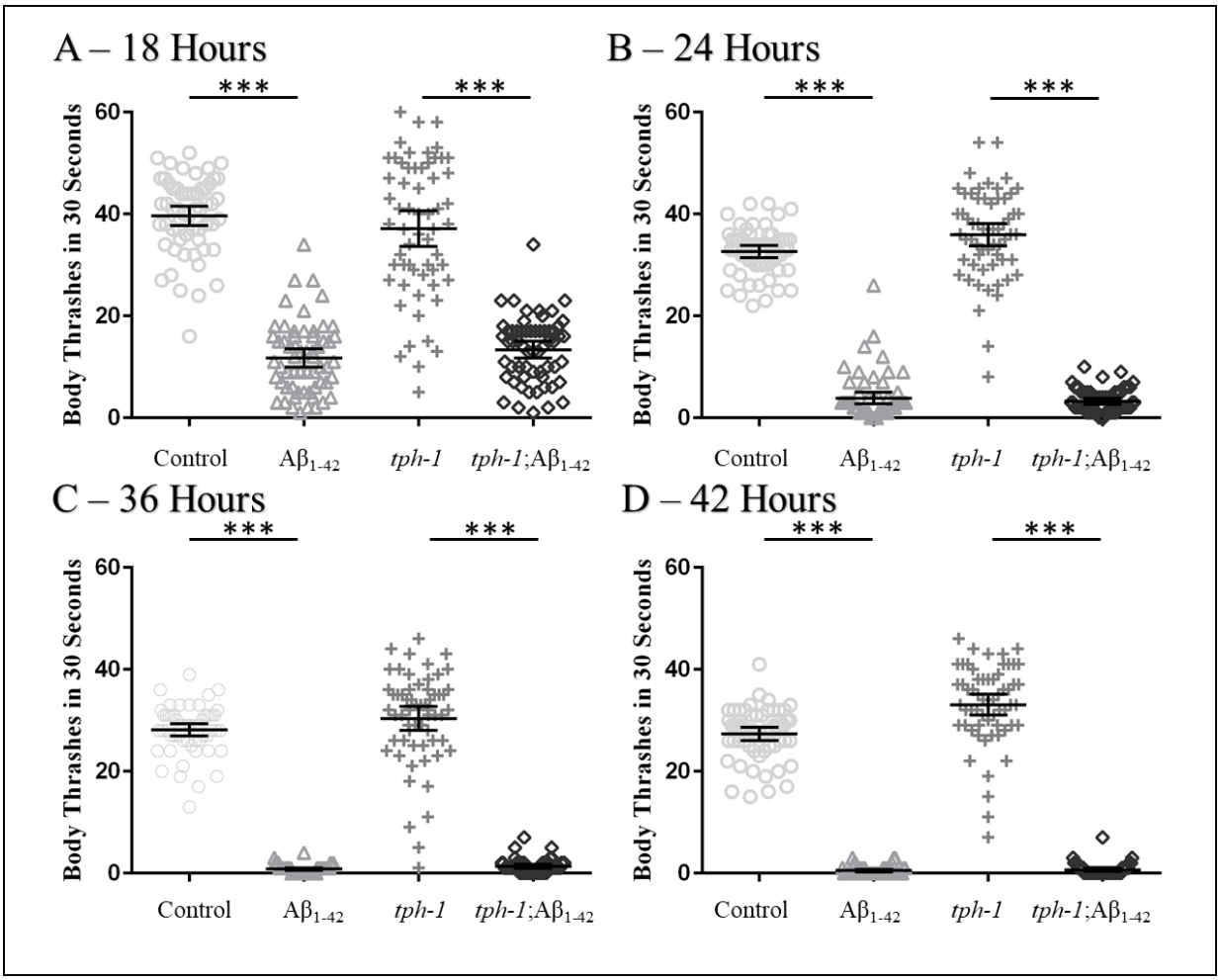

Figure 3.6: A non-functional TPH-1 does not alter the reduction in thrashing in Aβ3-42-expressing worms.

The thrashing behaviour was compared to determine whether any changes in the availability of serotonin would influence thrashing behaviour. Sixty worms of each strain were tested. The "Control" data is collected for worms that do not produce Aβ (CL2122). Panel (A) represents the thrashing data collected after 18 hours of treatment, (B) is the data after 24 hours of treatment, (C) shows the data after 36 hours of treatment, and (D) is the thrashing data after 42 hours of treatment. No significant difference was seen between GMC101 and *tph-1*;$A\beta_{1-42}$ (CEC218) worms at any time-point. Three asterisks show a significance level of $P < 0.001$.

3.7 The effects of Fluoxetine and nor-Fluoxetine on Aβ clearance through the mammalian serotonin transporter are inconclusive.

Confirmation of the role of MOD-5 in the Aβ-dependent paralysis phenotype was supported strongly by the *C. elegans* studies described above. The next challenge was to investigate the hypothesis that Aβ is able to be exported through SERT/MOD-5, thus SSRI treatment prevents its clearance. Although *C. elegans* provided a useful model to test the effects of Fluoxetine and nor-Fluoxetine on Aβ in a whole organism, to validate the involvement of SERT in Aβ transportation from the cell, mammalian cell culture was used. Cell culture provided a simpler and very controlled cellular model to display Aβ traffic. This allowed for a convenient model to compare Aβ levels within the cells to those presumably transported out into the culture media. It was hypothesized that if the SSRIs did prevent the movement of Aβ from the cell, it should be present more so within the cell; however, if it was still able to be cleared, the peptide should be observed within the culture media. In addition, mammalian cell culture allowed for an ideal method to model this movement within neuronal-like cells, as the *C. elegans* strains tested have Aβ accumulating within muscle cells. Preliminary data was produced in the Mousseau laboratory with HT22 mouse hippocampal cells. This initial test was performed to detect any effects of a range of Fluoxetine concentrations on the location of Aβ, whether within the cells or having been transported to the culture media. Increasing levels of Fluoxetine showed Aβ within the cell, while the lower concentrations had Aβ detection within the media (Figure 13). To further these studies, confirmation that HT22 was an appropriate cell line to test the effects of Fluoxetine on the accumulation of Aβ and where it localizes needed to be determined. The cell line to be used needed to have reasonable levels of SERT and the machinery to cleave APP to Aβ. HEK293 and HT22 cells displayed the greatest levels of SERT (Figure 14).

HT22 and HEK293 were chosen to study going forward since the preliminary results were completed in HT22 and HEK293 had the most distinct SERT band present (Figure 14). Both strains were transfected with an empty pcDNA3.1 vector, the vector containing human APP_{WT}, or the vector containing human $APP_{Swe/Ind}$ (Swedish-Indiana allele of APP) and treated with the vehicle, 10μM Fluoxetine, or 25μM Fluoxetine. The transfection was confirmed using WBs with the hypothesis that the samples transfected with the APP would show higher levels of this protein. Figure 15 displays that the cells transfected with APP_{WT} and $APP_{Swe/Ind}$ contain more APP than the cells transfected with the empty vector in both HEK293 and HT22 cell lines.

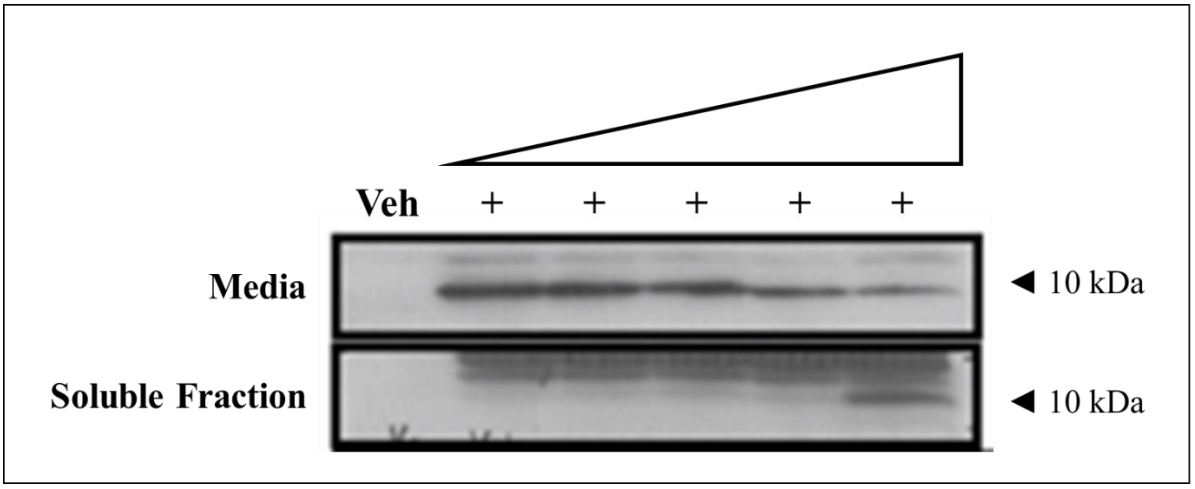

Figure 3.7: Increasing Fluoxetine concentrations influence the location of Aβ in the culture media and in lysates in HT22 cells (*unpublished data*, Pennington and Mousseau, 2012)**.**

IPs and urea WBs were used to compare the presence of Aβ in cells and their corresponding culture media after increasing concentrations of Fluoxetine treatment. Aβ levels can be seen to decrease in the media with increased Fluoxetine treatment and is detected within the soluble fraction by the highest concentration. Membranes were probed with 1:1000 6E10 in 5% BSA in 1xTBST.

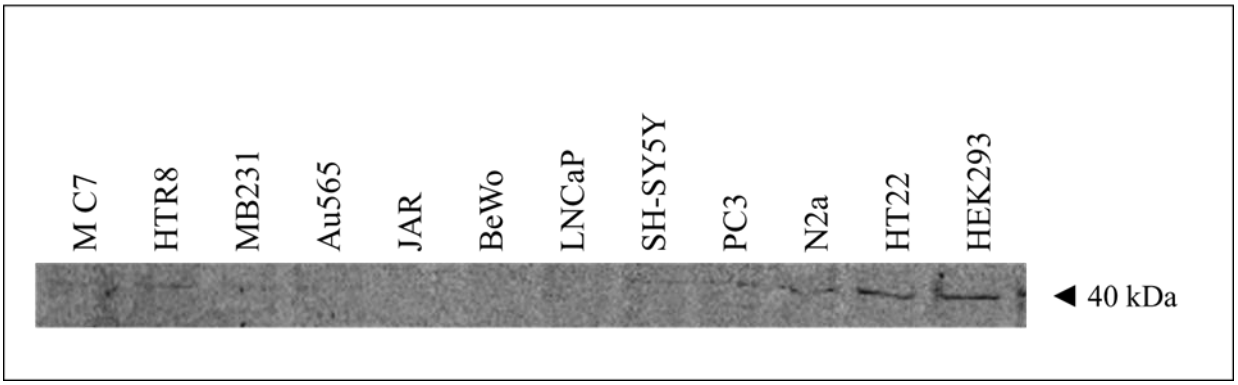

Figure 3.8: SERT expression is stronger in HT22 and HEK293 cell lines.

Cell pellets were lysed and tested with a 10% Western blot for SERT expression. SERT appears to be present within some of the cell lines tested but is most clear within HT22 and HEK293 cell lines. The membranes were probed with 1:500 ST24A5 in 5% BSA in 1xTBST.

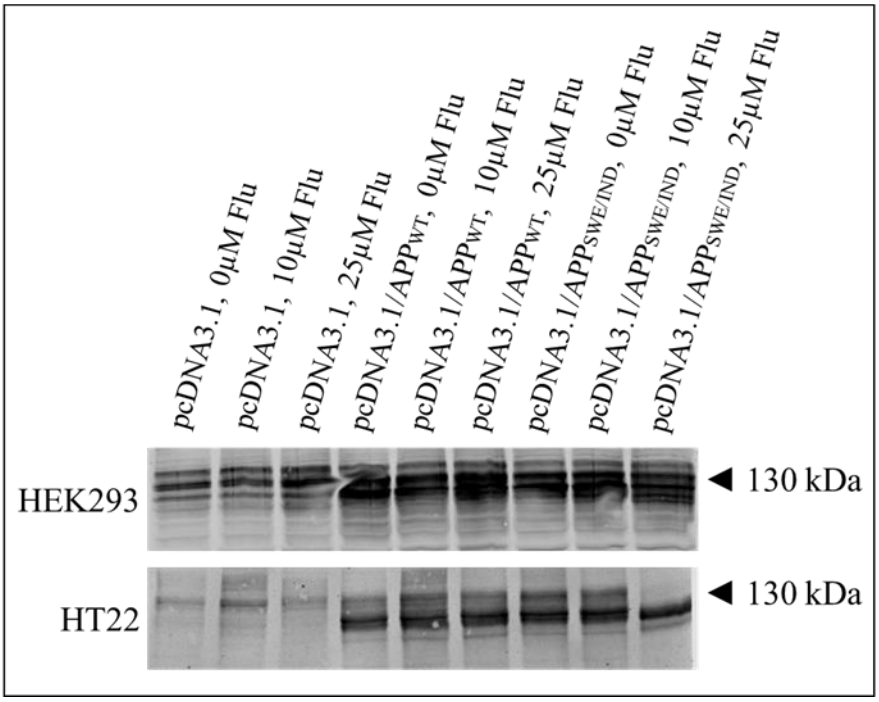

Figure 3.9: Overexpression of APP in HEK293 and HT22 cells is observed in all samples except those transfected with an empty vector, confirming a successful transfection.

Cells were transfected with either an empty pcDNA3.1 vector, or one containing APP_{WT} or $APP_{SWE/IND}$ and were treated with a vehicle, 10μM of Fluoxetine or 25μM Fluoxetine. Increased APP levels can be seen in all cell samples transfected with APP. Western blotting with 10% gels were used to test the samples and the membranes were probed with 1:1000 22C11 in 5% BSA in 1xTBST.

Once confirmed that the transfection was successful, IPs and WBs were used to concentrate and detect Aβ, whether in the soluble fraction (the supernatant after lysing the cell pellets) or within the culture media. For the soluble fraction of the cell sample, a sequential IP was used to remove specific fragments of APP; after C-TERM removed sAPPα, C99, and C83, the 6E10 antibody was used to isolate peptides containing amino acids 1-17 on the N-terminal of Aβ. WBs were then used to view whether Aβ was present within the soluble fraction of the HEK293 cells and the media (Figure 16). No amyloid variants around 10 kDa were detected in any of the treated cell samples. In contrast, the culture media from the samples that were transfected with APP_{WT} and $APP_{Swe/Ind}$ did contain Aβ around 10 kDa. No difference can be seen between the Fluoxetine treatments, but the media from cells transfected with $APP_{Swe/Ind}$ do show a greater amount of Aβ (Figure 16). Similar methods were completed in HT22 cells and culture media (Figure 17); WBs with the soluble fraction and media samples of the HT22 cells show that Aβ was not able to be detected in either the soluble sample or within the media (Figure 17).

The hypothesis described above is based on the idea that Aβ is able to be transported through SERT. To determine if any metabolite of APP is associating with SERT, the sequential IP described above was used to pull out sAPPα, C99, and C83, then Aβ, followed by probing the membranes to detect SERT. A sample of the soluble fraction was also tested to look for initial levels of SERT within the HEK293 and HT22 cells. Any physical interaction between sAPPα, C99, or C83 and SERT and if any association is present between Aβ and SERT in HEK293 cells is shown in Figure 18. In HEK293, it is not distinctly evident whether any of the four APP metabolites are physically associated with SERT. A very faint band can be seen in some C-TERM IP samples around 55 kDa, but no SERT detection is evident in the 6E10 IP, suggesting that Aβ is not bound to SERT in these samples. The first panel in Figure 18 shows that SERT is present within HEK293, confirming that the lack of interaction is not the result of the cells not containing SERT. The same procedures were completed with HT22 cells and are shown in Figure 19; SERT does appear to have some interaction with sAPPα, C99, or C83, but not with Aβ. The top panel faintly shows that SERT can be found within the cell samples, indicating that a lack of association between SERT and the APP products is not from SERT not being present. It appears that some association is present between an APP metabolite and SERT that is likely the 72 kDa variant, but as with HEK293, no binding has occurred between Aβ and SERT, as can be seen in the final panel.

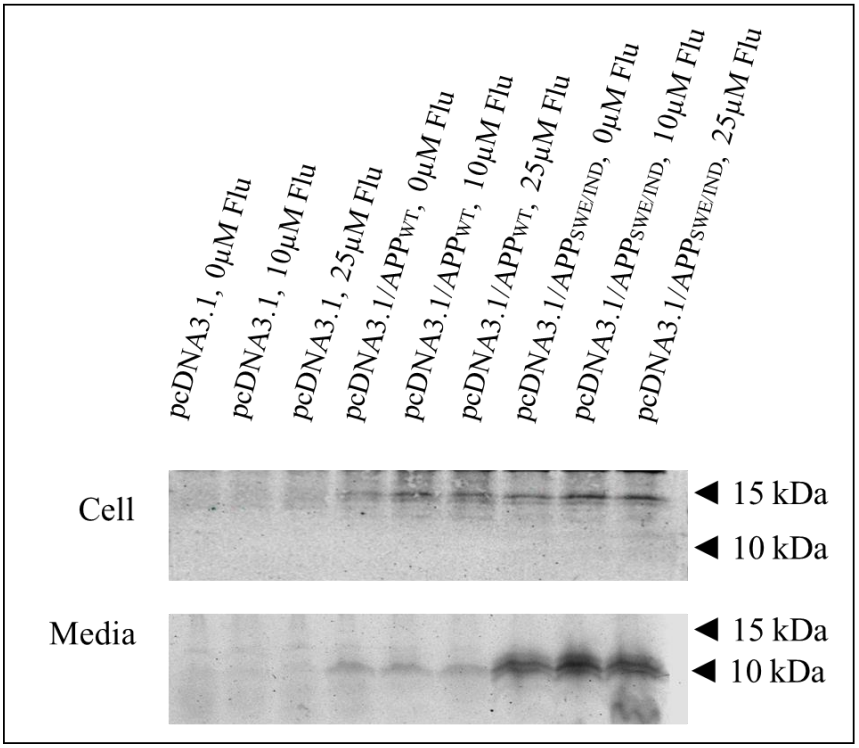

Figure 3.10: Fluoxetine does not prevent Aβ transport to the culture media in HEK293 cells.

After cells were transfected and treated in the same way described in Figure 15, IPs and urea WBs were utilized to isolate Aβ fragments containing amino acids 1-17 on the N-terminal by probing with 6E10. Aβ is undetectable within the soluble fraction of the cell and at least faintly evident within the corresponding culture media. Membrane of the cell soluble fraction was probed with 1:500 6E10 in 5% BSA in 1xTBST and the media membrane with 1:1000 6E10 in 5% BSA in 1xTBST.

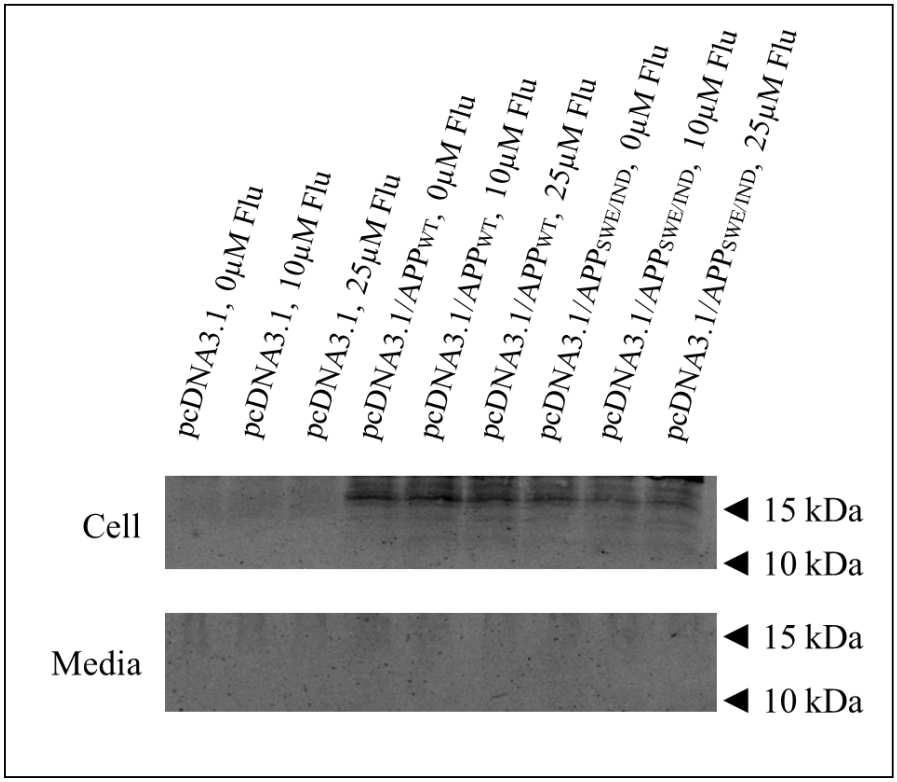

Figure 3.11: Fluoxetine does not prevent Aβ transport to the culture media in HT22 cells.

HT22 cells were transfected and treated as described in Figure 15. Unlike HEK293 cells, Aβ is unable to be detected within either set of samples, indicating that there are either issues with the detection method or this cell line was unable to produce the Aβ peptide. IPs and urea WBs pulled out Aβ fragments containing amino acids 1-17 on the N-terminal when probed with 1:500 6E10 in 5% BSA in 1xTBST.

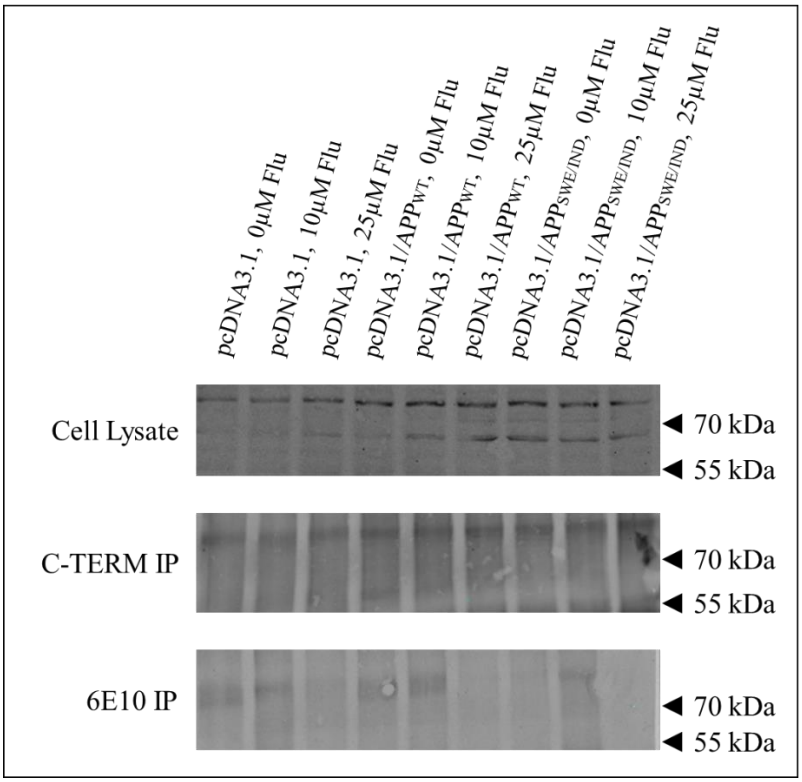

Figure 3.12: No interaction was observed between APP metabolites and SERT in HEK293 cells.

A sequential IP allowed sAPPα, C99, and C83 to be pulled out of the IP sample, before then isolating Aβ. After WBs using 7.5% gels, these samples were probed with anti-SERT, to search for any physical interaction between the APP metabolites and SERT. The image above also shows the initial SERT levels within the cells. Although SERT is present within all samples, any interaction between the four metabolites of APP and SERT cannot be observed. The membranes were probed twice with 1:500 anti-SERT in 5% BSA in 1xTBST.

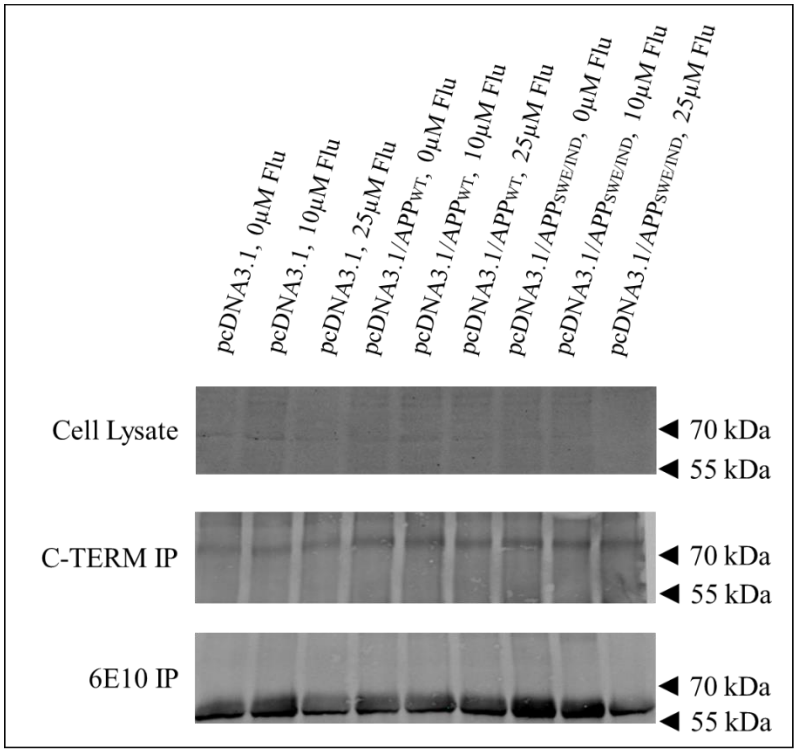

Figure 3.13: No interaction was observed between APP metabolites and SERT in HT22 cells.

The same procedure described for Figure 18 was used in HT22 cells. The image above shows whether SERT interacts with sAPPα, C99, or C83; if SERT is physically connected to Aβ; and the SERT levels within the HT22 cell samples. No association can be seen between the four metabolites of APP and SERT in the HT22 samples although SERT is able to be detected within the cell lysate. The strong band on the bottom panel is from IgG. The membranes were probed twice with 1:500 anti-SERT in 5%BSA in 1xTBST.

4 Discussion

4.1 Fluoxetine and nor-Fluoxetine promote intracellular Aβ peptide accumulation in *C. elegans*.

The premise of this work was to experimentally investigate a possible molecular mechanism explaining how SSRIs exacerbate Aβ toxicity, a theory that comes from clinical studies showing a correlation between specific early-life depression treatments and late-life AD. The finding by Kessing and colleagues that there is an association between the type of antidepressant treatment and the risk for AD development[120] implicates specifically SSRIs, but not other classes of antidepressant drugs, including other uptake inhibitors. *C. elegans* strains that ectopically expressed Aβ peptides in the body wall muscle and behaviour assays that quantify movement dysfunction associated with Aβ accumulation were used to observe the impact of Fluoxetine and nor-Fluoxetine. In addition, this organism was used to study components of the serotonin signaling pathway within a whole animal. Though the first assay used (testing paralysis on agar plates) suggested that SSRIs had no significant impact on Aβ-associated paralysis, these results could be the result of limitations of the technique and biased phenotypic scoring. When the experiments were repeated using a more quantitative readout phenotype (thrashing assay), it was observed that the SSRIs induced an exacerbated reduction in thrashing behaviour. This effect was associated with the production of $A\beta_{1-42}$, but not $A\beta_{3-42}$. These results confirmed a functional link between the mode of action of SSRIs and Aβ accumulation; however, this association is indirect as the change in Aβ accumulation inside the muscle cells has not been checked yet. It will be important to determine if a significant increase in $A\beta_{1-42}$ can be detected using WBs in Fluoxetine and nor-Fluoxetine treated animals compared to vehicle treated worms.

4.2 SERT/MOD-5 link serotonergic and Aβ pathways in the synapsis/neuromuscular junction to influence monoamine turnover and Aβ processing in worms.

Considering the conservation of Fluoxetine specificity to serotonin transporters, MOD-5 was an obvious candidate in modulating the effect of SSRIs. As a membrane transporter that has been shown to bind other neurotoxic ligands[163], MOD-5 could represent an export channel for Aβ peptides. Although the roles of extracellular and intracellular Aβ in the pathology of AD is still controversial, the removal of increasing loads of soluble intracellular Aβ peptides may prevent the formation of toxic plaques. In the artificial context of a transgenic model studied here, preventing

the clearance of Aβ leads to increasing accumulation of Aβ peptides in muscle tissue, evidenced by a systemic reduction in thrashing and, ultimately, paralysis of the whole organism.

This work is not the first to suggest that there is a link between Aβ accumulation in *C. elegans* and serotonin signalling. Using a similar experimental approach, Wu et al. showed that the extract (EGb 761) from *Ginkgo biloba* can inhibit both Aβ oligomerization in neurons and hypersensitivity to exogenous serotonin, suggesting a shared regulation[179]. Interestingly, the authors noticed that Aβ expressing lines with normal MOD-5 function were more sensitive to exogenous serotonin, a hallmark of *mod-5* mutants. This effect is completely suppressed by pre-treatment with the *G. biloba* extract, indicating that Aβ oligomerization in the neuron correlates with reduced import of serotonin from the synapsis. One interpretation of this finding is that Aβ peptides may compete with serotonin for binding to MOD-5 in the membrane of neurons, resulting in a diminished import of serotonin in higher intracellular Aβ load situations leading to longer residence of serotonin in the synaptic cleft and higher sensitivity for this active monoamine. Though biochemical proof of Aβ binding to SERT/MOD-5 is not yet available, evidence from *C. elegans* strongly suggest that MOD-5 represent a shared notch between the serotonin signalling branch and the Aβ clearance pathway. To further explore this network, it would be interesting to revisit these findings to test whether inhibition of MOD-5 with SSRI treatment can interfere with EGb 761-mediated suppression of Aβ oligomerization and deposition in neurons.

4.3 Lack of evidence of SERT-dependent Aβ export from mammalian cells.

Alternatively, both the HEK293 and HT22 cell lines did not appear to be affected by SSRI use. It was hypothesized that Fluoxetine would block SERT and cause Aβ to remain within the cell, where those treated with a vehicle would allow Aβ to be transported to the media. The lysates were tested and confirmed that the transfection was effective (Figure 15), thus the later experiments (determining the location of Aβ and whether it colocalizes with SERT) being unsuccessful was not because the cells were not expressing APP, nor that they do not express SERT as this was also confirmed in Figure 14 and in the first panels of Figures 18 and 19. It was hypothesized that with SSRI treatment, Aβ would bind to SERT. Sequential IPs were used to immunodeplete C99, C83, and sAPPα into one sample and Aβ into another, then were probed for SERT after WBs were ran. Following the hypothesis, if the APP metabolites associated with SERT, this should be detected when probing for the transporter. Although all samples did have

detectable levels of SERT, the HEK293 cells did not show any banding after the SERT probe. This was unsurprising as it was shown in Figure 16 that the HEK293 cells did not have detectable levels of Aβ within the cells but was observed within the media. This helps confirm that no association between Aβ and SERT occurred within these samples. The HT22 cells also had detectable SERT levels within the cell lysate samples but showed no association between SERT and Aβ. HT22 may not have been capable of producing Aβ, as only larger APP metabolites around 15 kDa appear to be present (Figure 17) and is reflected by Figure 19 where a faint band is present around 55 kDa after the C-TERM IP. As the data displayed in Figures 16 and 17 did not agree with the hypothesis, and no difference is evident between the vehicle and the two treatment concentrations of Fluoxetine, it appears that the cell lines chosen may not have been proper models or that the detection method used was not sensitive enough to perceive any differences. This is discussed further in Section 4.4.

4.4 Limitations of the worm and cell culture models

There are some limitations of the research described above. Firstly, the worm model used to study the effects of SSRIs on the accumulation of Aβ cannot be directly compared to the aggregation seen in human brains. Expression of Aβ occurs in body muscle cells in *C. elegans*, therefore, not directly affecting their neurons. Serotonin is known to have a multitude of roles in the human body, including vasoconstriction and coagulation, to name a few[180], and is taken up by many different tissues, such as smooth muscle, brain, spleen, liver, lungs, and gut[180]. The specific role of serotonin on body muscle cells and if MOD-5 is present in these cells is not well documented. However, regulation of pharyngeal pumping in worms is controlled by serotonin[181], indicating that it is possible for muscle cells within these nematodes to be regulated by this monoamine. It is clear in the thrashing experiments completed in this study that Fluoxetine and nor-Fluoxetine cause a significant effect in this worm model, but the precise action is unknown. The neuromuscular junction in *C. elegans* differs from vertebrates because the muscle cells extend axons towards the motor neurons and form synapses[182]; this location is likely where the SSRIs are acting to produce the effects described above. It is not clear whether the drugs used are acting on the muscle cell itself, producing the reduction in body bends, or directly on Aβ. As exogenous serotonin has been found to induce a number of behaviours in *C. elegans*, including slowed locomotion[181], it could be argued that the SSRIs are increasing serotonin levels within the worm,

resulting in the reduced thrashing. However, the results displayed in Figure 12 dispute this idea. CEC218 worms express human $A\beta_{1-42}$ and do not produce serotonin (*tph-1*), but still show the reduced levels of thrashing that are very similar to those observed in GMC101 worms, which can synthesize serotonin. It would follow that this change in serotonin availability or location caused by SSRIs in $A\beta_{1-42}$-expressing (GMC101) worms cannot be responsible for the reduced thrashing phenotype if no difference is seen in worms that cannot produce serotonin. This does not quell all other arguments that could be made about there being off-target effects causing the phenotype observed, however, whether these effects are the result of an increase in Aβ could be easily tested. Once the detection method for Aβ has been optimized, this could be verified by determining if the amount of Aβ within the worms is increased when treated with an SSRI, compared to the vehicle by lysing the worms and testing with a urea/SDS-PAGE gel and 6E10 primary antibody probing.

Another limitation of the worm model is that it has a human protein being produced within a non-human organism. The assumption used here is that the cellular environments within the worm muscle cells and the human neurons (these proteins are typically found in) are the same and allow for similar pathways to be present. If this assumption is incorrect, and the worms do not have the machinery to clear and metabolize this peptide, that would indicate that what we are seeing is not actually caused by SSRIs influencing Aβ. However, previous work has been done showing that *C. elegans* does have gene analogues to those present in humans, supporting the use of this model. These include *mitoferrin-1*, the mitochondrial solute carrier which, when knocked-down, reduces paralysis rate in GMC101 worms[183]; the presenilin homolog, *sel-12*[184]; and α-secretase, both of which can cleave human APP[185].

In addition, the amount of Fluoxetine or nor-Fluoxetine consumed by the worms is currently unknown. Although the plates are seeded with a specific concentration of the SSRIs, the worms are not going to have an internal concentration of either compound the same as that on the plates because of the cuticle and the internal amount is likely variable from worm to worm. The treatment is determined by the amount of *E. coli* lawn that is eaten; this variation may be a factor attributing to the range in thrashing seen across the worms. Mass spectrometry could allow the detection of the compounds after the worm has consumed them. As well, this may be used to detect specific differences in the chemical structures of compounds within the lysed worm solution, which could be used to determine if the worm can metabolize the drugs.

The mammalian cell culture also had some limitations; this model does not take a whole organism into account. Although cell culture does allow the effects of Fluoxetine to be tested in mammalian cells, this only shows effects at a cellular level and likely differs from what may happen in a whole organism. A rodent model could be an appropriate next step to determine if treatment with SSRIs increases the organism's risk for AD.

Following the work discussed, there are still a multitude of questions that need to be answered. Firstly, once the detection method is optimized, both Fluoxetine and nor-Fluoxetine need to be used to treat APP-transfected HEK293 and HT22 cells to determine if Fluoxetine and its metabolite produce similar effects, as seen in *C. elegans*. As well, multiple antidepressant drugs need to be tested in cell culture to display whether all SSRIs have similar actions regarding Aβ accumulation and localization and if other classes differ in effect. These objectives could be achieved similarly to the previous cell culture procedures, with the cells being transfected to express human APP, treated, IPs performed, and tested with urea/SDS-PAGE.

In this study only two concentrations of Fluoxetine were used for the cell culture treatments. After further tests are done to accept or reject the original hypothesis, a greater range of drug concentrations could show if the switch from seeing Aβ in the media to finding it in the cell occurs at a specific concentration or if the amount seen in each location is dose-dependent and gradually changes. If any interesting results were found when using other compounds, this technique could be employed as well.

Although *C. elegans* and cell culture are useful models for neurodegeneration and to screen the effects of antidepressant drugs without the extra interfering factors that a larger, more complex organism can give, these are only predictive models of this disorder. It would be interesting to study the effects of antidepressant drug use on AD development in a mouse or rat model, as these are evolutionarily closer to humans. How earlier use of antidepressant drugs compares to use later in life could be studied, as well as, if longer treatment shows a greater increased risk of late-life AD. At the end of the study, after being sacrificed, the brains of the animals could be tested for their Aβ burden. In addition, it has been reported that treatment with SSRIs at doses below the lowest typical treatment dose might be able to treat depression without increasing risk for AD[186]. A smaller dose could be tested to determine its efficacy. This could be an ideal treatment, if successful, as it could still prevent the uptake of serotonin, increasing its availability, while not saturating the transporter, allowing Aβ to leave the neuron. To be able to make confident

hypotheses about what the chronic effects of antidepressant drugs are in the human body, a mammalian model will need to be tested first.

Finally, there may be more than one binding site for SSRIs on SERT; this theory would explain why other uptake inhibitors do not display the same risk factor for AD as SSRIs. SSRIs may be binding to a site causing a conformational change within the transporter. This change could prevent Aβ from associating with the second binding site on SERT and halt its removal from the cell. Other drugs that display no increased risk for AD, such as TCAs[120], may bind to the second transporter binding site allowing the movement of Aβ to continue. This is supported by the finding that men and women have greater efficacy with different classes of antidepressant drugs and suggests that there may be other structural differences between male and female SERT. Determining whether two binding sites are present on the transporter, and if any differences can be detected between the sexes, could allow for more selective antidepressant drugs to be developed.

4.5 Clinical implications of the effects of SSRI usage on Aβ accumulation

Antidepressant drugs are one of the most commonly prescribed types of medications, with SSRIs continuing to increase in use[187], and has risen for almost four decades[188]. As well, other off-label uses of SSRIs have been found, increasing the number of people utilizing this type of drug. Unlike other antidepressant drug options, such as MAOIs, SSRIs appear to be a safer and more convenient choice when selecting a compound to prescribe. Although other classes have more acute side effects to consider and monitor, SSRIs may have more serious chronic side effects if their use is continued for a longer duration. If these compounds can increase a person's risk for AD, they should not be the first option chosen when looking for a depression treatment without receiving more information from the patient. The family history and other AD risk factors, such as presence of affective disorders, need to be considered when prescribing an antidepressant drug. A meta-analysis by Moraros et al. found that individuals with AD are more likely to have been treated with antidepressant drugs, and that this association is more evident in people treated before the age of 65[161]. This effect could be the result of many factors. Rate of metabolism is different across age ranges causing those treated with antidepressant drugs in early adulthood to metabolize the drugs faster, producing more of the metabolites. The work described above in *C. elegans* suggests that nor-Fluoxetine has very similar effects on the accumulation of Aβ to that seen for

Fluoxetine. As nor-Fluoxetine has a longer half-life, and seemingly has the same effects as the parent compound, this could cause the heightened effects found in younger cohorts. As well, younger adults have a greater chance for an extended duration of treatment if a disorder presents at an earlier age compared to an elderly patient. This is not to say that SSRIs have no benefit, but that more consideration should be taken in the treatment process. As already stated, other types of antidepressant drugs do not show the same risk for AD as has been associated with SSRIs[120].

Another factor to consider is that the increased risk in AD development may not uniformly affect the population. With a theorised difference in efficacy between TCAs and SSRIs in males and females[130–133], women may be more likely to be prescribed an SSRI over other antidepressant drug options because of its higher success rate. TCAs were not found to cause an increased risk for AD development, so its use in males would likely not be an additional risk factor. Depression is more commonly diagnosed in women, thus if SSRIs are thought to have minimal side effects and have greater success in females, their use could be increasing the risk of AD in these women.

5 References

1. Moya-Alvarado G, Gershoni-Emek N, Perlson E, Bronfman FC. Neurodegeneration and Alzheimer's disease (AD). What can proteomics tell us about the Alzheimer's brain? *Mol Cell Proteomics*. 2016;15(2):409-425. doi:10.1074/mcp.R115.053330

2. Mental Health America. Alzheimer's Disease. http://www.mentalhealthamerica.net/alzheimers-disease. Published 2017.

3. Tang X, Holland D, Dale AM, Younes L, Miller MI. Shape abnormalities of subcortical and ventricular structures in mild cognitive impairment and Alzheimer's disease: detecting, quantifying, and predicting. *Hum Brain Mapp*. 2014;35(8):3701-3725. doi:10.1002/hbm.22431

4. Andreasen N, Minthon L, Davidsson P, et al. Evaluation of CSF-tau and CSF-Aβ42 as Diagnostic Markers for Alzheimer Disease in Clinical Practice. *Arch Neurol*. 2001;58:373-379.

5. Strittmatter WJ, Saunders AM, Schmechel D, et al. Apolipoprotein E: High-avidity binding to β-amyloid and increased frequency of type 4 allele in late-onset familial Alzheimer disease. *Proc Natl Acad Sci*. 1993;90(5):1977-1981. doi:10.1073/pnas.90.5.1977

6. Corder EH, Saunders AM, Strittmatter WJ, et al. Gene dose of apolipoprotein E type 4 allele and the risk of Alzheimer's disease in late onset families. *Science (80-).* 1993;261(5123):921-923.

7. Tanzi RE. The genetics of Alzheimer disease. *Cold Spring Harb Perspect Med*. 2012;2(10):1-10. doi:10.1101/cshperspect.a006296

8. Goate A, Chartier-Harlin MC, Mullan M, et al. Segregation of a missense mutation in the amyloid precursor protein gene with familial Alzheimer's disease. *Nature*. 1991;349(6311):704-706. doi:10.1038/349704a0

9. Suh Y-H, Checler F. Amyloid precursor protein, presenilins, and α-synuclein: molecular pathogenesis and pharmacological applications in Alzheimer's disease. *Pharmacol Rev*. 2002;54(3):469-525. doi:10.1124/pr.54.3.469

10. Reitz C, Mayeux R. Alzheimer disease: Epidemiology, diagnostic criteria, risk factors and biomarkers. *Biochem Pharmacol*. 2014;88(4):640-651. doi:10.1016/j.bcp.2013.12.024

11. Sherrington R, Rogaev EI, Liang Y, et al. Cloning of a gene bearing missense mutations in early-onset familial Alzheimer's disease. *Nature*. 1995;375(6534):754-760. doi:10.1038/375754a0

12. De Strooper B. Aph-1, Pen-2, and Nicastrin with presenilin generate an active γ-secretase complex. *Neuron*. 2003;38(1):9-12. doi:10.1016/S0896-6273(03)00205-8

13. Duff K, Eckman C, Zehr C, et al. Increased amyloid-β42(43) in brains of mice expressing mutant presenilin 1. *Nature*. 1996;383(6602):710-713. doi:10.1038/383710a0

14. Levy-Lahad E, Wijsman EM, Nemens E, et al. A familial Alzheimer's disease locus on

chromosome I. *Science (80-)*. 1995;269(1978):970-973. papers2://publication/uuid/EFC5558B-FCBA-4754-B291-E5933300E5DF.

15. Levy-lahad E, Wasco W, Poorkaj P, et al. Candidate gene for the chromosome 1 familial Alzheimer's disease locus. *Science (80-)*. 1995;269:973-977.

16. Scheuner D, Eckman C, Jensen M, et al. Secreted amyloid beta-protein similar to that in the senile plaques of Alzheimer's disease is increased in vivo by the presenilin 1 and 2 and APP mutations linked to familial Alzheimer's disease. *Nat Med*. 1996;2(8):864-870. doi:10.1038/nm0896-864

17. Citron M, Vigo-Pelfrey C, Teplow DB, et al. Excessive production of amyloid β-protein by peripheral cells of symptomatic and presymptomatic patients carrying the Swedish familial Alzheimer disease mutation. *Proc Natl Acad Sci*. 1994;91(25):11993-11997. doi:10.1073/pnas.91.25.11993

18. Jacobsen L, Madsen P, Moestrup SK, et al. Molecular characterization of a novel human hybrid-type receptor that binds the α2-macroglobulin receptor-associated protein. *J Biol Chem*. 1996;271(49):31379-31383. doi:10.1074/jbc.271.49.31379

19. Rogaeva E, Meng Y, Lee JH, et al. The neuronal sortilin-related receptor SORL1 is genetically associated with Alzheimer disease. *Nat Genet*. 2007;39(2):168-177. doi:10.1038/ng1943

20. Wegmann S, Yu JJ, Chinnathambi S, Mandelkow EM, Mandelkow E, Muller DJ. Human tau isoforms assemble into ribbon-like fibrils that display polymorphic structure and stability. *J Biol Chem*. 2010;285(35):27302-27313. doi:10.1074/jbc.M110.145318

21. Kidd M. Paired helical filaments in electron microscopy of Alzheimer's disease. *Nature*. 1963;197:192-193. doi:10.1038/197192b0

22. Braak H, Braak E. Neuropathological stageing of Alzheimer-related changes. *Acta Neuropathol*. 1991;82(4):239-259. doi:10.1007/BF00308809

23. Salloway S, Sperling R, Fox NC, et al. Two phase 3 trials of Bapineuzumab in mild-to-moderate Alzheimer's disease. *N Engl J Med*. 2014;370(4):322-333. doi:10.1056/NEJMoa1304839

24. Barthel H, Gertz HJ, Dresel S, et al. Cerebral amyloid-β PET with florbetaben (18F) in patients with Alzheimer's disease and healthy controls: A multicentre phase 2 diagnostic study. *Lancet Neurol*. 2011;10(5):424-435. doi:10.1016/S1474-4422(11)70077-1

25. Oddo S, Caccamo A, Shepherd JD, et al. Triple-transgenic model of Alzheimer's disease with plaques and tangles: Intracellular Aβ and synaptic dysfunction. *Neuron*. 2003;39(3):409-421. doi:10.1016/S0896-6273(03)00434-3

26. Selkoe DJ, Podlisny MB. Deciphering the genetic basis of Alzheimer's disease. *Annu Rev Genomics Hum Genet*. 2002;3(1):67-99. doi:10.1146/annurev.genom.3.022502.103022

27. Müller UC, Deller T, Korte M. Not just amyloid: Physiological functions of the amyloid precursor protein family. *Nat Rev Neurosci*. 2017;18(5):281-298. doi:10.1038/nrn.2017.29

28. Fisher S, Gearhart JD, Oster-Granite ML. Expression of the amyloid precursor protein gene in mouse oocytes and embryos. *Proc Natl Acad Sci*. 1991;88(5):1779-1782. doi:10.1073/PNAS.88.5.1779

29. Tyan S-H, Shih AY-J, Walsh JJ, et al. Amyloid precursor protein (APP) regulates synaptic structure and function. *Mol Cell Neurosci*. 2012;51(1-2):43-52. doi:10.1016/j.mcn.2012.07.009

30. Young-Pearse TL, Bai J, Chang R, Zheng JB, LoTurco JJ, Selkoe DJ. A critical function for β-Amyloid precursor protein in neuronal migration revealed by in utero RNA interference. *J Neurosci*. 2007;27(52):14459-14469. doi:10.1523/JNEUROSCI.4701-07.2007

31. Caillé I, Allinquant B, Dupont E, et al. Soluble form of amyloid precursor protein regulates proliferation of progenitors in the adult subventricular zone. *Dev Dis*. 2004;131(9):2173-2181. doi:10.1242/dev.01103

32. Herzig MC, Paganetti P, Staufenbiel M, Jucker M. BACE1 and mutated presenilin-1 differently modulate Aβ40 and Aβ42 levels and cerebral amyloidosis in APPDutch transgenic mice. *Neurodegener Dis*. 2007;4(2-3):127-135. doi:10.1159/000101837

33. Wild-Bode C, Yamazaki T, Capell A, et al. Intracellular generation and accumulation of amyloid β-peptide terminating at amino acid 42. *J Biol Chem*. 1997;272(26):16085-16088. doi:10.1074/jbc.272.26.16085

34. Arnold SE, Hyman BT, Flory J, Damasio AR, Van Hoesen GW. The topographical and neuroanatomic distribution of neurofibrillary tangles and neuritic plaques in the cerebral cortex of patients with Alzheimer's disease. *Cereb Cortex*. 1991;1:103-116.

35. Arriagada PV, Growdon JH, Hedley-Whyte ET, Hyman BT. Neurofibrillary tangles but not senile plaques parallel duration and severity of Alzheimer's disease. *Neurology*. 1992;42:631-639.

36. Hyman BT, Van Hoesen GW, Damasio AR, Barnes CL. Alzheimer's disease: Cell-specific pathology isolates the hippocampal formation. *Adv Sci*. 2008;225(4667):1168-1170. doi:10.1126/science.6474172

37. Ingelsson M, Fukumoto H, Newell KL, et al. Early Aβ accumulation and progressive synaptic loss, gliosis, and tangle formation in AD brain. *Neurology*. 2004;62(6):925-931. doi:10.1212/01.WNL.0000115115.98960.37

38. Blennow K, Dubois B, Fagan AM, Lewczuk P, De Leon MJ, Hampel H. Clinical utility of cerebrospinal fluid biomarkers in the diagnosis of early Alzheimer's disease. *Alzheimer's Dement*. 2015;11(1):58-69. doi:10.1016/j.jalz.2014.02.004

39. Johnson KA, Fox NC, Sperling RA, Klunk WE. Brain imaging in Alzheimer disease. *Cold Spring Harb Perspect Med*. 2012;2(4):1-23. doi:10.1101/cshperspect.a006213

40. Dubois B, Feldman HH, Jacova C, et al. Research criteria for the diagnosis of Alzheimer's disease: revising the NINCDS–ADRDA criteria. *Lancet Neurol*. 2007;6(8):734-746. doi:10.1016/S1474-4422(07)70178-3

41. Stopschinski BE, Diamond MI. The prion model for progression and diversity of neurodegenerative diseases. *Lancet Neurol*. 2017;16(4):323-332. doi:10.1016/S1474-4422(17)30037-6

42. Baker HF, Ridley RM, Duchen LW, Crow TJ, Bruton CJ. Experimental Induction of β-Amyloid Plaques and Cerebral Angiopathy in Primates. *Ann N Y Acad Sci*. 1993;695(1):228-231. doi:10.1111/j.1749-6632.1993.tb23057.x

43. Walker LC, Jucker M. Neurodegenerative Diseases: Expanding the Prion Concept. *Annu Rev Neurosci*. 2015;38(1):87-103. doi:10.1146/annurev-neuro-071714-033828

44. Prusiner SB. Novel Proteinaceous Infectious Particles Cause Scrapie Author. *Science (80-)*. 2013;216(4542):136-144.

45. Parchi P, Giese A, Capellari S, et al. Classification of sporadic Creutzfeldt-Jakob disease based on molecular and phenotypic analysis of 300 subjects. *Ann Neurol*. 1999;46(2):224-233. doi:10.1002/1531-8249(199908)46:2<224::AID-ANA12>3.0.CO;2-W

46. Scarmeas N, Stern Y, Mayeux R, Manly JJ, Schupf N, Luchsinger JA. Mediterranean diet and mild cognitive impairment. *Arch Neurol*. 2009;66(2):216-225. doi:10.1001/archneurol.2008.536

47. Gu Y, Nieves JW, Stern Y, Luchsinger JA, Scarmeas N. Food combination and Alzheimer disease risk: A protective diet. *Arch Neurol*. 2010;67(6):699-706. doi:10.1001/archneurol.2010.84

48. Dishman RK, Berthoud H-R, Booth FW, et al. Neurobiology of Exercise. *Obesity*. 2006;14(3):345-356. doi:10.1038/oby.2006.46

49. Xu W, Tan L, Wang H-F, et al. Meta-analysis of modifiable risk factors for Alzheimer's disease. *J Neurol Neurosurg Psychiatry*. 2015;86(12):1299-1306. doi:10.1136/jnnp-2015-310548

50. Leibson CL, Rocca WA, Hanson VA, et al. The risk of dementia among persons with diabetes mellitus: A population-based cohort study. *Ann N Y Acad Sci*. 1997;826:422-427. doi:10.1111/j.1749-6632.1997.tb48496.x

51. Luchsinger JA, Tang M-X, Stern Y, Shea S, Mayeux R, Sergievsky GH. Diabetes mellitus and risk of Alzheimer's disease and dementia with stroke in a multiethnic cohort. *Am J Epidemiol*. 2001;154(7):635-641.

52. Luchsinger JA. Adiposity, hyperinsulinemia, diabetes and Alzheimer's disease. An epidemiological perspective. *Eur J Pharmacol*. 2008;585(1):119-129.

53. Mayeux R, Ottman R, Maestre G, et al. Synergistic effects of traumatic head injury and apolipoprotein-ε4 in patients with Alzheimer's disease. *Neurology*. 1995;45:555-557.

54. Raffaitin C, Gin H, Empana J, et al. Metabolic syndrome and risk for incident Alzheimer's disease or vascular dementia: The three-city study. *Diabetes Care*. 2009;32(1):169-174. doi:10.2337/dc08-0272

55. Burton C, Campbell P, Jordan K, Strauss V, Mallen C. The association of anxiety and

depression with future dementia diagnosis: A case-control study in primary care. *Fam Pract*. 2013;30:25-30. doi:10.1093/fampra/cms044

56. Gallacher J, Bayer A, Fish M, et al. Does anxiety affect risk of dementia? Findings from the Caerphilly Prospective Study. *Psychosom Med*. 2009;71:659-666. doi:10.1097/PSY.0b013e3181a6177c

57. Beaudreau SA, Hara RO. Late-life anxiety and cognitive impairment: A review. *Am J Geriatr Psychiatry*. 2008;16(10):790-803. doi:10.1097/JGP.0b013e31817945c3

58. Diniz BS, Butters MA, Albert SM, Dew MA, Reynolds CF 3rd. Late-life depression and risk of vascular dementia and Alzheimer's disease: Systematic review and meta-analysis of community based cohort studies. *Br J Psychiatry*. 2013;202:329-335.

59. Saczynski JS, Beiser A, Seshadri S, Auerback S, Wolf PA, Au R. Depressive symptoms and risk of dementia: The Framingham Heart Study. *Neurology*. 2010;75:35-41.

60. Green RC, Cupples LA, Kurz A, et al. Depression as a risk factor for Alzheimer disease: The MIRAGE Study. *Arch Neurol*. 2003;60:753-759.

61. Golden RN, Gilmore JH. Serotonin and mood disorders. *Psychiatr Ann*. 1990;20:580-586. doi:10.3928/0048-5713-19901001-09

62. Meltzer CC, Smith G, Dekosky ST, et al. Serotonin in aging, late-life depression, and Alzheimer's disease: The emerging role of functional imaging. *Neuropsychopharmacology*. 1998;18(18):407-430.

63. Grudzien A, Shaw P, Weintraub S, Bigio E, Mash DC, Mesulam MM. Locus coeruleus neurofibrillary degeneration in aging, mild cognitive impairment and early Alzheimer's disease. *Neurobiol Aging*. 2007;28(3):327-335. doi:10.1016/j.neurobiolaging.2006.02.007

64. Rüb U, Del Tredici K, Schultz C, Thal DR, Braak E, Braak H. The evolution of Alzheimer's disease-related cytoskeletal pathology in the human raphe nuclei. *Neuropathol Appl Neurobiol*. 2000;26(6):553-567. doi:10.1046/j.0305-1846.2000.00291.x

65. Kessing LV. Cognitive impairment in the euthymic phase of affective disorder. *Psychol Med*. 1998;28(5):1027-1038. doi:10.1017/S0033291798006862

66. Ontario Ministry of Health and Longterm Care. Mental Health: Depression. http://health.gov.on.ca/en/public/publications/mental/depression.aspx. Published 2015.

67. Kupfer DJ, Frank E, Phillips ML. Major depressive disorder: New clinical, neurobiological, and treatment perspectives. *Lancet*. 2012;379(9820):1045-1055. doi:10.1016/S0140-6736(11)60602-8

68. Martin LA, Neighbors HW, Griffith DM. The experience of symptoms of depression in men vs women: Analysis of the national comorbidity survey replication. *J Am Med Assoc*. 2013;70(10):1100-1106. doi:10.1001/jamapsychiatry.2013.1985

69. Mental Health America. Mood Disorders. http://www.mentalhealthamerica.net/conditions/mood-disorders. Published 2017.

70. American Psychiatric Association. *Diagnostic and Statistical Manual of Mental*

Disorders. Washington: American Psychiatric Association; 2000.

71. Bruce ML. Psychosocial risk factors for depressive disorders in late life. *Biol Psychiatry*. 2002;52(3):175-184. doi:10.1016/S0006-3223(02)01410-5

72. Mill J, Petronis A. Molecular studies of major depressive disorder: the epigenetic perspective. *Mol Psychiatry*. 2007;12(9):799-814. doi:10.1038/sj.mp.4001992

73. Miguel-Hidalgo JJ, Rajkowska G. Morphological brain changes in depression: Can antidepressants reverse them? *CNS Drugs*. 2002;16(6):361-372. doi:10.2165/00023210-200216060-00001

74. Soares JC, Mann JJ. The anatomy of mood disorders-review of structural neuroimaging studies. *Biol Psychiatry*. 1997;41:86-106.

75. Sheline YI, Gado MH, Price JL. Amygdala core nuclei volumes are decreased in recurrent major depression. *Neuroreport*. 1998;9(9):2023-2028. doi:10.1097/00001756-199806220-00021

76. Sheline YI, Wang PW, Gado MH, Csernansky JG, Vannier MW. Hippocampal atrophy in recurrent major depression. *Proc Natl Acad Sci*. 1996;93:3908-3913.

77. Statistics Canada. Top five prescription medications used, by sex, age group and medication class, household population aged 25 to 79, Canada, 2007-2011. https://www150.statcan.gc.ca/n1/pub/82-003-x/2014006/article/14032/tbl/tbl4-eng.htm. Published 2015.

78. Zeller EA, Barsky J, Fouts JR, Kirchheimer WF, Van Orden LS. Influence of isonicotinic acid hydrazide (INH) and 1-isonicotinyl-2-isopropyl hydrazide (IIH) on bacterial and mammalian enzymes. *Experientia*. 1952;8(9):349-350. doi:10.1007/BF02174413

79. Glowinski J, Axelrod J. Inhibition of tritiated-noradrenaline uptake in the rat brain by antidepressant drugs. *Nature*. 1964;204(4965):1318-1319. doi:10.1038/2041318a0

80. Wong DT, Horng JS, Bymaster FP, Hauser KL, Molloy BB. A selective inhibitor of serotonin uptake: Lilly 110140, 3-(p-trifluoromethylphenoxy)-N-methyl-3-phenylpropylamine. *Life Sci*. 1974;15(3):471-479. doi:10.1016/0024-3205(74)90345-2

81. Coppen A. The biochemistry of affective disorders. *Br J Psychiatry*. 1967;113:1237-1264.

82. Berger P, Barchas JD. Monoamine oxidase inhibitors. In: Usdin E, Forrest IS, eds. *Psychotherapeutic Drugs*. New York: Marcel Dekker; 1977:1173-1216.

83. Fox HH. Synthetic tuberculostats. VI. Some sugar derivatives of isonicotinylhydrazine. *J Org Chem*. 1953;18(8):990-993. doi:10.1021/jo50014a013

84. Selikoff IJ, Robitzek EH, Ornstein GG. Treatment of pulmonary tuberculosis with hydrazine derivatives of isonicotinic acid. *J Am Med Assoc*. 1952;150:973-980.

85. Loomer HP, Saunders IC, Kline NS. A clinical and pharmacodynamic evaluation of iproniazid as a psychic energizer. *Psychiatr Res Reports Am Psychiatry Assoc*. 1958;8:129-141.

86. Sneader VW. *Drug Discovery: The Evolution of Modern Medicines.* Chichester: John Wiley & Sons Ltd.; 1985.

87. López-Muñoz F, Assion HJ, Alamo C, García-García P, Fangmann P. La introducción clínica de la iproniazida y la imipramina: medio siglo de terapéutica antidepresiva. *An Psiquiatr*. 2008;24(2):56-70.

88. López-Muñoz F, Alamo C, Juckel G, Assion H-J. Half a century of antidepressant drugs: on the clinical introduction of monoamine oxidase inhibitors, tricyclics, and tetracyclics. Part I: monoamine oxidase inhibitors. *J cCinical Psychopharmacol*. 2007;27(6):555-559. doi:10.1097/jcp.0b013e3181bb617

89. Blackwell B. Hypertensive crisis due to monoamine oxidase inhibitors. *Lancet*. 1963;2(7313):849-851.

90. Tansey T. Las instituciones públicas y privadas y el avance de la psicofarmacología. In: López-Muñoz F, Alamo C, eds. *Historia de La Psicofarmacología*. Madrid: Editorial Médica Panamericana; 2007:1165-1186.

91. Fangmann P, Assion H-J, Juckel G, González CÁ, López-Muñoz F. Half a century of antidepressant drugs. *J Clin Psychopharmacol*. 2008;28(1):1-4. doi:10.1097/jcp.0b013e3181627b60

92. Preskorn SH. *Farmacología Clínica de Los Inhibidores Selectivos de La Recaptación de Serotonina.* Caddo: Professional Communications, Inc; 1996.

93. Gumnick JF, Nemeroff CB. Problems with currently available antidepressants. *J Clin Psychiatry*. 2000;61 (Suppl:5-15. http://www.ncbi.nlm.nih.gov/pubmed/10910012.

94. Lambert O, Bourin M. SNRIs: Mechanism of action and clinical features. *Expert Rev Neurother*. 2002;2(6):849-858. doi:10.1586/14737175.2.6.849

95. Bortolato M, Chen K, Shih JC. The Degradation of Serotonin: Role of MAO. In: Muller CP, Jacobs BL, eds. *Handbook of Behavioural Neuroscience*. ; 2010:203-218.

96. Knoll J, Magyar K. Some puzzling pharmacological side effects of monoamine oxidase inhibitors. *Adv Biochem Psychopharmacol*. 1972;5:393-408.

97. Fowler CJ, Mantle TJ, Tipton KF. The nature of the inhibition of rat liver monoamine oxidase types A and B by the acetylenic inhibitors clorgyline, l-deprenyl and pargyline. *Biochem Pharmacol*. 1982;31(22):3555-3561. doi:10.1016/0006-2952(82)90575-5

98. Jahng JW, Houpt TA, Wessel TC, Chen K, Shih JC, Joh TH. Localization of monoamine oxidase A and B mRNA in the rat brain by in situ hybridization. *Synapse*. 1997;25:30-36.

99. Fuxe K. Evidence for the existence of monoamine neurons in the central nervous system III. The monoamine nerve terminal. *Zeitschrift fur Zellforsch*. 1965;65:573-596.

100. Westlund KN, Denney RM, Rose RM, Abell CW. Localization of distinct monoamine oxidase A and monoamine oxidase B cell populations in human brainstem. *Neuroscience*. 1988;25(2):439-456.

101. Rodríguez MJ, Saura J, Billett EE, Finch CC, Mahy N. Cellular localization of

monoamine oxidase A and B in human tissues outside of the central nervous system. *Cell Tissue Res*. 2001;304(2):215-220. doi:10.1007/s004410100361

102. Youdim MBH. Multiple forms of monoamine oxidase and their properties. In: Costa E, Sandler M, eds. *Monoamine Oxidases: New Vistas*. New York: Raven; 1972:67-77.

103. Anderson MC, Hasan F, McCrodden JM, Tipton KF. Monoamine oxidase inhibitors and the cheese effect. *Neurochem Res*. 1993;18(11):1145-1149. doi:10.1007/BF00978365

104. Lotufo-Neto F, Trivedi M, Thase ME. Meta-analysis of the reversible inhibitors of monoamine oxidase type A Moclobemide and Brofaromine for the treatment of depression. *Neuropsychopharmacology*. 1999;20(3):226-247. doi:10.1016/S0893-133X(98)00075-X

105. Ruhé HG, Mason NS, Schene AH. Mood is indirectly related to serotonin, norepinephrine and dopamine levels in humans: A meta-analysis of monoamine depletion studies. *Mol Psychiatry*. 2007;12(4):331-359. doi:10.1038/sj.mp.4001949

106. Bennett JL, Aghajanian GK. D-LSD binding and brain homogenates: Possible relationship to serotonin receptors. *Life Sci*. 1974;15(9):1935-1944.

107. Snyder SH, H.I. Y. Antidepressants and the muscarinic cholinergic receptor. *Arch Gen Psychiatry*. 1977;34:236-239.

108. Green JP, Maayani S. Tricyclic antidepressant drugs block histamine H receptors in the brain. *Nature*. 1977;267:192-193.

109. U'Prichard DC, Greenberg DA, Sheehan PP, Snyder SH. Tricyclic antidepressants: Therapeutic properties and affinity for α-noradrenergic receptor binding sites in the brain. *Science (80-)*. 1978;199(4325):197-198. doi:10.2307/1745161

110. Mayo Clinic. Tricyclic antidepressants and tetracyclic antidepressants. https://www.mayoclinic.org/diseases-conditions/depression/in-depth/antidepressants/art-20046983. Published 2017.

111. Reardon O, John P, Jay D. Treatment-resistant depression : Progress and limitations. *Treat Psychiatr Disord*. 1998;28(11):633-640.

112. Brent D, Emslie G, Clarke G, et al. Switching to another SSRI or to Venlafaxine with or without cognitive behavioral therapy for adolescents with SSRI-resistant depression. *J Am Med Assoc*. 2008;299(8):901-913.

113. Sokolski KN, Conney JC, Brown BJ, Demet EM. Once-daily high-dose pindolol for SSRI-refractory depression. *Psychiatry Res*. 2004;125:81-86. doi:10.1016/j.psychres.2003.12.006

114. Sánchez C, Bergqvist PBF, Brennum LT, et al. Escitalopram, the S-(+)-enantiomer of citalopram, is a selective serotonin reuptake inhibitor with potent effects in animal models predictive of antidepressant and anxiolytic activities. *Psychopharmacology (Berl)*. 2003;167(4):353-362. doi:10.1007/s00213-002-1364-z

115. Owens MJ, Knight DL, Nemeroff CB. Second-generation SSRIs: human monoamine

transporter binding profile of escitalopram and R-fluoxetine. *Biol Psychiatry*. 2001;50(5):345-350. doi:10.1016/S0006-3223(01)01145-3

116. Sánchez C, Meier E. Behavioral profiles of SSRIs in animal models of depression, anxiety and aggression. Are they all alike? *Psychopharmacology (Berl)*. 1997;129(3):197-205. doi:10.1007/s002130050181

117. Cipriani A, Koesters M, Furukawa TA, et al. Duloxetine versus other anti-depressive agents for depression. *Cochrane Database Syst Rev*. 2012;10(10):1-96. doi:10.1002/14651858.CD006533.pub2

118. Sanchez C, Reines EH, Montgomery SA. A comparative review of Escitalopram, Paroxetine, and Sertraline: Are they all alike? *Int Clin Psychopharmacol*. 2014;29(4):185-196. doi:10.1097/YIC.0000000000000023

119. Dale E, Bang-Andersen B, Sánchez C. Emerging mechanisms and treatments for depression beyond SSRIs and SNRIs. *Biochem Pharmacol*. 2015;95(2):81-97. doi:10.1016/j.bcp.2015.03.011

120. Kessing LV, Søndergård L, Forman JL, Andersen PK. Antidepressants and dementia. *J Affect Disord*. 2009;117(1-2):24-29. doi:10.1016/j.jad.2008.11.020

121. Sette M, Briley MS, Langer SZ. Complex inhibition of [3H]Imipramine binding by serotonin and nontricyclic serotonin uptake blockers. *J Neurochem*. 1983;40(3):622-628. doi:10.1111/j.1471-4159.1983.tb08026.x

122. Schloss P, Williams DC. The serotonin transporter: A primary target for antidepressant drugs. *J Psychopharmacol*. 1998;12(2):115-121. doi:10.1177/026988119801200201

123. Schloss P, Mayser W, Betz H. Neurotransmitter transporters: A novel family of integral plasma membrane proteins. *Fed Eur Biochem Socieities*. 1992;307(1):76-80.

124. Rudnick G, Clark J. From synapse to vesicle: The reuptake and storage of biogenic amine neurotransmitters. *Biochim Biophys Acta*. 1993;1144(3):249-263. doi:10.1016/0005-2728(93)90109-S

125. Kanner BI, Schuldiner S. Mechanism of transport and storage of neurotransmitters. *Crit Rev Biochem*. 1987;22(1):1-38. doi:10.3109/10409238709082546

126. Owens MJ, Nemeroff CB. Role of serotonin in the pathophysiology of depression: Focus on the serotonin transporter. *Clin Chem*. 1994;40(2):288-295. doi:10.1371/clinchem.2009.123752

127. Entsuah AR, Huang H, Thase ME. Response and remission rates in different subpopulations with major depressive disorder administered venlafaxine, selective serotonin reuptake inhibitors, or placebo. *J Clin Psychiatry*. 2001;62(11):869-877. doi:http://dx.doi.org/10.4088/JCP.v62n1106

128. Quitkin FM, Stewart JW, McGrath PJ, et al. Are there differences between women's and men's antidepressant responses? *Am J Psychiatry*. 2002;159(11):1848-1854. doi:10.1176/appi.ajp.159.11.1848

129. Hildebrandt MG, Steyerberg EW, Stage KB, Passchier J, Kragh-Soerensen P. Are gender differences important for the clinical effects of antidepressants? *Am J Psychiatry*. 2003;160(9):1643-1650. doi:10.1176/appi.ajp.160.9.1643

130. Haykal RF, Akiskal HS. The long-term outcome of dysthymis in private practice: Clinical features, temperment, and the art of management. *J Clin Psychiatry*. 1999;60(8):508-518. doi:10.4088/JCP.v60n0802

131. Kornstein SG, Schatzberg AF, Thase ME, et al. Gender differences in treatment response to Sertraline versus Imipramine in chronic depression. *Am J Psychiatry*. 2000;157(9):1445-1452. doi:10.1176/appi.ajp.157.9.1445

132. Khan A, Brodhead AE, Schwartz KA, Kolts RL, Brown WA. Sex differences in antidepressant response in recent antidepressant clinical trials. *J Clin Psychopharmacol*. 2005;25(4):318-324. doi:10.1097/01.jcp.0000168879.03169.ce

133. Yang SJ, Kim SY, Stewart R, et al. Gender differences in 12-week antidepressant treatment outcomes for a naturalistic secondary care cohort: The CRESCEND study. *Psychiatry Res*. 2011;189(1):82-90. doi:10.1016/j.psychres.2010.12.027

134. Frank E, Carpenter LL, Kupfer DJ. Sex difference in recurrent depression: Are there any that are significant? *Am J Psychiatry*. 1988;145(1):41-45.

135. Old Age Depression Interest Group. How long should the elderly take antidepressants? *Br J Psychiatry*. 1993;162(2):175-182. doi:10.1192/bjp.162.2.175

136. Naito S, Sato K, Yoshida K, et al. Gender differences in the clinical effects of fluvoxamine and milnacipran in Japanese major depressive patients. *Psychiatry Clin Neurosci*. 2007;61(4):421-427. doi:10.1111/j.1440-1819.2007.01679.x

137. Meyer UA. Overview of enzymes of drug metabolism. *J Pharmacokinet Biopharm*. 1996;24(5):449-459. doi:10.1007/BF02353473

138. Miksys SL, Cheung C, Gonzalez FJ, Tyndale RF. Human CYP2D6 and mouse CYP2DS: Organ distribution in a humanized mouse model. *Drug Metab Dispos*. 2005;33(10):1495-1502. doi:10.1124/dmd.105.005488

139. Zanger UM, Schwab M. Cytochrome P450 enzymes in drug metabolism: Regulation of gene expression, enzyme activities, and impact of genetic variation. *Pharmacol Ther*. 2013;138(1):103-141. doi:10.1016/j.pharmthera.2012.12.007

140. Probst-Schendzielorz K, Viviani R, Stingl JC. Effect of Cytochrome P450 polymorphism on the action and metabolism of selective serotonin reuptake inhibitors. *Expert Opin Drug Metab Toxicol*. 2015;11(8):1219-1232. doi:10.1517/17425255.2015.1052791

141. Mitchell SJ, Kane AE, Hilmer SN. Age-related changes in the hepatic pharmacology and toxicology of Paracetamol. *Curr Gerontol Geriatr Res*. 2011;2011:1-14. doi:10.1155/2011/624156

142. Sramek JJ, Murphy MF, Cutler NR. Sex differences in the psychopharmacological treatment of depression. *Dialogues Clin Neurosci*. 2016;18(4):447-457.

143. Hilmer SN, Shenfield GM, Le Couteur DG. Clinical implications of changes in hepatic drug metabolism in older people. *Ther Clin Risk Manag*. 2005;1(2):151-156. http://www.pubmedcentral.nih.gov/articlerender.fcgi?artid=1661619&tool=pmcentrez&rendertype=abstract.

144. Mathers CD, Stevens GA, Boerma T, White RA, Tobias MI. Causes of international increases in older age life expectancy. *Lancet*. 2015;385(9967):540-548. doi:10.1016/S0140-6736(14)60569-9

145. Erdö F, Denes L, De Lange E. Age-associated physiological and pathological changes at the blood-brain barrier: A review. *J Cereb Blood Flow Metab*. 2017;37(1):4-24. doi:10.1177/0271678X16679420

146. Schmucker DL. Age-related changes in liver structure and function: Implications for disease? *Exp Gerontol*. 2005;40(8-9):650-659. doi:10.1016/j.exger.2005.06.009

147. Gury C, Cousin F. Pharmacokinetics of SSRI antidepressants: Half-life and clinical applicability. *Encephale*. 1999;25(5):470-476.

148. Waade RB, Molden E, Refsum H, Hermann M. Serum concentrations of antidepressants in the elderly. *Ther Drug Monit*. 2012;34(1):25-30. doi:10.1097/FTD.0b013e318241dce0

149. Yonkers KA, Kando JC, Cole JO, Blumenthal S. Gender differences in pharmacokinetics and pharmacodynamics of psychotropic medication. *Am J Psychiatry*. 1992;149(5):587-595.

150. Holladay JW, Dewey MJ, Yoo SD. Pharmacokinetics and antidepressant activity of fluoxetine in transgenic mice with elevated serum alpha-1-acid glycoprotein levels. *Drug Metab Dispos*. 1998;26(1):20-24.

151. Hodes GE, Hill-Smith TE, Suckow RF, Cooper TB, Lucki I. Sex-specific effects of chronic Fluoxetine treatment on neuroplasticity and pharmacokinetics in mice. *J Pharmacol Exp Ther*. 2010;332(1):266-273. doi:10.1124/jpet.109.158717

152. Ferguson JM, Hill H. Pharmacokinetics of Fluoxetine in elderly men and women. *Gerontology*. 2006;52(1):45-50. doi:10.1159/000089825

153. Hutson WR, Roehrkasse RL, Wald A. Influence of gender and menopause on gastric emptying and motility. *Gastroenterology*. 1989;96(1):11-17. doi:10.1016/0016-5085(89)90758-0

154. Gershon H, Gershon D. Caenorhabditis elegans—a paradigm for aging research: Advantages and limitations. *Mech Ageing Dev*. 2002;123:261-274.

155. McColl G, Roberts BR, Pukala TL, et al. Utility of an improved model of amyloid-beta (Aβ1-42) toxicity in Caenorhabditis elegans for drug screening for Alzheimer's disease. *Mol Neurodegener*. 2012;7(57):1-9. doi:10.1186/1750-1326-7-57

156. Nurrish S, Ségalat L, Kaplan JM. Serotonin Inhibition of Synaptic Transmission. *Neuron*. 1999;24(1):231-242. doi:10.1016/S0896-6273(00)80835-1

157. Hall AM, Roberson ED. Mouse models of Alzheimer ' s disease. *Brain Res Bull*.

2012;88(1):259-273. doi:10.1016/j.brainresbull.2011.11.017.Mouse

158. Holmes A, Yang RJ, Lesch K-P, Crawley JN, Murphy DL. Mice lacking the serotonin transporter exhibit 5-HT1A receptor-mediated abnormalities in tests for anxiety-like behavior. *Neuropsychopharmacology*. 2003;28(12):2077-2088. doi:10.1038/sj.npp.1300266

159. Ownby RL, Crocco E, Acevedo A, John V, Loewenstein D. Depression and risk for Alzheimer disease. *Arch Gen Psychiatry*. 2006;63(5):530-538. doi:10.1001/archpsyc.63.5.530

160. Kessing LV, Forman JL, Andersen PK. Do continued antidepressants protect against dementia in patients with severe depressive disorder? *Int Clin Psychopharmacol*. 2011;26(6):316-322. doi:10.1097/YIC.0b013e32834ace0f

161. Moraros J, Nwankwo C, Patten SB, Mousseau DD. The association of antidepressant drug usage with cognitive impairment or dementia, including Alzheimer disease: A systematic review and meta-analysis. *Depress Anxiety*. 2017;34(3):217-226. doi:10.1002/da.22584

162. Lee FJS, Liu F, Pristupa ZB, Niznik HB. Direct binding and functional coupling of α-synuclein to the dopamine transporters accelerate dopamine-induced apoptosis. *Fed Am Soc Exp Biol*. 2018;15:916-926.

163. Wersinger C, Rusnak M, Sidhu A. Modulation of the trafficking of the human serotonin transporter by human alpha-synuclein. *Eur J Neurosci*. 2006;24(1):55-64. doi:10.1111/j.1460-9568.2006.04900.x

164. Lavedan C. The synuclein family. *Genome Res*. 1998;8(301):871-880.

165. Fay DS, Fluet A, Johnson CJ, Link CD. In Vivo Aggregation of β-Amyloid Peptide Variants. *J Neurochem*. 1998;71(4):1616-1625. doi:10.1046/j.1471-4159.1998.71041616.x

166. Brenner S. The genetics of Caenorhabditis elegans. *Genetics*. 1974;77(1):71-94. doi:10.1002/cbic.200300625

167. Ranganathan R, Sawin ER, Trent C, Horvitz HR. Mutations in the Caenorhabditis elegans serotonin reuptake transporter MOD-5 reveal serotonin-dependent and -independent activities of fluoxetine. *J Neurosci*. 2001;21(16):5871-5884. doi:21/16/5871 [pii]

168. Sze JY, Victor M, Loer C, Shi Y, Ruvkun G. Food and metabolic signalling defects in a Caenorhabditis elegans serotonin-synthesis mutant. *Nature*. 2000;403(6769):560-564. doi:10.1038/35000609

169. Sulston J, Hodgkin J. Methods. In: Wood WB, ed. *The Nematode C. Elegans*. Cold Spring Harbor: Cold Spring Harbor Laboratory Press; 1988:587-606.

170. Ren M, Feng H, Fu Y, Land M, Rubin CS. Protein kinase D is an essential regulator of C. elegans innate immunity. *Immunity*. 2009;30(4):521-532. doi:10.1016/j.immuni.2009.03.007

171. Dostal V, Link CD. Assaying β-amyloid toxicity using a transgenic C. elegans model. *J*

Vis Exp. 2010;44:4-7. doi:10.3791/2252

172. Zamberlan DC, Arantes LP, Machado ML, Golombieski R, Soares FAA. Diphenyl-diselenide suppresses amyloid-β peptide in Caenorhabditis elegans model of Alzheimer's disease. *Neuroscience*. 2014;278:40-50. doi:10.1016/j.neuroscience.2014.07.068

173. Hoffmann J, Twiesselmann C, Kummer MP, Romagnoli P, Herzog V. A possible role for the Alzheimer amyloid precursor protein in the regulation of epidermal basal cell proliferation. *Eur J Cell Biol*. 2000;79(12):905-914. doi:10.1078/0171-9335-00117

174. Taddio A, Ito S, Koren G. Excretion of Fluoxetine and its metabolite, in human breast milk. *J Clin Pharmacol*. 1996;36:42-47.

175. Buckingham SD, Sattelle DB. Fast, automated measurement of nematode swimming (thrashing) without morphometry. *BMC Neurosci*. 2009;10(84):1-6. doi:10.1186/1471-2202-10-84

176. Nurrish S, Ségalat L, Kaplan JM. Serotonin inhibition of synaptic transmission: Gα(o) decreases the abundance of UNC-13 at release sites. *Neuron*. 1999;24(1):231-242. doi:10.1016/S0896-6273(00)80835-1

177. Kullyev A, Dempsey CM, Miller S, et al. A genetic survey of Fluoxetine action on synaptic transmission in Caenorhabditis elegans. *Genetics*. 2010;186(3):929-941. doi:10.1534/genetics.110.118877

178. Ramoz LL. Food-dependent swimming-induced paralysis in C. elegans: A novel serotonin transporter dependent phenotype. 2010.

179. Wu Y, Wu Z, Butko P, et al. Amyloid-β-Induced Pathological Behaviors Are Suppressed by Ginkgo biloba Extract EGb 761 and Ginkgolides in Transgenic Caenorhabditis elegans. *J Neurosci*. 2006;26(50):13102-13113. doi:10.1523/JNEUROSCI.3448-06.2006

180. Sirek A, Sirek O V. Serotonin: A review. *Can Med Assoc J*. 1970;102(8):846-849. http://www.pubmedcentral.nih.gov/articlerender.fcgi?artid=1946699&tool=pmcentrez&rendertype=abstract.

181. Horvitz HR, Chalfie M, Trent C, Sulston JE, Evans PD. Serotonin and octopamine in the nematode Caenorhabditis elegans. *Science (80-).* 1982;216(8):1012-1015.

182. Croll NA. *The Behaviour of Nematodes.* (Arnold E, ed.). London; 1970.

183. Huang J, Chen S, Hu L, et al. Mitoferrin-1 is involved in the progression of Alzheimer's disease through targeting mitochondrial iron metabolism in a Caenorhabditis elegans model of Alzheimer's disease. *Neuroscience*. 2018;385:90-101. doi:10.1016/j.neuroscience.2018.06.011

184. Levitan D, Doyle TG, Brousseau D, et al. Assessment of normal and mutant human presenilin function in Caenorhabditis elegans. *Proc Natl Acad Sci*. 1996;93:14940-14944.

185. Link CD. C. elegans models of age-associated neurodegenerative diseases: Lessons from transgenic worm models of Alzheimer's disease. *Exp Gerontol*. 2006;41(10):1007-1013. doi:10.1016/j.exger.2006.06.059

186. Kauffman JM. Selective serotonin reuptake inhibitor (SSRI) drugs: More risks than benefits? *Am Physicians Surg*. 2009;14(1):7-12.

187. Kantor ED, Rehm CD, Haas JS, Chan AT, Giovannucci EL. Trends in prescription drug use among adults in the United States from 1999-2012. *J Am Med Assoc*. 2015;314(17):1818-1831. doi:10.1001/jama.2015.13766

188. Pratt LA, Brody DJ, Gu Q. Antidepressant use in persons aged 12 and over: United States, 2005-2008. *NCHS Data Brief*. 2011;127(76):1-8. http://www.ncbi.nlm.nih.gov/pubmed/22617183.

6 Appendices

Appendix A: Western Blot Constituents

Table A.1: Urea/SDS-PAGE Recipe

Components	Resolving Gel (12%T/5%C/8M Urea)	Stacking Gel (6%T/5%C)	Comb Gel (7.5%T/5%C)
Separation Buffer	2.5mL		
Stacking Buffer		1.0mL	
Comb Buffer			1.5mL
40% Acrylamide	3.0mL	300µL	562.5µL
Urea	4.8g		
10% SDS	100µL	20µL	30µL
ddH_2O		670µL	867.5µL
10% APS	40µL	8µL	24µL
TEMED	5µL	2µL	3µL
Total Volume	**10mL**	**2mL**	**3mL**

Separation Buffer: 9.7 g Tris + 1.1 mL H_2SO_4 in 50 mL ddH_2O for a final concentration of 1.6 M Tris + 0.4 M H_2SO_4

Stacking Buffer: 8.4 g Bistris + 555 µL H_2SO_4 in 50 mL ddH_2O for a final concentration of 0.8 M Bistris + 0.2 M H_2SO_4

Comb Buffer: 7.5 g Bistris + 2.6 g Bicine in ddH_2O in 50 mL ddH_2O for a final concentration of 0.72 M Bistris + 0.32 M Bicine

Table A.2: Western Blot Ingredients

Component	**Resolving Gel**		**Stacking Gel**
	7.5%	**10%**	
dH_2O	4.84mL	4.01mL	3.00mL
Buffer A	2.50mL	2.50mL	
30% Acrylamide/Bis	2.50mL	3.33mL	0.67mL
Buffer C			1.25mL
10% SDS	100µL		50µL
10% APS	50µL		25µL
TEMED	10µL		5µL
Total Volume	**10mL**		**5mL**

Buffer A: 18.45 g Tris Base + 77.0 g Tric HCl + 2.0 g SDS diluted to 500 mL dH_2O to a final pH of 8.8

Buffer C: 30.0 g Tric HCl + 2.0 g SDS diluted to 500 mL dH_2O to a final pH of 6.8

Appendix B: Calculated Statistical Values

Table B.1: Paralysis Results

Strain	Treatment	Vehicle	χ^2 Value	P Value	Sample Size
CL2120	Fluoxetine	Live	2.842	0.241	218
		Dead	2.069	0.355	219
GMC101		Live	1.241	0.538	228
		Dead	0.687	0.709	224
CL2120	nor-Fluoxetine	Live	1.807	0.405	231
		Dead	0.488	0.783	231
GMC101		Live	1.824	0.402	233
		Dead	0.135	0.935	217

Table B.2: Thrashing results from CL2122 worms treated with Fluoxetine

Time (Hours)	Treatments Compared	H Value	Z value	P Value	Sample Size
18	Overall	11.706	N/A	0.003	165
	Vehicle - 1µM	N/A	-1.302	0.193	51, 55
	Vehicle - 10µM	N/A	-3.365	0.001	51, 59
	1µM - 10µM	N/A	-2.097	0.036	55, 59
24	Overall	2.117	N/A	0.347	180; 60, 60, 60
	Vehicle - 1µM	N/A	N/A	N/A	60, 60
	Vehicle - 10µM	N/A	N/A	N/A	60, 60
	1µM - 10µM	N/A	N/A	N/A	60, 60
36	Overall	10.616	N/A	0.005	180
	Vehicle - 1µM	N/A	-2.555	0.011	60, 60
	Vehicle - 10µM	N/A	-3.052	0.002	60, 60
	1µM - 10µM	N/A	-0.269	0.788	60, 60
42	Overall	0.887	N/A	0.642	178
	Vehicle - 1µM	N/A	N/A	N/A	59, 59
	Vehicle - 10µM	N/A	N/A	N/A	59, 60
	1µM - 10µM	N/A	N/A	N/A	59, 60

Table B.3: Thrashing results from CL2120 worms treated with Fluoxetine

Time (Hours)	Treatments Compared	H Value	Z value	P Value	Sample Size
18	Overall	3.609	N/A	0.165	176
	Vehicle - 1µM	N/A	N/A	N/A	60, 60
	Vehicle - 10µM	N/A	N/A	N/A	60, 56
	1µM - 10µM	N/A	N/A	N/A	60, 56
24	Overall	2.833	N/A	0.243	180; 60, 60, 60
	Vehicle - 1µM	N/A	N/A	N/A	60, 60
	Vehicle - 10µM	N/A	N/A	N/A	60, 60
	1µM - 10µM	N/A	N/A	N/A	60, 60
36	Overall	0.934	N/A	0.627	180; 60, 60, 60
	Vehicle - 1µM	N/A	N/A	N/A	60, 60
	Vehicle - 10µM	N/A	N/A	N/A	60, 60
	1µM - 10µM	N/A	N/A	N/A	60, 60
42	Overall	1.059	N/A	0.589	175
	Vehicle - 1µM	N/A	N/A	N/A	60, 58
	Vehicle - 10µM	N/A	N/A	N/A	60, 57
	1µM - 10µM	N/A	N/A	N/A	58, 57

Table B.4: Thrashing results from GMC101 worms treated with Fluoxetine

Time (Hours)	Treatments Compared	H Value	Z value	P Value	Sample Size
18	Overall	11.935	N/A	0.003	165
	Vehicle - 1µM	N/A	-0.276	0.783	57, 56
	Vehicle - 10µM	N/A	-3.216	0.001	57, 58
	1µM - 10µM	N/A	-2.714	0.007	56, 58
24	Overall	20.585	N/A	<0.001	180
	Vehicle - 1µM	N/A	-3.410	0.001	60, 60
	Vehicle - 10µM	N/A	-4.237	<0.001	60, 60
	1µM - 10µM	N/A	-1.087	0.277	60, 60
36	Overall	11.338	N/A	0.003	180
	Vehicle - 1µM	N/A	-2.295	0.022	60, 60
	Vehicle - 10µM	N/A	-3.268	0.001	60, 60
	1µM - 10µM	N/A	-0.979	0.328	60, 60
42	Overall	27.241	N/A	<0.001	179
	Vehicle - 1µM	N/A	-3.859	<0.001	59, 60
	Vehicle - 10µM	N/A	-4.906	<0.001	59, 60
	1µM - 10µM	N/A	-1.263	0.207	60, 60

Table B.5: Thrashing results from CL2122 worms treated with nor-Fluoxetine

Time (Hours)	Treatments Compared	H Value	Z value	P Value	Sample Size
18	Overall	0.884	N/A	0.643	180
	Vehicle - 1µM	N/A	N/A	N/A	60, 60
	Vehicle - 10µM	N/A	N/A	N/A	60, 60
	1µM - 10µM	N/A	N/A	N/A	60, 60
24	Overall	5.635	N/A	0.060	180
	Vehicle - 1µM	N/A	N/A	N/A	60, 60
	Vehicle - 10µM	N/A	N/A	N/A	60, 60
	1µM - 10µM	N/A	N/A	N/A	60, 60
36	Overall	10.357	N/A	0.006	179
	Vehicle - 1µM	N/A	-2.548	0.011	60, 60
	Vehicle - 10µM	N/A	-2.981	0.003	60, 59
	1µM - 10µM	N/A	-0.355	0.723	60, 59
42	Overall	0.094	N/A	0.954	180
	Vehicle - 1µM	N/A	N/A	N/A	120
	Vehicle - 10µM	N/A	N/A	N/A	120
	1µM - 10µM	N/A	N/A	N/A	120

Table B.6: Thrashing results from CL2120 worms treated with nor-Fluoxetine

Time (Hours)	Treatments Compared	H Value	Z value	P Value	Sample Size
18	Overall	0.899	N/A	0.638	179
	Vehicle - 1µM	N/A	N/A	N/A	60, 60
	Vehicle - 10µM	N/A	N/A	N/A	60, 59
	1µM - 10µM	N/A	N/A	N/A	60, 59
24	Overall	3.916	N/A	0.141	180
	Vehicle - 1µM	N/A	N/A	N/A	60, 60
	Vehicle - 10µM	N/A	N/A	N/A	60, 60
	1µM - 10µM	N/A	N/A	N/A	60, 60
36	Overall	3.912	N/A	0.141	179
	Vehicle - 1µM	N/A	N/A	N/A	60, 60
	Vehicle - 10µM	N/A	N/A	N/A	60, 59
	1µM - 10µM	N/A	N/A	N/A	60, 59
42	Overall	3.795	N/A	0.150	177
	Vehicle - 1µM	N/A	N/A	N/A	59, 59
	Vehicle - 10µM	N/A	N/A	N/A	59, 59
	1µM - 10µM	N/A	N/A	N/A	59, 59

Table B.7: Thrashing results from GMC101 worms treated with nor-Fluoxetine

Time (Hours)	Treatments Compared	H Value	Z value	P Value	Sample Size
18	Overall	2.124	N/A	0.346	180
	Vehicle - 1µM	N/A	N/A	N/A	60, 60
	Vehicle - 10µM	N/A	N/A	N/A	60, 60
	1µM - 10µM	N/A	N/A	N/A	60, 60
24	Overall	12.096	N/A	0.002	179
	Vehicle - 1µM	N/A	-2.516	0.012	60, 60
	Vehicle - 10µM	N/A	-3.288	0.001	60, 59
	1µM - 10µM	N/A	-0.964	0.335	60, 59
36	Overall	17.195	N/A	<0.001	180
	Vehicle - 1µM	N/A	-2.903	0.004	60, 60
	Vehicle - 10µM	N/A	-3.984	<0.001	60, 60
	1µM - 10µM	N/A	-1.173	0.241	60, 60
42	Overall	26.773	N/A	<0.001	179
	Vehicle - 1µM	N/A	-3.807	<0.001	60, 59
	Vehicle - 10µM	N/A	-4.830	<0.001	60, 60
	1µM - 10µM	N/A	-1.330	0.183	59, 60

Table B.8: Thrashing results from CEC215 strain comparison

Time (Hours)	Strains Compared	H Value	Z value	P Value	Sample Size
18	Overall	174.663	N/A	<0.001	240
	CL2122-GMC101	N/A	-9.338	<0.001	60, 60
	CL2122-MT9772	N/A	-3.557	<0.001	60, 60
	GMC101-CEC215	N/A	-4.079	<0.001	60, 60
	MT9772-CEC215	N/A	-9.032	<0.001	60, 60
24	Overall	183.798	N/A	<0.001	239
	CL2122-GMC101	N/A	-9.431	<0.001	60, 60
	CL2122-MT9772	N/A	-0.171	0.864	60, 60
	GMC101-CEC215	N/A	-5.334	<0.001	60, 59
	MT9772-CEC215	N/A	-9.407	<0.001	60, 59
36	Overall	188.630	N/A	<0.001	240
	CL2122-GMC101	N/A	-9.484	<0.001	60, 60
	CL2122-MT9772	N/A	-3.198	0.001	60, 60
	GMC101-CEC215	N/A	-4.697	<0.001	60, 60
	MT9772-CEC215	N/A	-9.515	<0.001	60, 60
42	Overall	189.784	N/A	<0.001	238
	CL2122-GMC101	N/A	-9.491	<0.001	60, 60
	CL2122-MT9772	N/A	-4.243	<0.001	60, 60
	GMC101-CEC215	N/A	-5.065	<0.001	60, 58
	MT9772-CEC215	N/A	-9.462	<0.001	60, 58

Table B.9: Thrashing results from CEC218 strain comparison

Time (Hours)	Strains Compared	H Value	Z value	P Value	Sample Size
18	Overall	155.069	N/A	<0.001	240
	CL2122-GMC101	N/A	-9.272	<0.001	60, 60
	CL2122-MT15434	N/A	-0.688	0.491	60, 60
	GMC101-CEC218	N/A	-1.735	0.083	60, 60
	MT15434-CEC218	N/A	-8.115	<0.001	60, 60
24	Overall	180.057	N/A	<0.001	239
	CL2122-GMC101	N/A	-9.435	<0.001	60, 60
	CL2122-MT15434	N/A	-2.920	0.003	60, 60
	GMC101-CEC218	N/A	-0.533	0.594	60, 59
	MT15434-CEC218	N/A	-9.409	<0.001	60, 59
36	Overall	181.848	N/A	<0.001	240
	CL2122-GMC101	N/A	-9.543	<0.001	60, 60
	CL2122-MT15434	N/A	-2.738	0.006	60, 60
	GMC101-CEC218	N/A	-2.311	0.021	60, 60
	MT15434-CEC218	N/A	-9.314	<0.001	60, 60
42	Overall	192.552	N/A	<0.001	240
	CL2122-GMC101	N/A	-9.629	<0.001	60, 60
	CL2122-MT15434	N/A	-5.189	<0.001	60, 60
	GMC101-CEC218	N/A	-0.561	0.575	60, 60
	MT15434-CEC218	N/A	-9.596	<0.001	60, 60